Polymerization of hyperbranched polysaccharides by combined biocatalysis

Jeroen van der Vlist

Polymerization of hyperbranched polysaccharides
by combined biocatalysis

Jeroen van der Vlist

PhD thesis
University of Groningen
The Netherlands

January 2011

Printed by Ipskamp B.V.
Enschede,The Netherlands

Cover photo: branched vein system of a leaf
(Bert van 't Hul / stock.xchng)

ISSN 1570-1530
ISBN 978-90-367-4729-5 (print)
ISBN 978-90-367-4730-1 (electronic)
Zernike Institute PhD thesis series 2011-05

University of Groningen
Zernike Institute
for Advanced Materials

RIJKSUNIVERSITEIT GRONINGEN

Polymerization of hyperbranched polysaccharides by combined biocatalysis

Proefschrift

ter verkrijging van het doctoraat in de
Wiskunde en Natuurwetenschappen
aan de Rijksuniversiteit Groningen
op gezag van de
Rector Magnificus, dr. F. Zwarts,
in het openbaar te verdedigen op
vrijdag 28 januari 2011
om 16.15 uur

door

Jeroen van der Vlist
geboren op 25 oktober 1978
te Gouda

Promotor :	Prof. dr. K. Loos
Beoordelingscommissie :	Prof. dr. L. Dijkhuizen
	Prof. dr. P. Mischnick
	Prof. dr. A. Gandini

TABLE OF CONTENTS

CHAPTER 1

General introduction

1.1 CARBOHYDRATE CHEMISTRY

1.1.1 Glucose based carbohydrates

Carbohydrates or saccharides are one of the four major classes of biomolecules. Proteins, nucleic acids and lipids are the other three. Carbohydrates consist of an aldehyde group (aldoses) or ketone group (ketoses) with multiple hydroxy groups. The simplest carbohydrates are the monosaccharides that exist, due to a stereo center, in two configurations (D and L). Aldoses with six carbon atoms (hexoses) have even four stereo centers resulting in 16 stereoisomers, D-glucose being one of them.

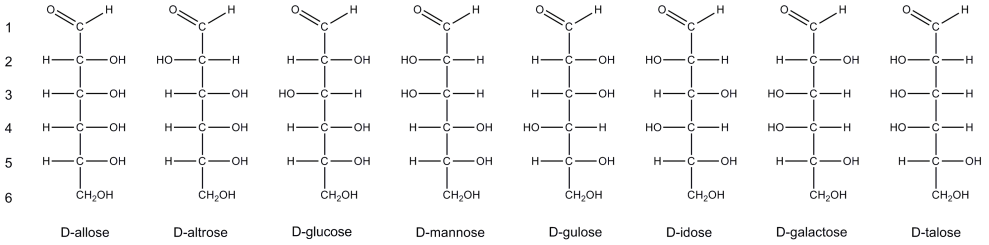

FIGURE 1.1: Fischer projections of 8 of the 16 hexoses (only the D stereoisomers are shown).

Although a linear structure of glucose occurs, the ring structure is the predominant configuration in solution (>99%). The aldehyde group can react intramolecular with the C5 hydroxy group to form a pyranose ring. An additional stereo center is created at the C1 atom with this cyclization and as a result, there are two different ring structures. In the α configuration, the hydroxyl group attached to C1 is axial positioned while in the β configuration the hydroxyl group is equatorially positioned. The β configuration is energetically favoured and the ratio of α:β anomers is 36:63 in solution[1].

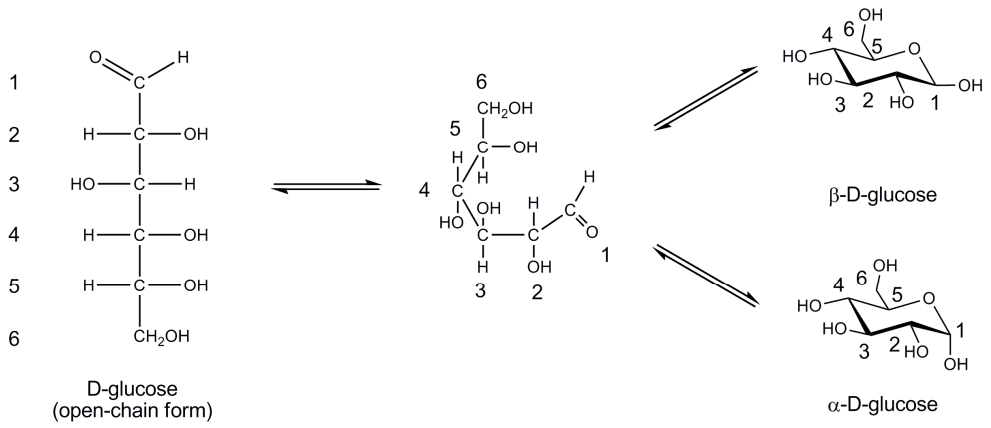

FIGURE 1.2: The open-chain form of D-glucose and the cyclic α and β configurations. The carbon atoms are numbered from 1 to 6, starting from the aldehyde group.

1.1.2 Polysaccharides

Polysaccharides are monosaccharides linked together by glycosidic bonds. The notation used to distinguish different glycosidic bonds consists of the notation α or β (the 2 possible anomers of cyclic glucose) followed by the carbon numbers which actually join the monosaccharides between brackets. For example, the linkage that connects the two D-glucose residues of the disaccharide maltose, which are joined at the C1 and C4 position, is written as: $\alpha(1\rightarrow4)$.

Besides the multiple linking positions and linking types, monosaccharides can have different ring sizes, various stereoisomers and can carry different substituents. Hence, it is not difficult to imagine that there is a huge variety of polysaccharides. Some abundant homopolysaccharides constructed from D-glucose are summarized below.

Dextran consists of $\alpha(1\rightarrow6)$ linked D-glucose residues and is the energy storage polysaccharide of yeasts and bacteria. Branching can occur at $\alpha(1\rightarrow2)$, $\alpha(1\rightarrow3)$ and $\alpha(1\rightarrow4)$ depending on the source[2]. Dextran is highly soluble in water, lacks nonspecific cell binding and resists protein adsorption, which makes dextran an interesting biomaterial for implantable purposes[3].

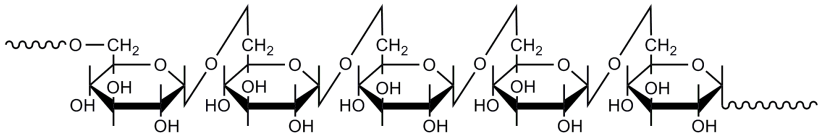

FIGURE 1.3: Linear chain of dextran, α(1→6) linkage.

Amylose is an α(1→4) linked glucan and is the linear component of starch. Although the composition of starch from each plant is unique, most starches contain 20 to 25 % amylose. The degree of polymerization of amylose varies also with the origin. Amylose from potato or tapioca starch has a DP of 1000 to 6000 while amylose from maize or wheat amylose has a degree of polymerization varying between 200 and 1200[4]. Due to intramolecular hydrogen bonding of the hydroxyl groups, amylose tends to wind up in a left-handed double stranded helix[5]. This helical conformation, with a relatively hydrophobic inner part, can be filled with water molecules but also with more hydrophobic compounds, such as fatty acids[6].

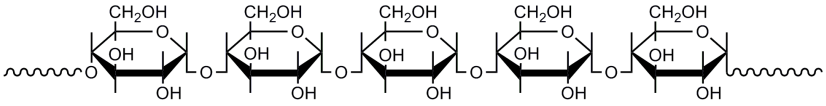

FIGURE 1.4: Structure of amylose chain, α(1→4) linkage.

Cellulose is one of the most abundant biopolymers in the biosphere[7]. Almost half of the cell wall material of wood constitutes of cellulose but it is also produced by algae, bacteria and prokaryotes[8]. Cellulose is built up from β(1→4) linked D-glucose residues and is the isomer of amylose. In nature, most cellulose is synthesized as crystalline microfibrils. Within these microfibrils the cellulose chains are parallel aligned and forms intermolecular hydrogen bonding between neighbouring chains. The degree of polymerization varies by origin. Cotton and other plant fibers have for example DP values in the 800 – 10000 range while wood cellulose has a DP in the range of 300 to 1700[9].

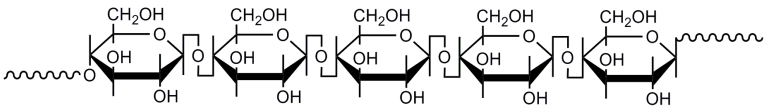

FIGURE 1.5: Structure of cellulose, β(1→4) linkage.

Chitin like cellulose is a β(1→4) linked polyglucan but has an acetamido attached to C2 instead of a hydroxy group. Exoskeletons of insects are constructed from chitin and it is present in the cell walls of most fungi and many algae. Chitin is the second most abundant polysaccharide. Chitin itself is a hydrophobic polymer and insoluble in aqueous solutions at neutral pH. However, the (often incomplete) N-deactetylation of chitin increases the water solubility and provides primary amines for further chemical modification[10]. The (partly) N-deacetylated analogue of chitin is known as chitosan and has been investigated for different biomedical applications[11].

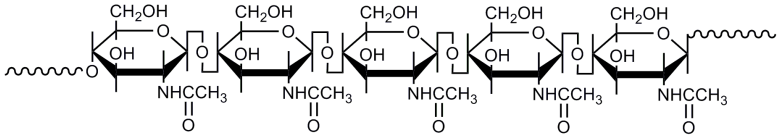

FIGURE 1.6: Structure of chitin, β(1→4) linkage.

Amylopectin and *glycogen* are branched α(1→4) linked D-glucose polysaccharides with a DP in the range of 60 000 and 6 000 000[12,13]. Branching occurs at the α(1→6) position. Amylopectin is the branched energy storage polymer of plants while glycogen is the energy storage polymer of mammals. Glycogen has typically branch lengths of 10 D-glucose units while amylopectin has branch lengths between 24 and 30 D-glucose residues. Another major difference is the branching pattern. While the branching pattern of glycogen is random, the branching points of amylopectin are clustered in regions[14]. A stable opalescent solution is obtained when glycogen or amylopectin are dissolved in water.

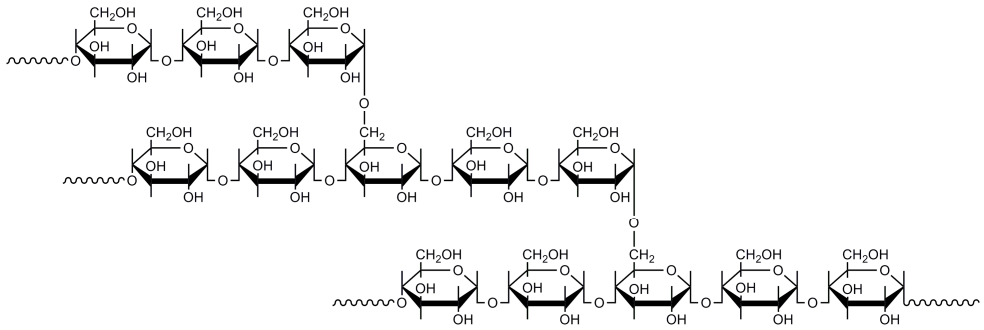

FIGURE 1.7: Part of the branched structure of glycogen. Amylopectin is branched in a similar way to glycogen but with the difference that the branch points are clustered.

1.1.3 Polysaccharides in industry

Polysaccharides are an abundant source of raw materials that are interesting due to their biodegradable, biocompatible and renewable character. Saccharides are expected to play an increasingly relevant role as raw material in the future and, in particular, as a potential candidate to replace petrol-based materials. Already, polysaccharides find their way in many different fields of industry. A short overview is given in TABLE 1.1.

TABLE 1.1: Polysaccharide processing industries and used polysaccharides.

Industry	Polysaccharide	Main function
Paper	Cellulose, starch	Structural material, coating
Food	Starch	Rheological control, texturizer
Biomedical	Dextran, chitosan, hyaluronan	Drug carrier, wound dressing
Package	Starch/cellulose derivatives	Reduction of synthetic polymers
Coating	Starch	Rheological control
Adhesive	Starch	Tackifier
Textile	Cellulose (cotton)	Woven fabric

Many polysaccharides that are industrially used are chemically or enzymatically modified to tailor the properties needed. Most enzymatic modifications are based on the specific hydrolysis of certain glycosidic linkages.

The industrial use of the enzyme glucoamylase in the starch processing industry is a good example of how enzymes can improve commercial processes[15]. This enzyme

was industrially introduced in the early 1960's and is able to hydrolyze starch with a conversion of >95% into D-glucose. The catalytic activity of this amylase surpassed the previously used acid catalyzed hydrolysis of starch. Furthermore, products are obtained with a higher yield and with a higher degree of purity. Since then, the traditional acid catalyzed hydrolysis of starch is completely replaced by enzyme catalyzed hydrolysis.

1.2 ENZYMES AS CATALYSTS

In nature, enzymes fulfil the function of catalysts. A catalyst is a substance that accelerates a reaction but undergoes no net chemical change. By providing an alternative reaction path (grey pathway in FIGURE 1.8) the reaction can proceed with lower activation energy (E_a).

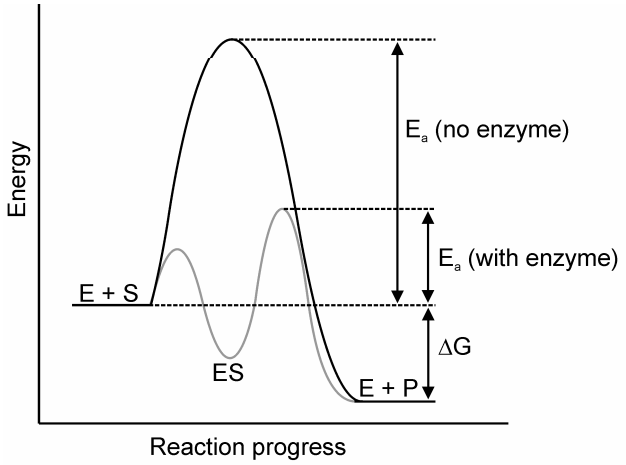

FIGURE 1.8: Transition state diagram of a typical enzyme catalyzed (grey line) and uncatalyzed reaction (black line). Where E is enzyme, S is substrate, ES is enzyme-substrate intermediate and P is product.

Enzymes are responsible for almost all biosynthetic processes in living cells. These biosynthetic reactions proceed under mild and neutral conditions at low temperatures and with quantitative conversion. This, together with the high catalytic activity and selectivity, makes enzymes highly dedicated catalysts. The reaction rates of enzyme catalyzed reactions are typically 10^6 to 10^{12} times greater than the uncatalyzed reactions but can be as high as 10^{17}.[16] In general, the selectivity is higher than conventional catalysts and side products are rarely formed.

The urge to use enzymes in (organic) chemistry becomes evident if the above described advances are considered. The first attempts to utilize enzymes *in vitro* in organic solvents are attributed to Klibanov and co workers[17,18]. Especially the enzyme family of lipases are investigated because they are stable in organic solvents, do not need a cofactor, accept a wide range of substrates and they are able to produce chiral products. Biologically active (and chiral) compounds obtained via lipase catalyzed reactions are summarized in a review by Theil[19].

Enzymes made their introduction as catalyst in polymer science as well[20-23]. At present, enzymes from four of the six enzyme classes are known to induce or catalyze polymerizations. Some examples are shown in TABLE 1.2.

TABLE 1.2: Polymers obtained via an enzyme catalyzed polymerization.

Enzyme class	Enzymes inducing polymerization	Typical polymers
I. Oxidoreducates	horse radish peroxidase	polyanilines[24], polyphenols[25,26], polystyrene[27], polymethyl methacrylate[28]
II. Transferases	prenyltransferase PHA synthase hyaluronan synthase phosphorylase	cis-1,4-polyisoprene[29-31] polyesters [32,33] hyaluronan[34,35] amylose[36-38]
III. Hydrolases	cellulase, chitinase, xylanase papain lipase *Candida antartica* CALB hyaluronidase	cellulose[39], chitin[40,41], xylan[42,43] (oligo)peptides[44-47] polyesters[48-50], polycarbonates[51-53] hyaluronan[54-56]
IV. Lyases		
V. Isomerases		
VI. Ligases	cyanophycin synthetase	cyanophycin[57]

1.3 BIOSYNTHETIC PRODUCTION OF POLYSACCHARIDES

In the starch processing industry enzymes are mainly used to hydrolyze or modify polysaccharides. However, the synthesis of polysaccharides with the aid of enzymes is also attractive and provides an alternative to the classical synthetic methods. The classical chemical synthetic approaches are, in many cases, inadequate to provide substantial quantities of saccharides. The difficulties arise from realizing complete regio- and stereo-control of the glycosylating process.

At present, no such methods are available because, in chemical synthesis, most of the difficulties arise from the laborious regio- and stereochemical control. Most synthetic approaches are therefore based on the modification or degradation of naturally occurring polysaccharides resulting in less than perfect products.

Biocatalytic synthetic pathways are very attractive as they have many advantages such as mild reaction conditions, high enantio-, regio-, chemoselectivity and enzymes are non-toxic natural catalysts. In enzymatic methods for glycoside and saccharide synthesis, no selective protection/deprotection steps are necessary and control of configuration at newly formed anomeric centers is absolute[58]. At present, enzymes from the families of hydrolases and transferases are known to produce polysaccharides *in vitro*.

1.3.1 Polysaccharides produced by hydrolases

Glycosidases (EC 3.2.1.x) have been used extensively to catalyze the formation of polysaccharides. The native action of glycosidases is to hydrolyze glycosidic linkages of glucans in the presence of water. These types of enzyme catalyzed reactions are reversible and hence the glycosidic bond formation is possible if the glycosyl substrate (the monomer) has a good leaving group and if the reaction conditions, with respect to substrate concentration, temperature and solvent quality, are well chosen.

This field is greatly inspired by the seminal work of Professor Shiro Kobayashi and his co-workers who succeeded in synthesizing:

- cellulose from β-cellobiosyl fluoride with cellulase[59-61],
- amylose from α-D-maltosyl fluoride with α-amylase[62],
- xylan from β-xylobiosyl fluoride with xylanase[42,43],
- chitin from N,N-diacetylchitobiose oxazoline with chitinase[63],
- keratan from Galβ(1→4)GlcNAc(6S) and Gal(6S)β(1→4) GlcNAc(6S) oxazoline with keratanase II[64].
- Furthermore, Kobayashi et al. were able to show that hyaluronidase is able to catalyze the *in vitro* synthesis of hyaluronan[65], chondroitin[66], chondroitin sulfate[67], their derivatives[66,68] and non-natural glycosaminoglycans[69].

1.3.2 Polysaccharides produced by transferases

Glycosyltransferases (EC 2.4.x.x) catalyze the transfer of a sugar moiety from an activated donor sugar onto saccharide and non-saccharide acceptors. They can be divided into the Leloir and non-Leloir types according to the type of glycosyl donors they use[70]. Non-Leloir glycosyltransferases typically use glycosyl phosphates as donors, while Leloir glycosyltransferases use sugar nucleotides as donors and transfer the monosaccharide with either retention (retaining enzymes) or inversion (inverting enzymes) of the configuration of the anomeric center.

Glycosyltransferases are among others reported to synthesize:

- hyaluronan with hyaluronan synthase[55,55],
- amylose with amylosucrose[71,72],
- branched α-glucans with glucansucrases[73].

In this thesis, two enzymes from the class of glycosyltransferases are used and outlined in the following section – phosphorylase and branching enzyme.

PHOSPHORYLASE

Phosphorylase (EC 2.4.1.1) belongs to the group of non-Leloir glycosyltransferases and requires the activated donor substrate glucose-1-phosphate. Phosphorylase is in this study used to produce linear $\alpha(1\rightarrow4)$ linked glucans *in vitro*.

In vivo, linear $\alpha(1\rightarrow4)$ linked glucans are synthesized from ADP-glucose by the enzyme glycogen synthase (EC 2.4.1.1)[74-77]. The enzyme as well as the monomer is quite sensitive and therefore most researchers (at least in the field of polymer science) prefer to use phosphorylase for the synthesis of synthetic amylose. *In vivo* phosphorylase is mainly involved in the breakdown of starch in order to gain energy. The terminal non-reducing glucose residues from α-glucans are phosphorolytically removed to yield a glucose-1-phosphate molecule. The product, glucose-1-phosphate, is subsequently inter-converted to glucose-6-phosphate by the action of phosphoglucomutase (EC 5.4.2.2.). Glucose-6-phosphate has different fates. It is for example a precursor in the pentose phosphate pathway (PPP) and it can be converted to α-D-glucose and to pyruvate via the glycolysis pathway (see FIGURE 1.9).

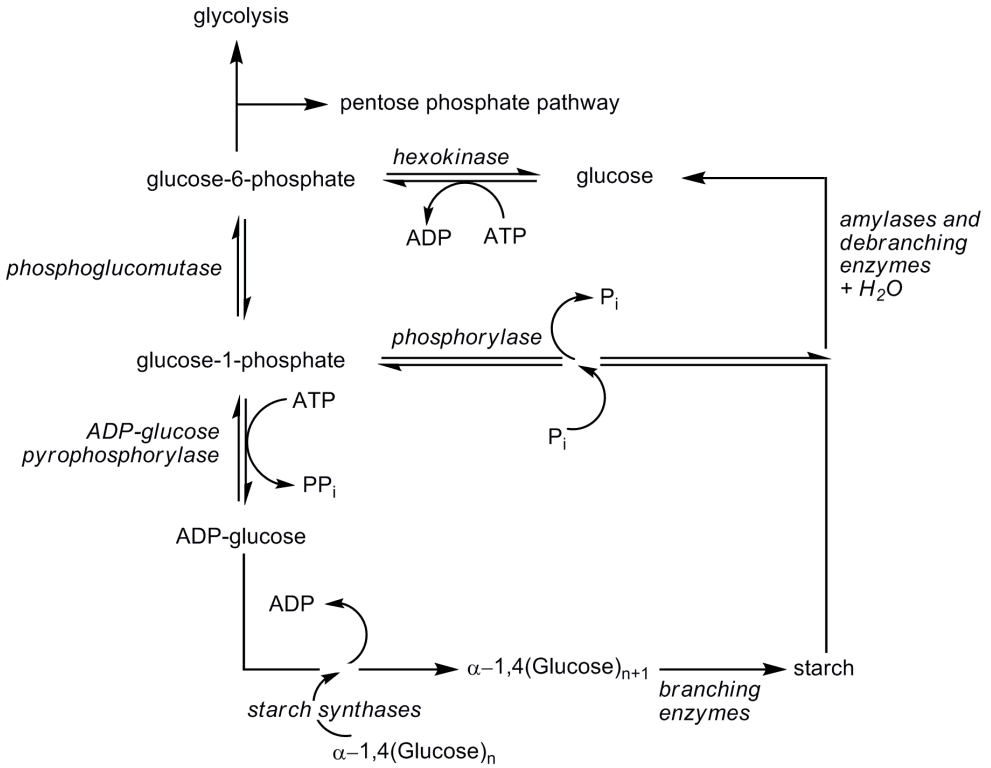

FIGURE 1.9: Simplified view of starch metabolism[78].

However, under the appropriate conditions, the catalytic action of phosphorylase can be reverted and linear synthetic amylose can be synthesized with the release of inorganic phosphate (P_i) (see FIGURE 1.10). Polymerization will only occur if a linear $\alpha(1\rightarrow4)$ primer of at least 3 glucose residues is present[79].

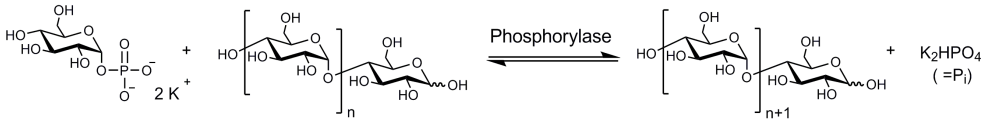

FIGURE 1.10: Catalytic action of phosphorylase.

The existence of a phosphorylating enzyme (phosphorylase) in a higher plant was first reported by Iwanoff[80] who observed that an enzyme, he found in the germinating vetches Vicia sativa, liberates inorganic phosphate from organic phosphorous compounds. Shortly thereafter, the same enzyme was found in other vetches and wheat[81,82], rice and coleseed[83], barley and malt etc. Bodńar[84] was the first to report a progressive disappearance of inorganic phosphate (thus the reverse reaction) while incubating suspended flour from ground peas in a phosphate buffer.

Cori and Cori demonstrated that animal tissues contain an enzyme which acts upon glycogen as well[85-88]. Cori, Colowick and Cori suggested that the product of this reaction is α-glucopyranose-1-phosphoric acid (also called Cori-ester), which was confirmed later by Kiessling[89] and Wolfrom and Pletcher[90].

The most intensively studied phosphorylases are rabbit muscle phosphorylase and the potato phosphorylase. Over 75% of the key active-site residues from muscle phosphorylase is analogous to potato phosphorylase[91]. An important difference is the need for a co-factor in the case of muscle phosphorylase while potato phosphorylase has no regularity characteristics[91] and follows normal Michaelis-Menten kinetics[92]. The affinity towards substrates also differs. Muscle phosphorylase acts on branched polysaccharides and less on linear variants while potato phosphorylase acts on both linear and branched polysaccharides[85,93].

Potato phosphorylase can be found in two different forms that are inter-convertible. These so-called isozymes have different properties in terms of kinetics, molecular weight and activity. The “slow isozyme” has a mass of 209 KDa and the “fast isozyme” has a mass of 165 KDa. The names slow and fast refer to the migration speed in a polyacrylamide electrophoresis. Furthermore the slow isozyme is more pronounced in young potato tubers and favours the metabolic pathway (i.e. synthesis of starch) while the fast isozyme is mainly found in sprouting potato tubers and favours the catabolic pathway (i.e. breakdown of starch)[94].

The fact that glycogen phosphorylase can be used to polymerize amylose was first demonstrated by Schäffner and Specht[95] in 1938 using yeast phosphorylase. Shortly after, the same behaviour was also observed for other phosphorylases from yeast by Kiessling[96,97], muscles by Cori, Schmidt and Cori[98], pea seeds[99], potatoes by Hanes[100] and preparations from liver by Ostern and Holmes[101], Cori, Cori and Schmidt[102] and Ostern, Herbert and Holmes[103]. These results opened up the field of enzymatic polymerizations of amylose using glucose-1-phosphate as monomer and can be considered as the first experiments ever to synthesize biological macromolecules *in vitro*. Pfannemüller[104-108] et al. showed in the 1960’s and 70’s that it is possible to obtain carbohydrate containing amphiphiles with various alkyl chains via amide bond formation. For this, maltooligosaccharides were oxidized to the according aldonic acid lactones, which could subsequently be coupled to alkylamines. Subsequently, the alkyl-oligosaccharides where utilized as primer for the phosphorylase catalyzed elongation of the polysaccharide resulting in sugar based surfactants.

BRANCHING ENZYME

The formation of the α(1→4,6) glucosyl branches of amylopectin and glycogen is catalyzed by branching enzymes (BE, EC 2.4.1.18). BE's belong to the glycosyltransferases according to the Enzyme Commission (EC) classification. However, the Carbohydrate-Active enZYmes Database (CAZy)[109,110] uses an amino-acid-sequence-based classification and classifies GBE_{DG} as a hydrolase rather than a transferase. The CAZy database is currently the best classification system for carbohydrate-active enzymes. Until recently it was believed that all GBEs belong to glycoside hydrolase family 13 (GH13). However, GBEs belonging to the GH57 family are also known[111,112].

The branching enzyme itself is not able to induce polymerization. Instead it catalyzes the formation of $\alpha(1\rightarrow6)$ branch points by the hydrolysis of an $\alpha(1\rightarrow4)$ glycosidic linkage and subsequent inter- or intra-chain transfer of the non-reducing terminal fragment to the C6 hydroxyl position of an α-glucan (see FIGURE 1.11).

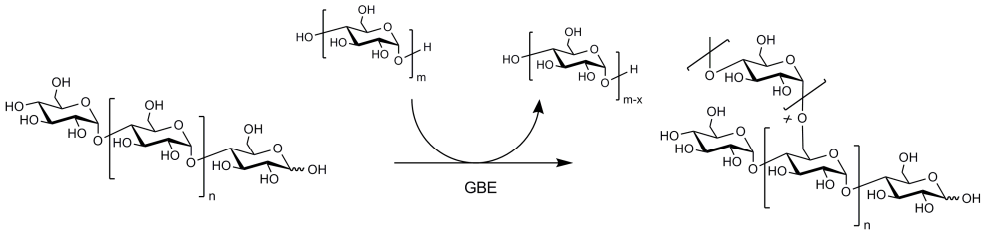

FIGURE 1.11: Catalytic action of the branching enzyme.

The branching enzyme, also known as the Q-enzyme, has been isolated from various sources, including potato tubers[113-117], maize[118-120], teosinte[121], sorghum[122], rice[123], *Pisum sativum*[124], spinach[125,126], mammalian muscle[127], *Escherichia coli*[128,129] and rabbit liver[130]. The first evidence of the action of a branching enzyme was found in potato juice[131]. It is the branching enzyme that is responsible for the branched structure of glycogen as well as amylopectin. Next to the intra- and inter-chain transfer as proved by Whelan[132] in potato branching enzyme, Takata[133,134] proposes a third possibility: backbiting, resulting in intramolecular cyclization of the chain.

In potatoes[135] and maize[136], at least 2 distinct isozymes have been identified, while only one form is found in most bacteria. Depending on the source, the branching enzyme prefers different donors and acceptors. Furthermore, the various branching enzymes may have different specificities in the length of the transferred chain. For example, starch branching enzyme I (SBEI) from maize, preferentially transfers long chains and is more active on amylose while the isozyme SBEII, is more active on

amylopectin and transfers shorter chains[137]. Many branching enzymes have been over expressed in *E. coli* bacterium[134,137-142] to study the exact mechanism in more detail. Palomo Reixach et al.[142] over expressed the glycogen branching enzyme of *Deinococcus geothermalis* (GBE_{DG}) in *E. coli.* When incubated with amylose V, a branching pattern with a side chain distribution corresponding to a degree of branching of 11 % was found.

The GBE_{DG} is an interesting branching enzyme as it transfers rather short fragments resulting in a highly branched structure. Thereby, the optimum activity is in the same pH- and temperature range of potato phosphorylase, making it possible to execute an enzyme catalyzed tandem polymerization together with potato phosphorylase.

1.4 COMBINED BIOCATALYSIS

In nature, a cascade of enzyme catalyzed reactions is involved for the biosynthesis of starch. When selecting the appropriate enzymes and reaction circumstances reactions with multiple enzymes can be performed *in vitro*.

Synthetic glycogen was first *in vitro* synthesized by Cori[143] in 1943 via the cooperative action of muscle phosphorylase and branching enzymes isolated from rat liver and rabbit heart. The substrate glucose-1-phosphate was used as starting material. This method was repeated by others with phosphorylases and branching enzymes from various sources[127,144-146]. Waldmann[147] used sucrose phosphorylase and glucan phosphorylase in a 1-pot synthesis to produce synthetic amylose from sucrose. Sucrose phosphorylase promotes the synthesis of glucose-1-phosphate from inorganic phosphate and sucrose while glucan phosphorylase catalyzes the amylose chain formation from glucose-1-phosphate. Kuriki[148] proposed to extend this reaction by adding a branching enzyme which would result in branched α-glucans from sucrose and inorganic phosphate. Since sucrose and inorganic phosphate are cheaper than the rather expensive glucose-1-phosphate, sucrose phosphorylase may by a key enzyme to make these reactions industrially attractive. The combined action of branching enzyme with starch synthase[149,150] and glycogen synthase[129,151,152] has been reported as well and resulted in synthetic glycogen.

Here we report the polymerization of hyperbranched polyglucans by the combined biocatalysis of potato phosphorylase and GBE_{DG} (see FIGURE 1.12).

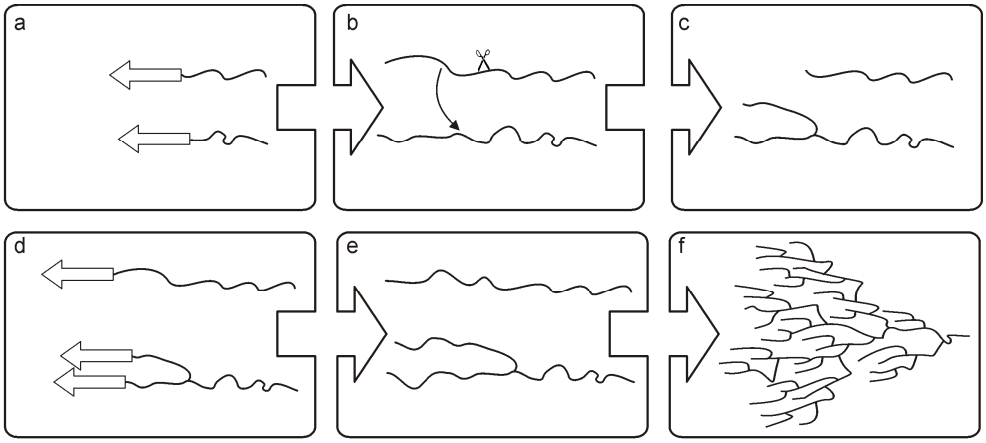

FIGURE 1.12: The combined action of phosphorylase and the branching enzyme. ***a)*** *Phosphorylase catalyzes the chain elongation from linear primers.* ***b, c)*** *The branching enzyme catalyzes the hydrolytic chain scission of an $\alpha(1\rightarrow4)$ linkage and transfers the non-reducing terminal fragment to a C6 hydroxyl position.* ***d)*** *Phosphorylase uses the newly formed non-reducing chain ends (branches) as primer sites and elongates them.* ***e)*** *When the side chains are long enough, the branching enzyme again starts the process as depicted in figures b and c .* ***f)*** *After multiple cycles in which phosphorylase elongates the chains and the branching enzyme reshuffles the non-reducing terminal fragments, a hyperbranched polysaccharide is formed.*

1.5 HYPERBRANCHED POLYMERS

The first known branched polymers are the branched α-glucans, dextran, amylopectin and glycogen. Staudinger[153] identified them as branched macromolecules in 1937 and the linking pattern was clarified by Meyer and Berneld[154,155] in 1940. Although the branched α-glucans are *hyperbranched*, the term was first introduced by Kim and Webster[156,157] in 1988 for the hyperbranched polyphenylenes they synthesized. In 2009 the IUPAC defined a hyperbranched polymer as: "A polymer composed of highly branched macromolecules in which any linear subchain may lead in either direction to at least two other subchains"[158].

Hyperbranched polysaccharides and hyperbranched polymers in general behave different than their linear analogues. The compact and globular shape of hyperbranched polymers diminishes the amount of entanglements with other polymer chains. Consequently, the viscosity of a hyperbranched polymer solution is low as compared to their linear analogues. Furthermore, the multiple end groups of a hyperbranched polymer make it possible to tailor the chemical, thermal and solution properties.

1.5.1 The degree of branching

In 1952, Flory[159] published his theoretical work on polycondensates consisting of multifunctional AB_m monomers. An AB_m monomers consist of an *A* functionality and multiple *B* functionalities (≥2). The *A* functionality is complementary to *B* and the only reaction in the system that can take place is the coupling of *A* to *B*. As can be seen in FIGURE 1.13, three types of incorporation modes are possible: dendritic (D), linear (L) and terminal (T).

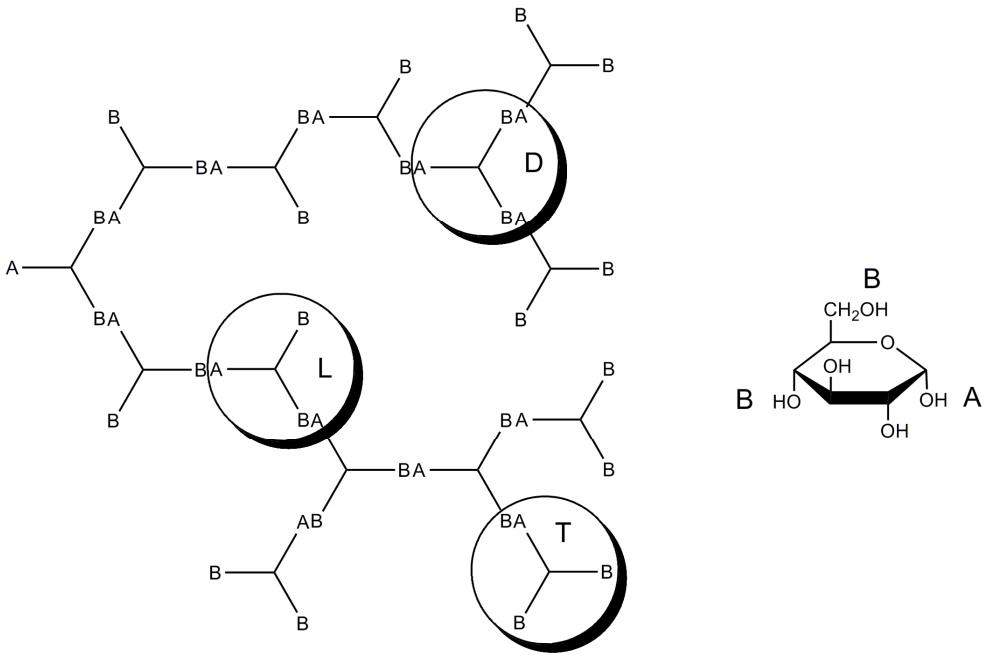

FIGURE 1.13: Schematic representation of a hyperbranched polymer constructed from AB_2 monomers (left) and an α-D-glucose residue presented as an AB_2 monomer (right).

Glycogen, and the structures synthesized in this research, can be seen as an AB_2/AB copolymer. The reducing group at C1 acts as the *A* functionality and the hydroxy groups at C4 and C6 act as the *B* functionalities. The linear, AB, monomer is via the C1 and C4 incorporated and the dendritic AB_2 monomer is incorporated by the C1, C4 and C6. The C2, C3 and C5 hydroxy groups do not participate because of the regiospecifity of the enzymes involved in the biosynthesis of glycogen.

A relation for the degree of branching (DB) can be established with a dendrimer as reference point. A dendritic structure, consisting of solely dendritic and terminal groups, represents a degree of branching of 100%. Therefore, the degree of

branching is defined as the number of D and T monomers divided by the total number of monomers incorporated[160,161] (see EQUATION 1.1).

$$DB = \frac{D+T}{D+T+L} \qquad 1.1$$

However, the term *degree of branching* is also attributed to the amount of dendritic units per polymer. This definition reflects the number of branching points per molecule rather than comparing a hyperbranched polymer with a dendrimer.

$$DB = \frac{D}{D+T+L} \qquad 1.2$$

In general EQUATION 1.1 is used to calculate the DB for synthetic hyperbranched polymers. However, the DB of natural polymers such as polysaccharides is often calculated with EQUATION 1.2. The outcomes of EQUATIONS 1.1 and 1.2 differ by a factor 2 since the terminal groups are excluded in the latter equation.

Since we compare our hyperbranched polysaccharide structures with natural branched polymers such as glycogen and amylopectin rather than with dendritic structures we use EQUATION 1.2 to calculate the degree of branching.

1.6 BIOCONJUGATES

Polymers consisting of two parts, both synthetic and natural in origin are known as polymer bioconjugates or polymer bio-hybrids. The conjugation of synthetic polymers with peptides[162,163], proteins[164], DNA[165] or enzymes[166] have been reported. Initially bio-hybrids were designed for use in the pharmaceutical industry[167] but due to the broad properties and the endless variations, bioconjugates can be found in applications varying from bio-sensor, artificial enzymes, biometric systems and light-harvesting systems to photonic materials and nano-electronic devices[168,169].

Polysaccharide and sugar based bioconjugates, also known as glycoconjugates, are systems that contain both a synthetic and a sugar based part. The sugar moiety can be found in the form of pendant side groups attached to a synthetic polymer backbone or attached to the end group of a synthetic polymer [106,170-181]. Furthermore, glycodendrimers, carbohydrate coated dendrimers and star-polymers in various forms have been synthesized[182-188].

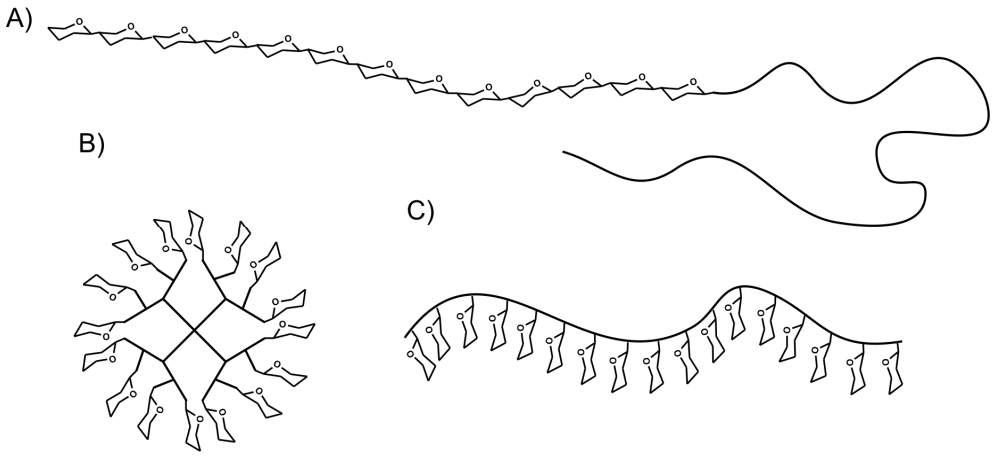

FIGURE 1.14: Graphical representation of A) linear glyco diblock copolymer. B) glucan coated dendrimer. C) polymer with pendant sugar groups. For simplification purposes, hydroxy groups and protons are not shown.

1.6.1 Bioconjugation

There are different synthetic strategies to couple polymers to saccharides. Some of them are summarized below. In this thesis, all coupling reactions have been performed using the method of reductive amination. This method works without any modification of the saccharide moiety unlike most of the other strategies mentioned below.

CLICK CHEMISTRY

Sharpless[189] introduced the idea of "click" chemistry in 2001. One of the most popular "click" reactions is based on the azide alkyne Huisgen cycloaddition in which an azide reacts with an alkyne in the presence of Cu(I)[190]. The utilization of "click" chemistry has been demonstrated for a range of carbohydrates[174,191-194].

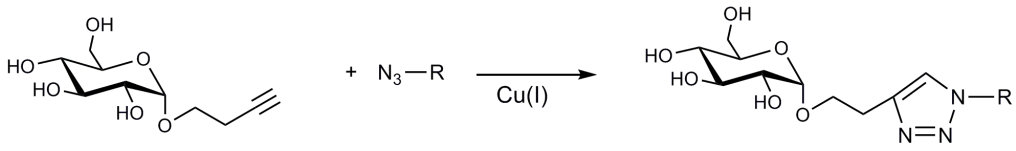

FIGURE 1.15: Coupling of an alkynyl glucose residue with an azide functionalized substrate.

COUPLING VIA A MALTOHEPTAONOLACTONE INTERMEDIATE

Oxidation of the terminal reducing group of a saccharide with bromine[108,195] or sodium periodate[196] results in the formation of a lactone. This lactone can be coupled to amine functionalized substrates. The amide bond formed can be enzymatically cleaved when needed.

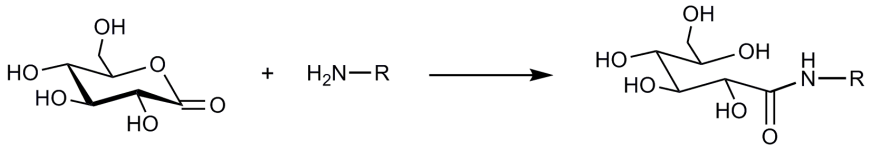

FIGURE 1.16: Coupling of a glucose lactone to an amine functionalized substrate.

COUPLING VIA GLYCOSYLAMINES

Via a reaction presented by Kochetkov[197], unprotected oligosaccharides can be converted to their corresponding glycosylamines. The anomeric hydroxyl group is hereby converted to an amino group upon treatment with aqueous ammonium carbonate. The resulting amine end-functionalized saccharide can be coupled to carboxylic acid functionalized substrates via an amide linkage. The long reaction times, the sometimes unstable glycosylamines and low yields are however disadvantageous.

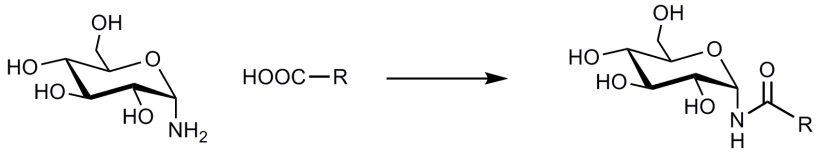

FIGURE 1.17: Formation of an amide linkage between an glycosylamine and a carboxy acid

COUPLING VIA REDUCTIVE AMINATION

Metal hydrides, for example substituted borohydrides, are capable of reducing a variety of organic functional groups. The reducing power and thus the selectivity of

the borohydride ion is greatly influenced by its substituents. Sodium cyanoborohydride is for example a much milder and more selective reducing agent than sodium borohydride due to the electron withdrawing cyanogroup[198].

Sodium cyanoborohydride can reduce aldehydes and ketones to their corresponding alcohols at a pH of 3-4. At a higher pH (pH 6-8) and in the presence of an primary or secondary amine, the reduction of the imine is favoured above the reduction of the carbonyl group and hence reductive amination is possible[199]. This highly selective reducing agent provides a simple and efficient method to couple the terminal reducing group of a saccharide to amine functionalized substrates[200].

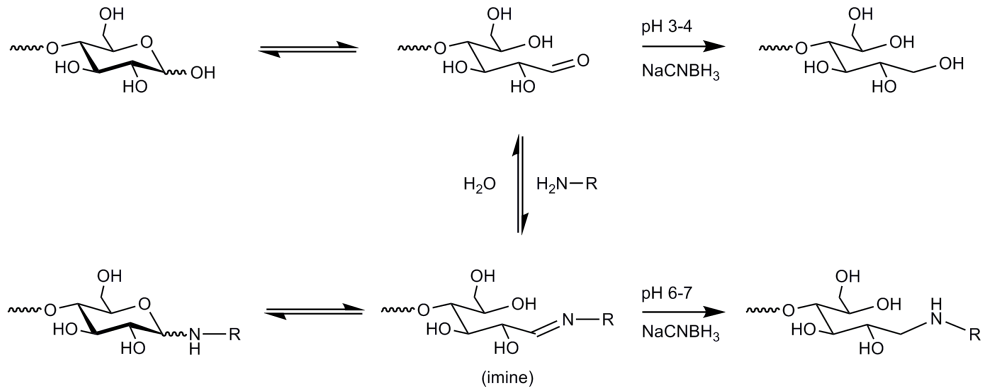

FIGURE 1.18: Reductive amination of the terminal reducing group of a saccharide with an amine functionalized substrate.

1.7 OUTLINE OF THIS THESIS

The primary aim of the work described in this thesis, is the *in vitro* synthesis of a synthetic hyperbranched polysaccharide via a biocatalytic pathway. Two enzymes that are normally involved in the biosynthesis of starch and glycogen are selected for this purpose. Via a combined biocatalysis, artificial hyperbranched polysaccharides can be obtained *in vitro* on the gram scale.

CHAPTER 2 describes the isolation and purification of potato phosphorylase as well as the cloning, expression and purification of the glycogen branching enzyme *Deinococcus geothermalis* (GBE_{DG}). The optimal reaction conditions for the use of both enzymes in a one-pot synthesis are studied and the branching pattern of the obtained product is investigated with MALDI-ToF mass spectrometry and ^{1}H-NMR spectroscopy.

CHAPTER 3 describes the grafting procedure of maltoheptaose primer onto Si substrates. The primer grafting density and the layer thickness is studied. With the enzymatic elongation of the primers, hyperbranched polysaccharides are grown from the substrates, resulting in covalently bond hyperbranched polysaccharide brushes. The primer, and thus brush, density as well as the thickness of the layer is determined by ellipsometry and surface analysis is performed with X-ray photoelectron spectroscopy (XPS) and atomic force microscopy (AFM).

The synthesis and purification of two- and three functional primers are described in *CHAPTER 4*. Subsequent use of these multivalent primers in an enzyme catalyzed reaction yields hyperbranched polymeric bioconjugates. The dimensions of the resulting bioconjugates are determined with dynamic light scattering.

CHAPTER 5 describes the enzymatic synthesis of biohybrid block copolymers. Poly(ethylene glycol) is functionalized with an amine group via a Mitzunobu Staudinger reaction. Subsequent coupling of maltoheptaose to the polymer yields a macroprimer. This macroprimer is used as starting site for the enzyme catalyzed polymerization and yields a block copolymer consisting of a linear poly ethylene glycol block and a hyperbranched amylose block.

1.8 REFERENCES

1. D. Voet, J.G. Voet, and C.W. Pratt. In *Fundamentals of Biochemistry*, 206-232, Wiley, **2006**
2. M. Naessens, A. Cerdobbel, W. Soetaert, E.J. Vandamme, *J. Chem. Technol. Biotechnol.*, **2005**, *80,* 845-860
3. S.P. Massia, J. Stark, D.S. Letbetter, *Biomaterials*, **2000**, *21,* 2253-2261
4. M.J.E.C. van der Maarel, B. van der Veen, J.C.M. Uitdehaag, H. Leemhuis, L. Dijkhuizen, *J. Biotechnol.*, **2002**, *94,* 137-155
5. B. Pfannemüller, *Biopolymers*, **1971**, *10,* 243-261
6. R.E. Rundle, F.C. Edwards, *J. Am. Chem. Soc.*, **1943**, *65,* 2200-2203
7. I.M. Saxena, R.M. Brown, *Annals of Botany*, **2005**, *96,* 9-21
8. R.M. Brown, *Journal of Polymer Science Part A-Polymer Chemistry*, **2004**, *42,* 487-495
9. D. Klemm, B. Heublein, H.P. Fink, A. Bohn, *Angewandte Chemie-International Edition*, **2005**, *44,* 3358-3393
10. M.N.V.R. Kumar, *Reactive & Functional Polymers*, **2000**, *46,* 1-27
11. E. Khor, L.Y. Lim, *Biomaterials*, **2003**, *24,* 2339-2349
12. V. Thiemann, B. Saake, A. Vollstedt, T. Schafer, J. Puls, C. Bertoldo, R. Freudl, G. Antranikian, *Appl. Microbiol. Biotechnol.*, **2006**, *72,* 60-71
13. D.J. Manners, *Carbohydr. Polym.*, **1991**, *16,* 37-82
14. A.M. Smith, *Current Opinion in Plant Biology*, **1999**, *2,* 223-229
15. W.D. Crabb, J.K. Shetty, *Current Opinion in Microbiology*, **1999**, *2,* 252-256
16. A. Radzicka, R. Wolfenden, *Science*, **1995**, *267,* 90-93
17. A. Zaks, A.M. Klibanov, *Proc. Natl. Acad. Sci. U. S. A.*, **1985**, *82,* 3192-3196
18. A. Zaks, A.M. Klibanov, *J. Biol. Chem.*, **1988**, *263,* 3194-3201
19. F. Theil, *Chemical Reviews*, **1995**, *95,* 2203-2227
20. A.R.A. Palmans and A. Heise, *Enzymatic Polymerisation*, Springer, **2010**
21. R.A. Gross, A. Kumar, B. Kalra, *Chemical Reviews*, **2001**, *101,* 2097-2124
22. H.N. Cheng and R.A. Gross, *Green Polymer Chemistry: Biocatalysis and Biomaterials*, American Chemical Society, **2010**
23. K. Loos, *Biocatalysis in Polymer Chemistry*, 1st edition, Wiley, **2010**
24. P. Xu, A. Singh, and D. Kaplan. In *Enzyme-Catalyzed Synthesis of Polymers*, 71-94, K. Kobayashi, H. Ritter, D. Kaplan, Springer, **2006**
25. M. Schnitzer, M. Barr, R. Hartenstein, *Soil Biol. Biochem.*, **1984**, *16,* 371-376
26. J.S. Dordick, M.A. Marletta, A.M. Klibanov, *Biotechnol. Bioeng.*, **1987**, *30,* 31-36
27. A. Singh and D. Kaplan. In *Enzyme-Catalyzed Synthesis of Polymers*, 211-224, K. Kobayashi, H. Ritter, D. Kaplan, Springer, **2006**
28. B. Kalra, R.A. Gross, *Biomacromolecules*, **2000**, *1,* 501-505
29. D.R. Light, M.S. Dennis, *J. Biol. Chem.*, **1989**, *264,* 18589-18597
30. S. Madhavan, G.A. Greenblatt, M.A. Foster, C.R. Benedict, *Plant Physiol.*, **1989**, *89,* 506-511
31. B.L. Archer, B.G. Audley, *Adv. Enzymol. Relat. Areas Mol. Biol.*, **1967**, *29,* 221-&
32. C.T. Nomura, S. Taguchi, *Appl. Microbiol. Biotechnol.*, **2007**, *73,* 969-979
33. J.N. Lu, R.C. Tappel, C.T. Nomura, *Polymer Reviews*, **2009**, *49,* 226-248

34. K.J. Williams, K.M. Halkes, J.P. Kamerling, P.L. DeAngelis, *J. Biol. Chem.*, **2006**, *281,* 5391-5397
35. W. Jing, P.L. DeAngelis, *J. Biol. Chem.*, **2004**, *279,* 42345-42349
36. B. Pfannemüller, W. Burchard, *Die Makromolekulare Chemie*, **1969**, *121,* 1-17
37. B. Pfannemüller, E. Husemann, *Starch*, **1968**, *20,* 351-362
38. B. Pfannemüller, *Starch*, **1968**, *20,* 351
39. S. Kobayashi, K. Kashiwa, T. Kawasaki, S. Shoda, *J. Am. Chem. Soc.*, **2002**, *113,* 3079-3084
40. S. Kobayashi, T. Kiyosada, S.i. Shoda, *J. Am. Chem. Soc.*, **1996**, *118,* 13113-13114
41. M. Faijes, A. Planas, *Carbohydr. Res.*, **2007**, *342,* 1581-1594
42. S. Kobayashi, X. Wen, S. Shoda, *Macromolecules*, **1996**, *29,* 2698-2700
43. M. Fujita, S.i. Shoda, S. Kobayashi, *J. Am. Chem. Soc.*, **1998**, *120,* 6411-6412
44. G. Anderson, P.L. Luisi, *Helvetica chemica acta*, **1979**, *62,* 488-493
45. H.D. Jakubke, P. Kuhl, A. Könnecke, *Angew. Chem. -Int. Edit.*, **1985**, *24,* 85-93
46. R. Jost, E. Brambilla, J.C. Monti, P.L. Luisi, *Helv. Chim. Acta*, **1980**, *63,* 375-384
47. A. Ferjancic, A. Puigserver, H. Gaertner, *Biotechnol. Lett.*, **1991**, *13,* 161-166
48. M. de Geus, J. Peeters, M. Wolffs, T. Hermans, A.R.A. Palmans, C.E. Koning, A. Heise, *Macromolecules*, **2005**, *38,* 4220-4225
49. A. Cordova, T. Iversen, K. Hult, *Polymer*, **1999**, *40,* 6709-6721
50. Z. Jiang, C. Liu, R.A. Gross, *Macromolecules*, **2008**, *41,* 4671-4680
51. D.A. Abramowicz, C.R. Keese, *Biotechnol. Bioeng.*, **1989**, *33,* 149-156
52. R.L. Rodney, J.L. Stagno, E.J. Beckman, A.J. Russell, *Biotechnol. Bioeng.*, **1999**, *62,* 259-266
53. R.L. Rodney, B.T. Allinson, E.J. Beckman, A.J. Russell, *Biotechnol. Bioeng.*, **1999**, *65,* 485-489
54. K.J. Williams, K.M. Halkes, J.P. Kamerling, P.L. DeAngelis, *J. Biol. Chem.*, **2006**, *281,* 5391-5397
55. W. Jing, P.L. DeAngelis, *J. Biol. Chem.*, **2004**, *279,* 42345-42349
56. P.L. DeAngelis, L.C. Oatman, D.F. Gay, *J. Biol. Chem.*, **2003**, *278,* 35199-35203
57. A. Bröker and A. Steinbüchel. In *Biocatalysis in Polymer Chemistry*, 247-276, K. Loos, Wiley, **2010**
58. J. van der Vlist and K. Loos. In *Biocatalysis in Polymer Chemistry*,K. Loos, Wiley, **2010**
59. S. Kobayashi, K. Kashiwa, T. Kawasaki, S. Shoda, *J. Am. Chem. Soc.*, **1991**, *113,* 3079-3084
60. J.H. Lee, R.M. Brown, S. Kuga, S. Shoda, S. Kobayashi, *Proc. Natl. Acad. Sci. U. S. A.*, **1994**, *91,* 7425-7429
61. S. Kobayashi, L.J. Hobson, J. Sakamoto, S. Kimura, J. Sugiyama, T. Imai, T. Itoh, *Biomacromolecules*, **2000**, *1,* 168-173
62. S. Kobayashi, J. Shimada, K. Kashiwa, S.I. Shoda, *Macromolecules*, **1992**, *25,* 3237-3241
63. J. Sakamoto, J. Sugiyama, S. Kimura, T. Imai, T. Itoh, T. Watanabe, S. Kobayashi, *Macromolecules*, **2000**, *33,* 4155-4160
64. M. Ohmae, K. Sakaguchi, T. Kaneto, S. Fujikawa, S. Kobayashi, *ChemBioChem*, **2007**, *8,* 1710-1720
65. S. Kobayashi, H. Morii, R. Itoh, S. Kimura, M. Ohmae, *J. Am. Chem. Soc.*, **2001**, *123,* 11825-11826

66. S. Kobayashi, S. Fujikawa, M. Ohmae, *J. Am. Chem. Soc.*, **2003**, *125,* 14357-14369
67. S. Fujikawa, M. Ohmae, S. Kobayashi, *Biomacromolecules*, **2005**, *6,* 2935-2942
68. H. Ochiai, M. Ohmae, T. Mori, S. Kobayashi, *Biomacromolecules*, **2005**, *6,* 1068-1084
69. S. Kobayashi, M. Ohmae, H. Ochiai, S.I. Fujikawa, *Chemistry-A European Journal*, **2006**, *12,* 5962-5971
70. L.F. Leloir, *Science*, **1971**, *172,* 1299
71. G. Potocki-Veronese, J.L. Putaux, D. Dupeyre, C. Albenne, M. Remaud-Simeon, P. Monsan, A. Buleon, *Biomacromolecules*, **2005**, *6,* 1000-1011
72. J.L. Putaux, G. Potocki-Veronese, M. Remaud-Simeon, A. Buleon, *Biomacromolecules*, **2006**, *7,* 1720-1728
73. S. Kralj, G.H. van Geel-Schutten, H. Rahaoui, R.J. Leer, E.J. Faber, M.J.E.C. van der Maarel, L. Dijkhuizen, *Appl. Environ. Microbiol.*, **2002**, *68,* 4283-4291
74. J.E. Ugalde, A.J. Parodi, R.A. Ugalde, *Proc. Natl. Acad. Sci. U. S. A.*, **2003**, *100,* 10659-10663
75. S.G. Ball, M.K. Morell, *Annual Review of Plant Biology*, **2003**, *54,* 207-233
76. S.G. Ball, M.H.B.J. van de Wal, R.G.F. Visser, *Trends in Plant Science*, **1998**, *3,* 462-467
77. H.P. Guan, P.L. Keeling, *Trends in Glycoscience and Glycotechnology*, **1998**, *10,* 307-319
78. A. Buléon, P. Colonna, V. Planchot, S. Ball, *International Journal of Biological Macromolecules*, **1998**, *23,* 85-112
79. W.J. Whelan, J.M. Bailey, *Biochem. J.*, **1954**, *58,* 560-569
80. L. Iwanoff, *Ber. d. Deutch. bot. Ges.*, **1902**, *20,* 366
81. W. Zaleski, *Ber. d. Deutch. bot. Ges.*, **1906**, *24,* 285
82. W. Zaleski, *Ber. d. Deutch. bot. Ges.*, **1911**, *29,* 146
83. U. Suzuki, K. Yoshimura, M. Takaishi, *Tokyo Kagaku Kaishi*, **1906**, *27*
84. J. Bodnár, *Biochem. Z.*, **1925**, *165,* 1-15
85. G.T. Cori, C.F. Cori, *J. Biol. Chem.*, **1936**, *116,* 129-132
86. G.T. Cori, C.F. Cori, *J. Biol. Chem.*, **1936**, *116,* 119-128
87. C.F. Cori, S.P. Colowick, G.T. Cori, *J. Biol. Chem.*, **1937**, *121,* 465-477
88. G.T. Cori, C.F. Cori, *Proc. Soc. Exp. Biol. Med.*, **1937**, *36,* 119
89. W. Kiessling, *Biochem. Z.*, **1938**, *298,* 421
90. M.L. Wolfrom, D.E. Pletcher, *J. Am. Chem. Soc.*, **1941**, *63,* 1050-1053
91. T. Fukui, S. Shimomura, K. Nakano, *Mol. Cell. Biochem.*, **1982**, *42,* 129-144
92. Y.P. Lee, *Biochim. Biophys. Acta*, **1960**, *43,* 18-24
93. S.H. Goldemberg, *Biochim. Biophys. Acta*, **1962**, *56,* 357-&
94. K.N. Shivaram, *Zeitschrift for Naturforschung. section C*, **1976**, *31C,* 424-431
95. A. Schäfner, H. Specht, *Naturwissenschaften*, **1938**, *26,* 494
96. W. Kiessling, *Naturwissenschaften*, **1939**, *27*
97. W. Kiessling, *Biochem. Z.*, **1939**, *302,* 50
98. C.F. Cori, G. Schmidt, G.T. Cori, *Science*, **1939**, *89*
99. C.S. Hanes, *Proc. Roy. Soc. B*, **1940**, *128,* 421-450
100. C.S. Hanes, *Proc. Roy. Soc. B*, **1940**, *129,* 174-208
101. P. Ostern, E. Holmes, *Nature*, **1939**, *144,* 34
102. G.T. Cori, C.F. Cori, G. Schmidt, *J. Biol. Chem.*, **1939**, *129,* 629-639
103. P. Ostern, D. Herbert, E. Holmes, *Biochem. J.*, **1939**, *33*

104. G. Ziegast, B. Pfannemüller, *Die Makromolekulare Chemie*, **1984**, *185,* 1855-1866
105. W.N. Emmerling, B. Pfannemüller, *Starch*, **1981**, *33,* 202-208
106. G. Ziegast, B. Pfannemüller, *Macromol. Rapid. Comm.*, **1984**, *5,* 373-379
107. W.N. Emmerling, B. Pfannemüller, *Makromol. Chem.*, **1983**, *184,* 1441-1458
108. W.N. Emmerling, B. Pfannemüller, *Makromolekulare Chemie-Macromolecular Chemistry and Physics*, **1978**, *179,* 1627-1633
109. www.cazy.org
110. B.L. Cantarel, P.M. Coutinho, C. Rancurel, T. Bernard, V. Lombard, B. Henrissat, *Nucleic Acids Res.*, **2009**, *37,* D233-D238
111. S.B. Darling, *Progress in Polymer Science*, **2007**, *32,* 1152-1204
112. M. Palomo, T. Pijning, T. Booiman, J. Dobruchowska, J. van der Vlist, S. Kralj, A. Planas, J.P. Kamerling, B.W. Dijkstra, M.J.E.C. van der Maarel, L. Dijkhuizen, H. Leemhuis, *J. Biol. Chem.*, **2010**
113. H.L. Griffin, Y.V. Wu, *Biochemistry*, **1968**, *7,* 3063-3072
114. H.L. Griffin, Y.V. Wu, *Biochemistry*, **1971**, *10,* 4330-4335
115. G.H. Vos-Scheperkeuter, J.G. de Wit, A.S. Ponstein, W.J. Feenstra, B. Witholt, *Plant Physiol.*, **1989**, *90,* 75-84
116. A.S. Ponstein, G.H. Vos-Scheperkeuter, W.J. Feenstra, B. Witholt, *Food Hydrocolloids*, **1987**, *1,* 497-498
117. G.H. Vos-Scheperkeuter, A.S. Ponstein, J.G. de Wit, W.J. Feenstra, G.T. Oostergetel, E.F.J. van Bruggen, B. Witholt, *Food Hydrocolloids*, **1987**, *1,* 387-391
118. C.D. Boyer, J. Preiss, *Carbohydr. Res.*, **1978**, *61,* 321-334
119. R.A. Pisigan, E.J. del Rosario, *Phytochemistry*, **1976**, *15,* 71-73
120. J.L. Ozbun, J.S. Hawker, E. Greenberg, C. Lammel, J. Preiss, E.Y.C. Lee, *Plant Physiol.*, **1973**, *51,* 1-5
121. D. Boyer, B. Fisher, *Phytochemistry*, **1984**, *23,* 737
122. D.J. Manners, *Carbohydr. Polym.*, **1989**, *11,* 87-112
123. C.D. Boyer, J. Preiss, *Plant Physiol.*, **1981**, *67,* 1141-1145
124. G.L. Matters, C.D. Boyer, *Phytochemistry*, **1981**, *20,* 1805-1809
125. J.L. Ozbun, J.S. Hawker, J. Preiss, *Biochem. J.*, **1972**, *126,* 953-&
126. J.S. Hawker, J.L. Ozbun, H. Ozaki, E. Greenberg, J. Preiss, *Arch. Biochem. Biophys.*, **1974**, *160,* 530-551
127. B.I. Brown and D.H. Brown. In *Complex Carbohydrates*, 395-403, E.F. Neufeld, V. Ginsberg, Academic Press, **1966**
128. C. Boyer, J. Preiss, *Biochemistry*, **1977**, *16,* 3693-3699
129. K. Kawaguchi, J. Fox, E. Holmes, C. Boyer, J. Preiss, *Arch. Biochem. Biophys.*, **1978**, *190,* 385-397
130. J. Larner. In *Methods in Enzymology*, 222-225, Academic Press, **1955**
131. W.N. Haworth, S. Peat, E.J. Bourne, *Nature*, **1944**, *154,* 236
132. D. Borovsky, E.E. Smith, W.J. Whelan, *Eur. J. Biochem.*, **1976**, *62,* 307-312
133. H. Takata, T. Takaha, S. Okada, M. Takagi, T. Imanaka, *J. Bacteriol.*, **1996**, *178,* 1600-1606
134. H. Takata, K. Ohdan, T. Takaha, T. Kuriki, S. Okada, *The Japanese Society of Applied Glycoscience*, **2003**, *50,* 15-20
135. L. Andersson, R. Andersson, R.E. Andersson, U. Rydberg, H. Larsson, P. Åman, *Carbohydr. Polym.*, **2002**, *50,* 249-257

136. Y. Takeda, H. Guan, J. Preiss, *Carbohydr. Res.*, **1993**, *240,* 253-263
137. H. Guan, T. Kuriki, M. Sivak, J. Preiss, *Plant Biology*, **1995**, *92,* 964-967
138. M.C. Abad, K. Binderup, J. Rios-Steiner, R.K. Arni, J. Preiss, J.H. Geiger, *J. Biol. Chem.*, **2002**, *277,* 42164-42170
139. H. Takata, T. Takaha, T. Kuriki, S. Okada, M. Takagi, T. Imanaka, *Appl. Environ. Microbiol.*, **1994**, *60,* 3096-3104
140. M.J.E.C. van der Maarel, A. Vos, P. Sanders, L. Dijkhuizen, *Biocatal. Biotransform.*, **2003**, *21,* 199-207
141. E.J. Kim, S.I. Ryu, H.A. Bae, N.T. Huong, S.B. Lee, *Food Chem.*, **2008**, *110,* 979-984
142. M. Palomo Reixach, S. Kralj, M.J.E.C. van der Maarel, L. Dijkhuizen, *Appl. Environ. Microbiol.*, **2009**, *75*
143. G.T. Cori, C.F. Cori, *J. Biol. Chem.*, **1943**, *151,* 57-63
144. W. Praznik, G. Rammesmayer, T. Spies, *Carbohydr. Res.*, **1992**, *227,* 171-182
145. C. Boyer, J. Preiss, *Biochemistry*, **1977**, *16,* 3693-3699
146. D. Borovsky, E.E. Smith, W.J. Whelan, *Eur. J. Biochem.*, **1975**, *59,* 615-625
147. H. Waldmann, D. Gygax, M.D. Bednarski, W.R. Shangraw, G.M. Whitesides, *Carbohydr. Res.*, **1986**, *157,* C4-C7
148. M. Yanase, T. Takaha, T. Kuriki, *J. Sci. Food. Agric.*, **2006**, *86,* 1631-1635
149. W. Goldner, H. Beevers, *Phytochemistry*, **1989**, *28,* 1809-1812
150. P.L. Dang, C.D. Boyer, *Phytochemistry*, **1988**, *27,* 1255-1259
151. A. Matsumoto, T. Nakajima, K. Matsuda, *Journal of Biochemistry*, **1990**, *107,* 118-122
152. A. Matsumoto, T. Nakajima, K. Matsuda, *Journal of Biochemistry*, **1990**, *107,* 123-126
153. H. Staudinger, E. Husemann, *Annalen der Chemie*, **1937**, *527,* 195-236
154. K.H. Meyer, M. Wertheim, P. Bernfeld, *Helv. Chim. Acta*, **1940**, *23,* 865-875
155. K.H. Meyer, P. Bernfeld, *Helv. Chim. Acta*, **1940**, *23,* 875-885
156. Y.H. Kim, O.W. Webser, *Polym. Prepr. (Am. Chem. Soc. , Div. Polym. Chem.)*, **1988**, *29,* 310-311
157. Y.H. Kim, O.W. Webster, *J. Am. Chem. Soc.*, **1990**, *112,* 4592-4593
158. M. Baron, K.H. Hellwich, M. Hess, K. Horie, A.D. Jenkins, R.G. Jones, J. Kahovec, P. Kratochvil, W.V. Metanomski, W. Mormann, R.F.T. Stepto, J. Vohlidal, E.S. Wilks, *Pure Appl. Chem.*, **2009**, *81,* 1131-1183
159. P.J. Flory, *J. Am. Chem. Soc.*, **1952**, *74,* 2718-2723
160. C.J. Hawker, R. Lee, J.M.J. Frechet, *J. Am. Chem. Soc.*, **2002**, *113,* 4583-4588
161. D. Holter, A. Burgath, H. Frey, *Acta Polym.*, **1997**, *48,* 30-35
162. F.M. Veronese, B. Sacca, P.P. de Laureto, M. Sergi, P. Caliceti, O. Schiavon, P. Orsolini, *Bioconjugate Chem.*, **2001**, *12,* 62-70
163. F.M. Veronese, *Biomaterials*, **2001**, *22,* 405-417
164. A.J. Dirks, R.J.M. Nolte, J.J.L.M. Cornelissen, *Advanced Materials*, **2008**, *20,* 3953-3957
165. F.E. Alemdaroglu, A. Herrmann, *Organic & Biomolecular Chemistry*, **2007**, *5,* 1311-1320
166. F.M. Veronese, C. Mammucari, F. Schiavon, O. Schiavon, S. Lora, F. Secundo, A. Chilin, A. Guiotto, *Farmaco*, **2001**, *56,* 541-547
167. R. Duncan, *Nature Reviews Drug Discovery*, **2003**, *2,* 347-360

168. D.S. Goodsell, *Bionanotechnology: Lessons from nature*, Wiley, **2004**
169. C.M. Niemeyer and C.A. Mirkin, *Nanobiotechnology, Concepts, Applications and Perspectives*, Wiley, **2004**
170. W.T.E. Bosker, K. Ágoston, M.A. Cohen Stuart, W. Norde, J.W. Timmermans, T.M. Slaghek, *Macromolecules*, **2003**, *36,* 1982-1987
171. C. Houga, J. Giermanska, S. Lecommandoux, R. Borsali, D. Taton, Y. Gnanou, J.F. Le Meins, *Biomacromolecules*, **2009**, *10,* 32-40
172. O.S. Hernandez, G.M. Soliman, F.M. Winnik, *Polymer*, **2007**, *48,* 921-930
173. C. Houga, J.F. Le Meins, R. Borsali, D. Taton, Y. Gnanou, *Chemical Communications*, **2007***,* 3063-3065
174. C. Schatz, S. Louguet, J.F. Le Meins, S. Lecommandoux, *Angew. Chem. -Int. Edit.*, **2009**, *48,* 2572-2575
175. K.K. Upadhyay, J.F. Le Meins, A. Misra, P. Voisin, V. Bouchaud, E. Ibarboure, C. Schatz, S. Lecommandoux, *Biomacromolecules*, **2009**, *10,* 2802-2808
176. Y.L. Yang, K. Kataoka, F.M. Winnik, *Macromolecules*, **2005**, *38,* 2043-2046
177. K. Loos, A. Böker, H. Zettl, A.F. Zhang, G. Krausch, A.H.E. Müller, *Macromolecules*, **2005**, *38,* 873-879
178. K. Loos, A.H.E. Müller, *Biomacromolecules*, **2002**, *3,* 368-373
179. K. Loos, R. Stadler, *Macromolecules*, **1997**, *30,* 7641-7643
180. I. Otsuka, K. Fuchise, S. Halila, S. Fort, K. Aissou, I. Pignot-Paintrand, Y.G. Chen, A. Narumi, T. Kakuchi, R. Borsali, *Langmuir*, **2010**, *26,* 2325-2332
181. A. Narumi, Y. Miura, I. Otsuka, S. Yamane, Y. Kitajyo, T. Satoh, A. Hirao, N. Kaneko, H. Kaga, T. Kakuchi, *Journal of Polymer Science Part A-Polymer Chemistry*, **2006**, *44,* 4864-4879
182. A. Narumi, T. Kakuchi, *Polymer Journal*, **2008**, *40,* 383-397
183. K. Aoi, K. Itoh, M. Okada, *Macromolecules*, **1995**, *28,* 5391-5393
184. H. Kaga, S. Yamane, A. Narumi, T. Satoh, T. Kakuchi, *Macromolecular Symposia*, **2004**, *217,* 29-38
185. A. Narumi, S. Yamane, Y. Miura, H. Kaga, T. Satoh, T. Kakuchi, *Journal of Polymer Science Part A-Polymer Chemistry*, **2005**, *43,* 4373-4381
186. V. Ladmiral, E. Melia, D.M. Haddleton, *Eur. Polym. J.*, **2004**, *40,* 431-449
187. S.R.S. Ting, E.H. Min, P. Escalé, M. Save, L. Billon, M.H. Stenzel, *Macromolecules*, **2009**
188. D. Appelhans, H. Komber, M.A. Quadir, S. Richter, S. Schwarz, J. van der Vlist, A. Aigner, M. Müller, K. Loos, J. Seidel, K.F. Arndt, R. Haag, B. Voit, *Biomacromolecules*, **2009**, *10,* 1114-1124
189. H.C. Kolb, M.G. Finn, K.B. Sharpless, *Angew. Chem. -Int. Edit.*, **2001**, *40,* 2004
190. R. Huisgen, *Proceedings of the Chemical Society of London*, **1961***,* 357
191. S. Hotha, S. Kashyap, *J. Org. Chem.*, **2006**, *71,* 364-367
192. N. Xu, R. Wang, F.S. Du, Z.C. Li, *Journal of Polymer Science Part A-Polymer Chemistry*, **2009**, *47,* 3583-3594
193. W.H. Binder, R. Sachsenhofer, *Macromolecular Rapid Communications*, **2007**, *28,* 15-54
194. P. Wu, M. Malkoch, J.N. Hunt, R. Vestberg, E. Kaltgrad, M.G. Finn, V.V. Fokin, K.B. Sharpless, C.J. Hawker, *Chemical Communications*, **2005***,* 5775-5777
195. K. Loos, V. von Braunmühl, R. Stadler, *Macromol. Rapid. Comm.*, **1997**, *18,* 927-938

196. S.P. Massia, J. Stark, D.S. Letbetter, *Biomaterials*, **2000**, *21,* 2253-2261
197. L.M. Likhosherstov, O.S. Novikova, V.A. Derevitskaja, N.K. Kochetkov, *Carbohydr. Res.*, **1986**, *146,* C1-C5
198. C.F. Lane, *Synthesis-Stuttgart*, **1975***,* 135-146
199. R.F. Borch, M.D. Bernstei, H.D. Durst, *J. Am. Chem. Soc.*, **1971**, *93,* 2897-&
200. M. Yalpani, D.E. Brooks, *Journal of Polymer Science Part A-Polymer Chemistry*, **1985**, *23,* 1395-1405

CHAPTER 2

Synthesis of hyperbranched polysaccharides

SUMMARY

An enzymatic tandem reaction is described in which the enzymes phosphorylase and *Deinococcus geothermalis* glycogen branching enzyme (GBE_{DG}) catalyze the synthesis of branched polyglucans from maltoheptaose. Phosphorylase consumes glucose-1-phosphate (G-1-P) and polymerizes linear polyglucans while GBE_{DG} introduces branch points *in situ* on $\alpha(1\rightarrow6)$ positions by reshuffling short terminal oligosaccharides. The resulting hyperbranched polyglucans were analyzed via methylation analysis and a chemo enzymatic assay (involving the anthrone assay, BCA assay and the debranching assay with isoamylase). MALDI-ToF and ^{1}H-NMR were used to confirm the linkage pattern and the degree of branching.

2.1 INTRODUCTION

Polysaccharides fulfil in nature multiple functions. Cellulose fibres function as structural material in wood, starch is the energy storage molecule of plants and the chitin exoskeleton of insects protects the animal's body. These polysaccharides are high molecular weight and stereo regular biopolymers. These special properties are difficult to control with conventional polymer chemistry and hence most glycoscience is based on modifying existing polysaccharides rather than synthesizing them. In this chapter, a method is described to synthesize a polysaccharide from scratch. To obtain the above described properties enzymes are used (just like in nature) for the construction (see FIGURE 1.12).

All starting materials, biocatalysts and products as shown in this chapter can be derived from potatoes, illustrating the versatility of the potato as a renewable resource:

- Phosphorylase, in this research isolated from potato tubers, is the key enzyme of the polymerizations as shown in this chapter.
- The branching enzyme or Q-enzyme was first discovered in potato juice[1] and is responsible for the branched character of the amylopectin component in potato starch.
- In industry, cyclodextrins are enzymatically produced from potato starch. Cyclodextrin glycosyltransferase (CGTase; EC 2.4.1.19) is employed to obtain a mixture of α-, β-, and γ-cyclodextrins[2]. In this research, cyclodextrins are converted to maltoheptaose and used as a primer.
- The monomer used, glucose-1-phosphate (G-1-P and also known as Cori ester), was first found in frogs by Cori and Cori[3], but can also be isolated from potatoes[4] and plays a role in energy metabolism of plant and animal.
- Amylose and amylopectin are the main components of potato tubers. The structures as synthesized in this chapter are their synthetic analogues.

2.1.1 Synthesis of maltoheptaose

Linear $\alpha(1\rightarrow4)$ linked glucose residues, with a minimal length of three residues, are suitable as a primer site for the phosphorylase catalyzed polymerization. However, the reaction velocity differs significantly if the polymerization is primed with short primers[5-7], resulting in a broad molecular weight distribution[8]. Therefore, the synthesis of a monodisperse primer is of the utmost importance for the production of materials of uniform length.

The enzymatic and/or acid catalyzed hydrolysis of starch results in a mixture of different lengths of oligosaccharides that are capable of priming the reaction. The purification is, however, difficult. This method is therefore not suitable for our purposes, as broad molecular weight distributions, after enzymatic polymerization, are the most likely result.

However, the acid catalyzed hydrolysis of cyclodextrins results in monodisperse oligosaccharides (see FIGURE 2.1). Here we use a 7-membered cyclic dextrin, β-cyclodextrin, to obtain a linear primer of 7 glucose residues (maltoheptaose).

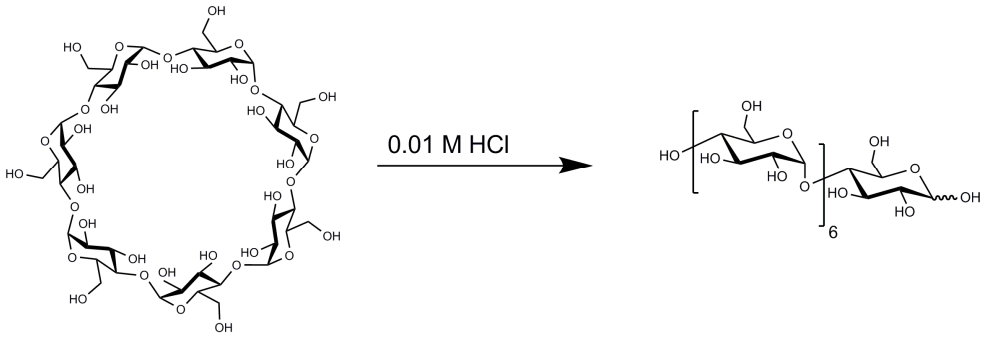

FIGURE 2.1: Acid catalyzed hydrolysis of β-cyclodextrin.

A concentrated solution of β-cyclodextrin was heated for 2 hours at reflux temperature in a diluted hydrochloric acid system. The glycosidic bonds were randomly cleaved from which about 10 % underwent a single cleavage resulting in maltoheptaose. A minor part had more than a single cleavage resulting in smaller oligosaccharides and about 90 % of the β-cyclodextrin is not cleaved at all. Unwanted smaller oligosaccharides were removed by precipitation in cold absolute ethanol. Maltoheptaose precipitates while the shorter oligosaccharides dissolve in small concentrations. The unreacted β-cyclodextrin can be removed by complexing the β-cyclodextrin with *p*-xylene. *P*-xylene fits in the hydrophobic interior of the cyclodextrin and forms an inclusion complex that is insoluble in water. The precipitated β-cyclodextrin complex can be re-used after thoroughly rinsing with water. The complete removal of β-cyclodextrin is of the utmost importance since it inhibits the phosphorylase enzyme in subsequent reactions[9]. The purity of the primer was checked with ^{1}H-NMR and MALDI-ToF.

A more efficient way to produce a monodisperse primer out of cyclodextrins is with the use of the enzyme cyclodextrinase. Cyclodextrinase from *K. oxytoca* converts 50 % from the cyclic form to the linear form[10]. However, the commercial availability of this enzyme is limited.

2.1.2 Isolation of potato phosphorylase

As mentioned before, potato tubers are a rich source of phosphorylase. This, together with the availability and the ease of isolation from the tubers makes the potato the ideal source of phosphorylase.

The isolation of phosphorylase starts with the disintegration of peeled potatoes, first with a kitchen blender and after that with an ultra-turrax blender. Sodium bisulfite was added as an anti-oxidant to prevent blackening of the potato slurry[11]. Phenol oxidases, in high concentrations present just below the skin of the potato, catalyze the oxidation of proteins inducing a blackening of the potato slurry and provoking a reduced enzyme activity[12]. The potato slurry was pressed through a kitchen towel and the solids were discarded. The remaining potato juice was a mixture of proteins, water soluble components and enzymes, including α-amylase. α-amylase is able to hydrolyze glycosidic $\alpha(1\rightarrow4)$ linkages and depolymerizes amylose. Removal of α-amylase is therefore necessary and can be done with a heat treatment at 55.5 °C. The α-amylase denaturates at this temperature and can be removed via centrifugation and/or filtration.

To isolate the phosphorylase enzyme from the potato juice, ammonium sulfate precipitation was used. Ammonium sulfate precipitation is the specific use of a salting-out technique in which the ionic strength of the solution is increased by the addition of ammonium sulfate. Enzymes precipitate at different salt concentrations making it possible to isolate phosphorylase. First, an ammonium sulfate concentration was chosen in which all unwanted enzymes precipitate. After removing the precipitate, the phosphorylase was salted-out and re-suspended in a citric acid buffer.

This enzyme suspension is already suitable for enzyme catalyzed polymerizations. Further purification results in a more pure phosphorylase suspension. Dialysis was in this research used to remove ammonium sulfate and an ultra filtration membrane was used to remove all components with molecular weights smaller than 100 kDa and to concentrate the solution.

SPECTROSCOPIC PHOSPHATE DETERMINATION

The phosphorylase catalyzed reaction can be followed by UV-spectroscopy. Since this reaction yields one inorganic phosphate (P_i) per cycle, a quantitatively spectroscopic determination of the [P_i] gives information about the amount of consumed G-1-P. Therefore, the molecular weight of the amylose chains produced can be calculated at any time of the reaction.

Fiske and Subbarow[13] developed a spectroscopic method to measure the [P_i] in blood and urine. The method is based on the formation of a blue phosphate molybdate complex that is reduced by a reducing agent to form phosphomolybdic acid. Phosphomolybdic acid is much more readily reduced to blue molybdous compounds than molybdic acid itself. However, the rather low pH that is used makes this method not directly suitable for the measurement of [P_i] in systems with labile phosphate esters like G-1-P as the esters will hydrolyze during the measurement[14]. With the addition of acetate buffer, the pH can be increased to pH 4-4.2. Under these conditions, the labile G-1-P is much more stable and will not contribute to the inorganic phosphate measurement.

2.1.3 Structural analysis of branched α-glucans

In order to resolve the linkage pattern of the branched α-glucans both chemical and enzyme based techniques are used. These techniques together with ^{1}H-NMR and MALDI-ToF provide information about the linkage pattern, average branch length, branch length distribution, number of non-reducing groups and the average degree of branching.

METHYLATION ANALYSIS

Methylation is a technique in which the free hydroxy groups of the polysaccharide are fully methylated. The methylated polysaccharides are subsequently cleaved by an acid catalyzed hydrolysis into the corresponding methylated monosaccharides. In the next two steps, the C1 hydroxy group is reduced to prevent ring closure and the remaining hydroxy groups are acetylated. The acetyl groups mark the original linkage position of the polysaccharide and give information about the linkage pattern (see FIGURE 2.2). The resulting partially methylated alditol acetates (PMAA's) were analyzed by GC-FID analysis and identified by retention time.

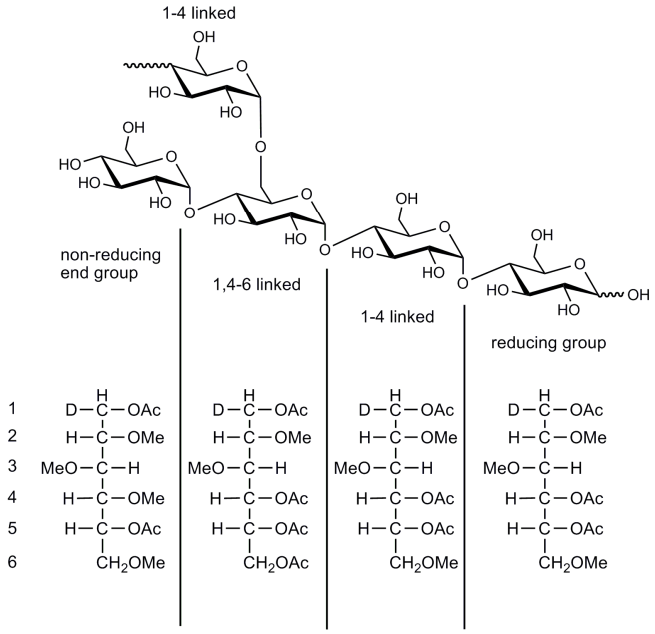

FIGURE 2.2: Fragment of a branched polysaccharide and the corresponding partially methylated alditol acetates. The acetyl groups mark the original linking position while the methyl groups mark the originally free hydroxy groups.

STRUCTURAL ANALYSIS VIA CHEMO ENZYMATIC WAYS

With a combination of methods, which rely on enzymatic or chemical assays, different glucose residues that are connected differently can be identified in a polysaccharide in order to elucidate the linking pattern and structure (see TABLE 2.1 and FIGURE 2.3).

TABLE 2.1: Enzymatic and chemical assays used for the structural analysis of polysaccharides.

Groups	abbreviation	Assay
Reducing groups	[red. groups]	2,2'-bicinchoninic acid (BCA)
Non-reducing end groups	[non. red. end groups]	Rapid Smith degradation (RSD)
Glucose residues	[glc. residues]	Anthrone

The degree of branching can be calculated when both the amount of non-reducing end groups (non. red. end groups) and reducing groups (red. groups) is known, together with the total amount of glucose residues (see EQUATION 2.1).

$$\text{degree of branching (\%)} = \frac{[\text{non.red. end groups}] - [\text{red. groups}]}{[\text{glc. residues}]} \qquad 2.1$$

With the Rapid Smith Degradation (RSD; oxidation with periodate, reduction with sodium borohydride and hydrolysis with sulphuric acid), the number of non-reducing end groups can be determined. The RSD assay produces glycerol from the non-reducing terminal groups of α-glucans and erythritol from the remaining glucose residues. Subsequently, the concentration of glycerol can be measured with a glycerol kinase assay[15]. It is important to prepare G-1-P free samples for the RSD assay as residual G-1-P is also converted to glycerol.

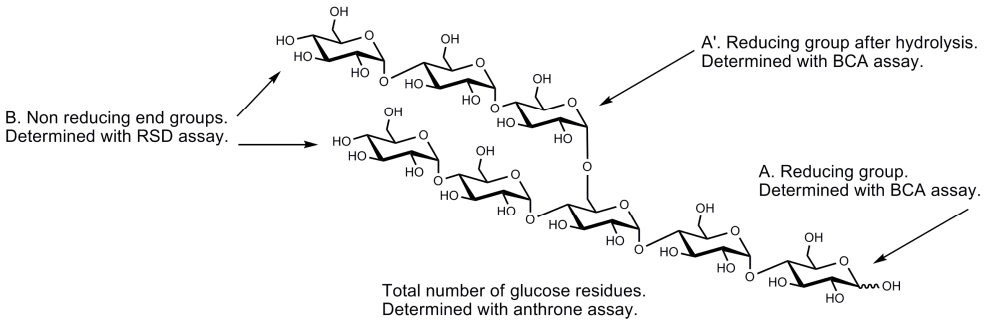

FIGURE 2.3: BCA assay, RDD assay and anthrone assay.

The amount of reducing groups can be assayed via the BCA method. In this assay, a copper ion (Cu^{2+}) is reduced by the reducing end of the carbohydrate. The reduced copper ion (Cu^{+}) forms a deep-blue complex with BCA and can be quantified with UV-VIS measurements. If the BCA assay is used before ([A]) and after ([A']) the specific hydrolysis of the α(1→6) glycosidic linkages, the amount of side chains can be calculated. α(1→6) Glycosidic linkages can be hydrolyzed by the enzyme isoamylase or pullulanase.

After the specific hydrolysis of branched polysaccharides, more reducing groups become available and hence colour development is more pronounced. When the BCA assay is performed *before* and *after* the specific hydrolysis of the α(1→6) linkages, the degree of branching can even be calculated without performing the RSD assay (see EQUATION 2.2).

The amount of glucose residues can be determined with the anthrone assay. The assay is based on the dehydration of glucose residues to furfural derivatives, e.g. hydroxymethylfurfural. Furfural derivatives react with anthrone to form a green-blue colour that can be quantified with UV-VIS measurements.

$$\text{degree of branching}\,(\%) = \frac{[A'] - [A]}{[\text{glc. residues}]} \cdot 100\% \qquad 2.2$$

DETERMINATION OF THE DEGREE OF BRANCHING WITH ^{1}H-NMR

The area below signals in a ^{1}H-NMR spectrum are proportional to the amount of protons responsible for the signal, and can be used to obtain quantitative information about the structure of the material. The ratio of the α/β anomers, the degree of polymerization, degree of branching and the average branch length of polysaccharides can be quantitatively determined[16]. Only good resolved and isolated signals with a high signal to noise ratio give accurate information and can be integrated.

TABLE 2.2: Chemical shift of the anomeric protons of maltoheptaose and the position of the H1(1→4,6) linkage of a branched glucan (^{1}H-NMR, 300 MHz, D_2O).

	Group	Chemical shift (ppm)[17]
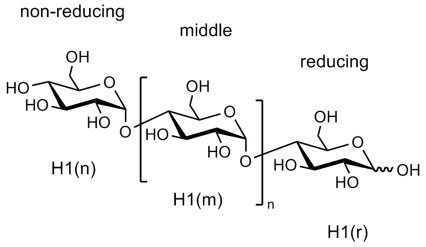	H1(r)α	5.23
	H1(r)β	4.65
	H1(m)	5.38
	H1(n)	5.33
	H1(1→4,6)	5.00

The anomeric protons of an α-D-glucose residue appear as isolated and good resolved signals between 4.0 and 5.5 ppm and meet the above described criteria (see FIGURE 2.4). The other protons of an α-D-glucose residue appear in the range of 3.2 to 3.9 ppm as a complex series of overlapping signals. In the case of an amylose chain or a branched amylose chain, anomeric protons are present in the non-reducing end group (H1(n)), the reducing group (H1(r)), glucose residues in the middle of a chain (H1(m)) and glucose residues at intersection points (H1(1→4,6)). All anomeric protons give signals at different chemical shifts due to small differences in chemical environment. TABLE 2.2 gives an overview of the chemical shift (expressed in ppm) of the different anomeric protons of a branched amylose.

The anomeric proton of α(1→4,6) linked sugar residues can be used to determine the amount of branch points while the anomeric proton of internal linked α-D-

glucose residues together with the non-reducing anomeric proton can be used to determine the total amount of glucose residues. The ratio of the surfaces below the signals gives the degree of branching, as follows from EQUATION 2.3.

$$\text{Degree of branching} = \frac{\text{H1}(1,4 \rightarrow 6)}{\text{H1(m)} + \text{H1(n)} + \text{H1}(1,4 \rightarrow 6)} \cdot 100\% \qquad 2.3$$

To enhance the ^{1}H- spectrum (see FIGURE 2.4) several precautions were taken:

- Hydroxy protons from the sugar residues were exchanged with deuterium in order to minimize interference in the ^{1}H-NMR measurement.
- The probe was tuned for each sample to ensure optimal signal-to-noise ratio (S/N).
- Measurements were done at 50 °C.
- HOD signal was pre-saturated before each measurement.
- The delay between pulses was 10 seconds to ensure complete relaxation. This is more than 5 times the slowest relaxing proton of a sugar residue (T_1 H4(n) <2.0 s[18]).

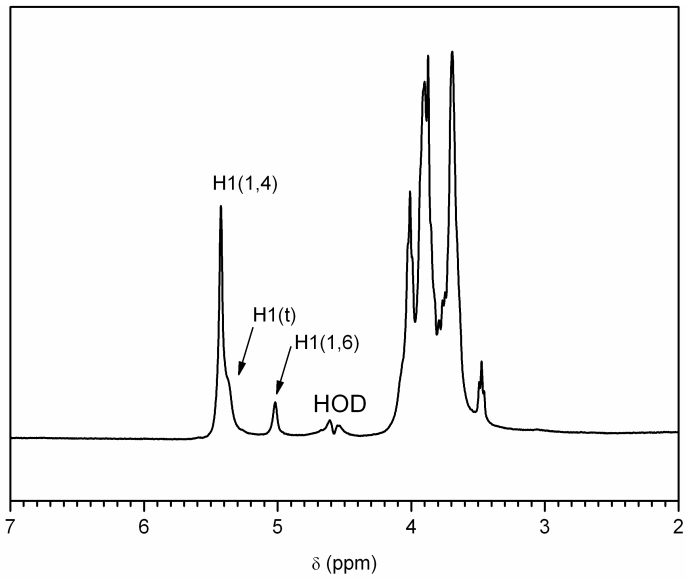

FIGURE 2.4: ^{1}H-NMR spectrum of a branched polysaccharide measured in D_2O at 50 °C. The HOD signal is visible as a small bump due to the pre-saturation.

2.2 EXPERIMENTAL

2.2.1 Materials and chemicals

β-Cyclodextrin hydrate (Fluka), α-D-glucose-1-phosphate disodium salt hydrate (Sigma), 3-(N-morpholino) propanesulfonic acid (MOPS, Sigma), tri sodium citrate (Merck) , ammoniummolybdate (Fluka), potassiumpyrosulfite (Fluka), sodium sulfite (Fluka), metol (Fluka), anthrone (Fluka), 2,2'-bicinchoninic acid (BCA, Fluka), ammonium sulfate (Merck), sodium bisulfite (Acros), *p*-xylene (Merck) and isoamylase (Aldrich) where used as received. Potatoes were bought at the local grossery. Starch V was a donation of Avebe (Foxhol, Groningen). Glycogen branching enzyme from *Deinococcus geothermalis* (GBE_{DG}) was kindly provided by M. Palomo Reixach, M.J.E.C. van der Maarel and L. Dijkhuizen from the Center for Carbohydrate Bioprocessing.

2.2.2 Analysis and equipment

UV-SPECTROSCOPY

UV-spectroscopy measurements were performed on a PYE Unicam SP8-200 UV/VIS spectrophotometer.

^{1}H-NMR SPECTROSCOPY

^{1}H-NMR spectra were recorded on a Varian VXR spectrometer operating at 300 or 400 MHz at ambient temperatures. Dimethyl-2-silapentane-5-sulfonic acid (DSS) was used as an external reference.

^{1}H-NMR spectra used for the determination of the degree of branching were recorded on a Varian Inova 500 MHz spectrometer at 50 °C with pre-saturation of the HOD resonance. 2,2-Dimethyl-2-silapentane-5-sulfonic acid (DSS) was used as an external reference. Complete relaxation of the protons was ensured by taking a 10 second pause between pulses.

INFRARED SPECTROSCOPY

ATR infrared spectra were recorded on a Bruker IFS88 spectrometer equipped with a MCT-A detector at a resolution of 4 cm^{-1} using an average of 50 scans for sample and reference.

MALDI-TOF

MALDI-ToF MS measurements were performed on a Voyager-DE PRO spectrometer in linear (positive ion) mode with 2,5-dihydroxybenzoic acid (DHB) as a matrix. The matrix solution was made by dissolving DHB (0.2 M) in a 1:1 v/v water/acetonitrile solution. Analyte solution was made by dissolving the product in water R.O. (4 $mg \cdot mL^{-1}$). Matrix and analyte were mixed in 1:1 v/v ratio. 5 µL of this mixture was deposited on the target and dried *in vacuo* at 40 °C.

GAS CHROMATOGRAPHY

GC-FID was performed with a RTX 5 Sil MS column (30 m x0.25 mm, Restek) using a temperature program (2 min isothermal at 140 °C, then heated to 260 °C with 8 °C/min)[19].

ISOLATION AND PURIFICATION OF POTATO PHOSPHORYLASE

2.5 kg potatoes were peeled, cleaned and shredded with a kitchen blender. 100 mL citrate buffer (pH 6.2, 50 mM, 0.02% NaN_3) and 500 ppm sodiumbisulfite were added to the potato slurry. All of the following preparations were performed while cooling in an ice bath if not otherwise stated. All centrifugation steps were done at 7500 rpm at 4 °C for 20 min. The potato slurry was mixed and disintegrated with an ultra-turrax for 10 min at 7000 rpm and pressed through a kitchen towel. The resulting potato juice was centrifuged to remove the remaining solids. The supernatant was heated to 55.5 °C for 40 min to denature the α-amylase. The potato juice was cooled, ammonium sulfate ($100\ g \cdot L^{-1}$) was added, and the mixture was stirred for 30 min. The potato juice was centrifuged and the solids were discarded. The supernatant was saturated with ammonium sulfate ($250\ g \cdot L^{-1}$) and stirred for 30 min. The precipitated phosphorylase was isolated by means of centrifugation. The phosphorylase was suspended in 200 mL citrate buffer and ammonium sulfate was added ($50\ g \cdot L^{-1}$). This mixture was stirred for 30 min. The phosphorylase suspension was centrifuged and the residue was re-suspended in citrate buffer (pH 6.2, 50 mM, 0.02 % NaN_3). The phosphorylase suspension was dialyzed against citrate buffer (pH 6.2, 50 mM, 0.02% NaN_3) and was concentrated with a stirred Amicon cell equipped with a Millipore ultra filtration membrane (100 kDA).

CLONING, EXPRESSION AND PURIFICATION OF THE GLYCOGEN BRANCHING ENZYME

Over expression of GBE_{DG} was achieved by overnight growth of *E. coli* BL21(DE3) Star cells containing the corresponding plasmid at 37 °C and 210 rpm in Luria-Bertani medium supplemented with 50 μg·mL^{-1} ampicillin. The cells were harvested by centrifugation (10 min at 10,000 x g). The pellets were re-suspended in 50 mM sodium phosphate buffer, pH 8.0, and the cells were disrupted by sonication (7 times for 15 s at 7 μm with 30 s intervals) and centrifuged (30 min at 15,000 x g).The enzyme was found as a soluble protein in the supernatant and purified by His tag affinity chromatography using a HiTrap chelating column (Amersham Parmacia, Uppsala, Sweden) charged with nickel sulfate. The enzyme was eluted with a linear gradient of 0 to 500 mM imidazol on an Åkta prime purification system (Amersham Pharmacia). Fractions containing the enzyme were pooled and dialyzed against sodium phosphate buffer (25 mM, pH 8.0).

ACTIVITY ASSAY PHOSPHORYLASE

150.4 mg (400 μmol) glucose-1-phosphate and 4.54 mg (4 μmol) maltoheptaose were dissolved in 3 mL citrate buffer (pH 6.2, 50 mM, 0.02% NaN_3). The pH was re-adjusted to pH 6.2, filled to 3.9 mL and heated to 37 °C. 100 μL Phosphorylase suspension was added and mixed. Immediately afterwards, a 100 μL aliquot (blanco) was taken and processed as described in the PARAGRAPH SPECTROSCOPIC PHOSPHATE DETERMINATION. After 10 min another 100 μL aliquot was taken and processed as described in PARAGRAPH SPECTROSCOPIC PHOSPHATE DETERMINATION. 1 unit is defined as the amount of phosphorylase suspension that can release 0.1 mg inorganic phosphate (P_i) per 3 min[20].

ACTIVITY ASSAY ISOAMYLASE

75 μL sodium acetate buffer (500 mM, pH 3.5), 350 μL 1% starch solution (must be heated to 80 °C for 0.5 hour before use) and 75 μL isoamylase solution were mixed and incubated for 15 minutes at 40 °C. The mixture was cooled to room temperature and 500 μL I_2/KI solution was added together with 11.5 mL water R.O. The absorption was measured on an UV-VIS spectrophotometer at a wavelength of 610 nm. One unit is defined as the increase in A_{610nm} of 0.1 in 1 hour and relative to a blanco sample.

ACTIVITY ASSAY GLYCOGEN BRANCHING ENZYME

The total activity of the enzyme was measured using the iodine assay[21], which is based on the formation of a blue complex between iodine-iodide and a linear $\alpha(1\rightarrow4)$ linked glucan of a certain length. The sum of the transglycosylation and the hydrolytic activity of the enzyme can be measured by monitoring the decrease in absorbance. The reaction mixtures contained 150 μL of 0.125% (W/V) amylose V (Avebe, Foxhol, The Netherlands) and 50 μL enzyme at the appropriate concentration (15 to 25 $mg \cdot mL^{-1}$). At different time intervals, aliquots of 15 mL were taken and the reaction was terminated by addition of 1.5 μL of 1 M NaOH and 150 μL of iodine reagent (0.01% [W/V] I_2, 0.1% [W/V] KI). One unit of enzyme activity is defined as the decrease in absorbance of 1.0 per min at 660 nm for amylose.

SYNTHESIS OF MALTOHEPTAOSE

500 g of β-cyclodextrin was dissolved in 2 L 0.01 M HCL and was refluxed for 2 hours. The mixture was neutralized with 1 M NaOH, slowly cooled to room temperature, and stored overnight at 4 °C. The precipitated β-cyclodextrin was removed by means of filtration. 20 mL of *p*-xylene was added to the filtrate and heated to 60 °C for 1 hour. The filtrate was then slowly cooled to room temperature and stored overnight at 4 °C. The resulting *p*-xylene/β-cyclodextrin complex was removed via filtration and the filtrate was concentrated to 200 mL via rotary evaporation. Again 20 mL of *p*-xylene was added to the filtrate and heated to 60 °C for 1 hour. The filtrate was cooled to room temperature and stored at 4 °C. The remaining β-cyclodextrin was removed as *p*-xylene/β-cyclodextrin complex via filtration. The filtrate was precipitated in 2 L cold ethanol and dried *in vacuo*. The resulting maltoheptaose appeared as an off-white powder in a yield of 10%.

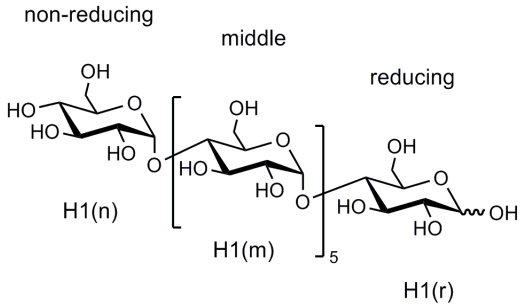

^{1}H-NMR (D_2O, 300 MHz) 5.39 ppm: H1(m) and H1(n) , 5.22 ppm: H1(r)α, 4.65 H1(r)β, 3.41 ppm: H4(m), 3.26 ppm: H2(r)β.
Melting point: 204.7 °C.
MALDI-ToF, 1173 m/z (M + Na)

SPECTROSCOPIC PHOSPHATE DETERMINATION

Preparation of the solutions:

1. (Reducing agent). 25 g Pyrosulfite and 1 g sodium sulfite were dissolved in 60 mL water R.O. 200 mg Metol was dissolved in 1 mL water R.O. The metal solution was added to the other solution and filled to 100 mL. This solution was stored in the dark.
2. (Buffer). 100 g Sodium acetate was dissolved in 250 mL water R.O.
3. (Complexing agent). 12.5 g Ammonium molybdate was dissolved in 100 mL water R.O. 125 mL 5 N sulphuric acid was added while stirring and filled with water R.O. to 250 mL.

Assay. A 10-100 μL aliquot was added to a 10 mL vial. 500 μL of solution **1.** and 1000 μL of solution **2.** were added and diluted with water R.O. After 10 min, 2 mL of solution **3.** was added and the vial was filled to 10 mL. The absorption was measured after 30 min at a wavelength of 716 nm.

TYPICAL ENZYME CATALYZED TANDEM POLYMERIZATION

Maltoheptaose (0.5 mM), G-1-P (25-500 mM), phosphorylase (5 $U.mL^{-1}$) and GBE_{DG} (250 $U.mL^{-1}$) were mixed and filled to 5 mL with 3-(N-morpholino) propanesulfonic acid buffer (MOPS, pH 7.0, 50 mM). When only phosphorylase was utilized, a citrate buffer (pH 6.2, 50mM) was used. Different ratio's G-1-P to primer were made by varying the G-1-P concentration. The solution depended on the enzymes used, was incubated at 37 °C (tandem polymerization) or 38°C (phosphorylase) and shaken. The released amount of phosphate was measured with a modified[14] method of Fiske and

Subbarow[13]. Upon reaching equilibrium conditions, the reaction was terminated by a heat treatment (5 min in boiling water). Denaturized enzymes were removed by means of centrifugation. Dialysis and lyophilization of the remaining solution yields the (hyperbranched) polysaccharides.

METHYLATION ANALYSIS

Preparation of 4.2 M sodium dimsyl. 0.5 g sodium hydride was dissolved in 5 mL dry DMSO at 50 °C in an ultrasonic bath.

Sample preparation. 2 mg dried sample was dissolved in 0.5 mL dry DMSO at 70 °C.

Methylation with CH_3I. 250 μL sodium dimsyl was added to the sample and mixed overnight at room temperature. While cooling on ice, 250 μL CH_3I was added and mixed for 1 hour. The methyl iodide was removed with a stream of nitrogen at 40 °C and 1.5 mL dichloro methane was added to the methylated samples. The solution was extracted by adding 1.5 mL water R.O. whereby the water layer was discarded. This extracting procedure was repeated 5 times and at last the dichloro methane was removed with a stream of nitrogen.

Hydrolysis with 2M TFA. 200 μL TFA was added to the dry sample and boiled for 1 hour. TFA was removed at 60 °C with a stream of nitrogen.

Reduction with $NaBD_4$. 400 μL $NaBD_4$ was added to the sample. The mixture was carefully shaken for 3 hours and the reduced product was lyophilized.

Acetylation. 80 μL acetic acid, 1.2 mL acetic anhydride and 40 μL 70% perchloric acid was added to the sample. While cooling on ice 4 mL water R.O. and 80 μL 1-methyl imidazole was added. The solution was extracted with 1 mL dichloro methane. 10 μL of the PMAA solution was used for the GC-FID analysis.

BCA ASSAY

Preparation. Solution **A**. 13.575g Na_2CO_3 , 6.05g $NaHCO_3$ and 0.475g Na_2BCA were dissolved in 250 mL water R.O. Solution **B**. 312.5 mg $CuSO_4.5H_2O$ and 315 mg lysine were dissolved in 250 mL water R.O.

Assay. Solution **A** and **B** were freshly mixed before the assay. 100 μL sample was incubated with 100 μL of reagent for 60 min at 80 °C in an oven. The samples were cooled on ice and the absorbance was measured at 550 nm. A calibration curve was made of maltose in the range of 10 – 70 μmol.

ANTHRONE ASSAY

Preparation. 60 mL water R.O. and 15 ml ethanol was mixed and cooled on ice. 400 mg of anthrone was dissolved in 200 ml of pure H_2SO_4. This anthrone solution was carefully added to the water/ethanol mixture. The anthrone solution was stored at 4 °C.

Assay. 1 ml sample and 10 ml anthrone reagents were mixed with a vortex stirrer and incubated for 10 min at 100 °C. The samples were allowed to cool down to room temperature before the absorbance was measured at a wavelength of 620 nm. A calibration curve was made of maltose in the range of 100 – 1000 μM.

2.3 RESULTS AND DISCUSSION

2.3.1 Optimum conditions for combined biocatalysis

Enzymes are usually only active within a narrow pH range. The pH influences the ionization states of the amino acid residues in the active site and the ionization of the substrate, which can result in a reduced catalytic activity. When two enzymes are used in a 1-pot synthesis, a compromise has to be found in reaction circumstances in a way that both enzymes perform the best.

The activity of potato phosphorylase as well as the activity of GBE_{DG} are measured with the corresponding activity assays, as described in the EXPERIMENTAL section, in different buffer systems with various pH values. The optimum activity of potato phosphorylase was found at a pH of 6.2 and the optimum activity of GBE_{DG} was found at a pH of 8.0 (see FIGURE 2.5). Therefore, the 1-pot systems, in which both enzymes are employed, are performed in a MOPS buffer at a pH of 7.0. Both enzymes were in this environment still active enough to catalyze the specific reactions.

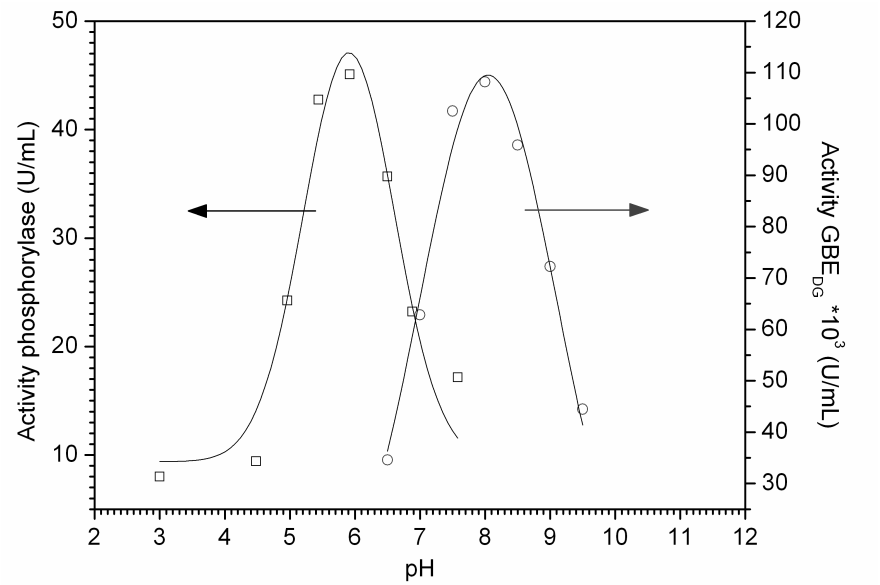

FIGURE 2.5: (□) Activity profile of potato phosphorylase and (○) GBE_{DG} at different pH values.

The temperature range in which both enzymes are active is, like the pH, restricted to a small bandwidth. The optimum temperature for GBE_{DG} was found to be 32 °C while the optimum temperature for the potato phosphorylase was 38 °C (see FIGURE 2.6). The combined biocatalysis is performed with good results at a temperature of 37 °C.

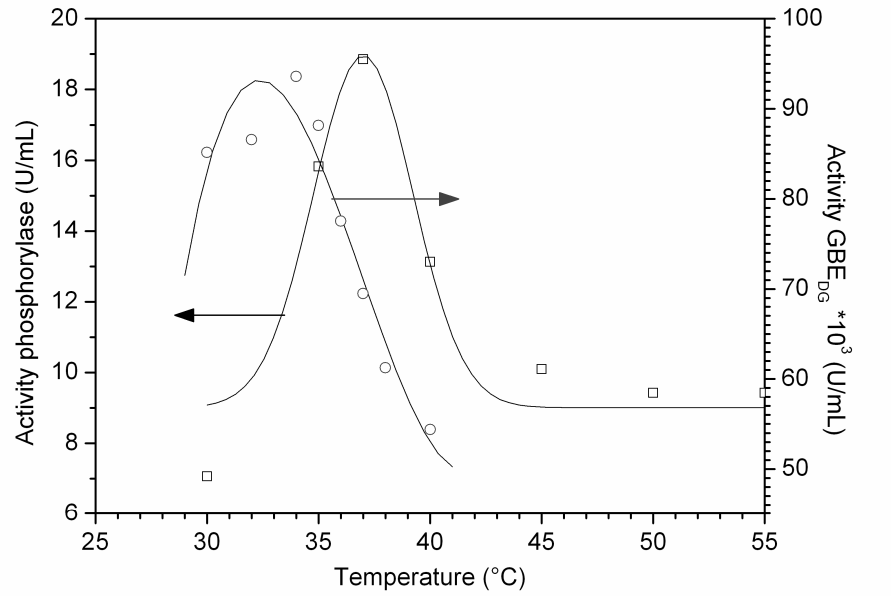

FIGURE 2.6: (□) Activity profile of potato phosphorylase and (○) GBE_{DG} between 30 and 55 °C.

2.3.2 Visual appearance of the reaction products

FIGURE 2.7 shows the difference between a polymerization performed in the presence of phosphorylase and GBE_{DG} (LEFT) and a polymerization performed in the presence of phosphorylase alone (RIGHT).

FIGURE 2.7: Reaction vials after polymerization.

The vial on the LEFT is the result of the combined catalyzed polymerization in which phosphorylase and GBE_{DG} are employed. The resulting hyperbranched polysaccharide (DP ~500) forms a stable opaque solution. The vial on the RIGHT is the result after incubation with phosphorylase alone. The synthetic, linear, amylose (DP ~500) precipitates during polymerization out of solution. This experiment gives us a visual proof that the combined action of the enzymes indeed produces a branched polyglucan, as only the branched structure is soluble.

In the following section a more detailed characterization of the obtained structures is described.

2.3.3 Kinetics of the phosphorylase catalyzed reaction

The phosphorylase catalyzed reaction behaves like a living polymerization including all following characteristics[8]:

- The polymer chain grows linear with time.
- Addition of G-1-P results in re-growth of the polymer chain.
- The termination step is absent.
- Polymers with a low polydispersity are obtained[22].

Since the phosphorylase driven reaction is an equilibrium reaction the linearity of monomer consumption diminishes when the concentration of G-1-P decreases (see FIGURE 2.8). In equilibrium about 70 % of the G-1-P is consumed, corresponding to an equilibrium constant (K) of 2.3.

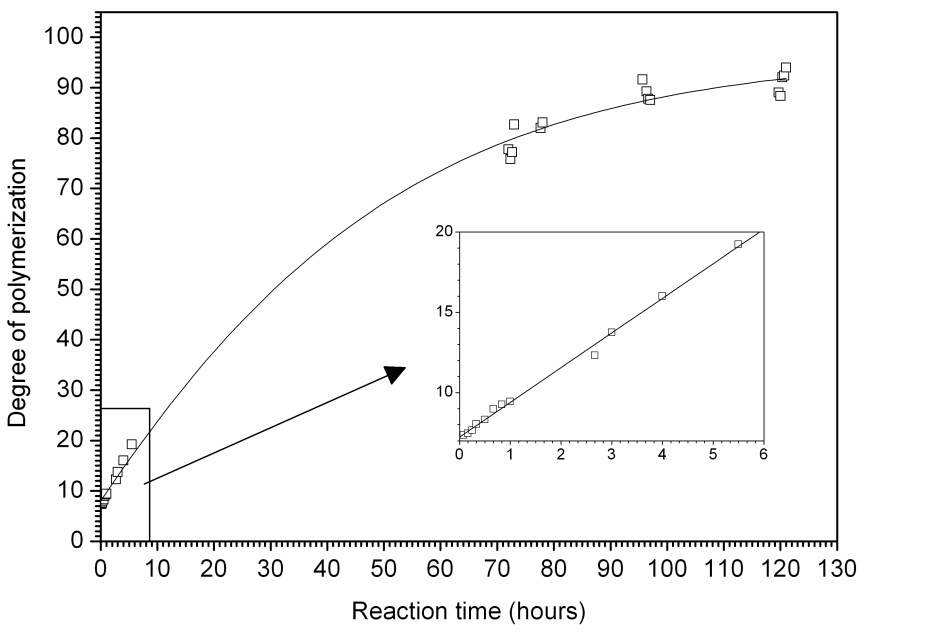

FIGURE 2.8: Typical reaction course of a phosphorylase driven polymerization. Reaction performed in 10 mL citrate buffer (pH 6.2, 50 mM) at 30 °C with a primer concentration of 2 mM, 360 mM G-1-P and 0.1 U.mL^{-1} phosphorylase.

The molecular weight of the synthetic amylose is solely dependent on the feed ratio G-1-P, analogue to a conventional anionic polymerization where the ratio of monomer over initiator determines the molecular weight. The degree of polymerization can be determined following EQUATION 2.4.

$$\text{Degree of polymerization} = \frac{[\text{G-1-P}]}{[\text{maltoheptaose}]} + 7 \qquad 2.4$$

where *7* represents the amount of glucose residues from the primer.

The initial reaction speed depends on the amount of potato phosphorylase and the concentration of primer molecules. In a later stage of the reaction, the decreasing concentration of monomer will become rate limiting.

When, next to the potato phosphorylase, GBE_{DG} is employed the reaction speed is no longer only dependent on these two parameters as GBE_{DG} introduces new branches *in situ*. Each newly introduced branch acts as an intramolecular primer site and increases the available points for polymer growth.

FIGURE 2.9 shows a phosphorylase driven reaction and is compared with a reaction in the presence of GBE_{DG}. In this particular case no difference in reaction speed is seen as phosphorylase is present in a rate limiting concentration. The increase in primer sites (as catalyzed by GBE_{DG}) can not be utilized completely by phosphorylase due to the rate limiting concentration of the enzyme. The advantage of this strategy is that the reaction products of the phosphorylase driven reaction and the combined biocatalysis can be compared at any time during polymerization. In terms of chemical structure and molecular architecture, the only difference is the branched character.

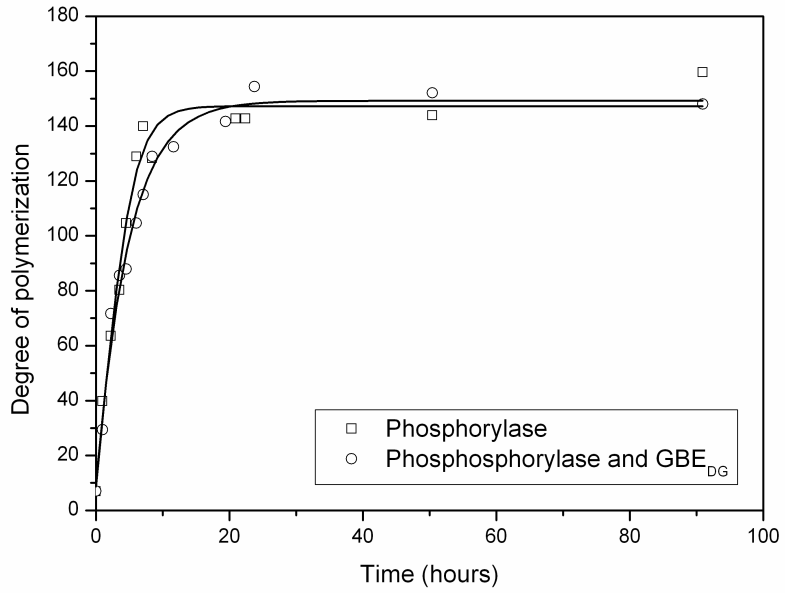

FIGURE 2.9: The reaction course of a phosphorylase driven polymerization with (○) and without GBE_{DG} (□).

FIGURE 2.10 shows the result of the obtained degree of polymerization in equilibrium conditions of reactions incubated with a fixed primer concentration and different feed ratio's of G-1-P. As shown in EQUATION 2.4, the degree of polymerization correlates linearly with the feed ratio G-1-P. This is experimental ly validated by the results as depicted in FIGURE 2.10. When GBE_{DG} is utilized, the same

correlation between the degree of polymerization and the feed ratio G-1-P is observed.

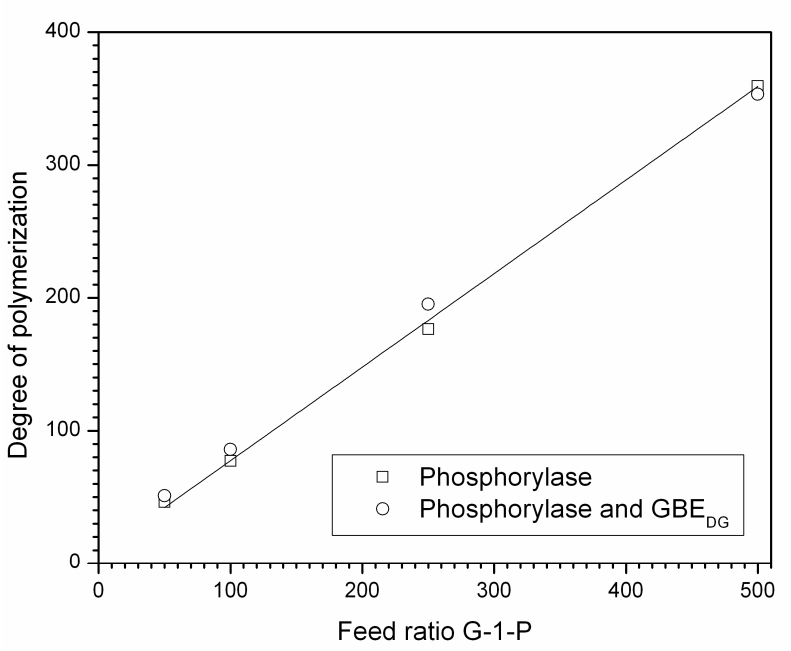

FIGURE 2.10: Degree of polymerization for different phosphorylase driven polymerizations (□) without GBE_{DG} and (○) with GBE_{DG} versus varying G-1-P feed ratios. The slope of the linear trend line represents the conversion of G-1-P and corresponds to 70 %. Reactions performed in 0.5 mL MOPS buffer (pH 7.0, 50 mM) at 37 °C with a primer concentration of 0.5 mM, 25-250 mM G-1-P, and 5 $U.mL^{-1}$ phosphorylase.

In conclusion, when the right reaction conditions are chosen no difference is seen in the reaction course. Both the phosphorylase driven reaction and the combined catalyzed reaction show the same kinetics. However, there is a difference with respect to the molecular architecture as the combined biocatalysis yields water soluble branched polysaccharides. By controlling the feed ratio of G-1-P, predetermined sizes of linear and branched structures are obtained depending on the enzymes used.

2.3.4 Degree of branching

During the enzyme catalyzed reaction the primer molecule grows due to the action of phosphorylase. *In situ* branch formation is realized by the utilization of GBE_{DG}. The minimum substrate length for GBE_{DG} is expected to be around 20 $\alpha(1\rightarrow4)$ linked glucose residues. This means that phosphorylase is in the initial stage of the reaction

the only active enzyme. When the growing primer exceeds the length of 20 glucose residues, GBE_{DG} is able to catalyze branch formation.

THEORETICAL DEGREE OF BRANCHING

The maximum degree of branching (DB) of polysaccharides as obtained via the combined biocatalysis correlates with the preferred glucan chain length (c.l.) that is transferred by GBE_{DG} (see EQUATION 2.5).

$$\lim_{DP\uparrow c.l.} DB(\%) = \left(\frac{1}{\text{chain length}} - \frac{1}{\text{degree of pol.}} \right) * 100\% \qquad 2.5$$

FIGURE 2.11 depicts the theoretical evolution of the average degree of branching with growing degree of polymerization as calculated by EQUATION 2.5. Three different average side chain lengths (DP 8, 9 and 10) are shown together with the corresponding maximum attainable degree of branching (dashed line in FIGURE 2.11).

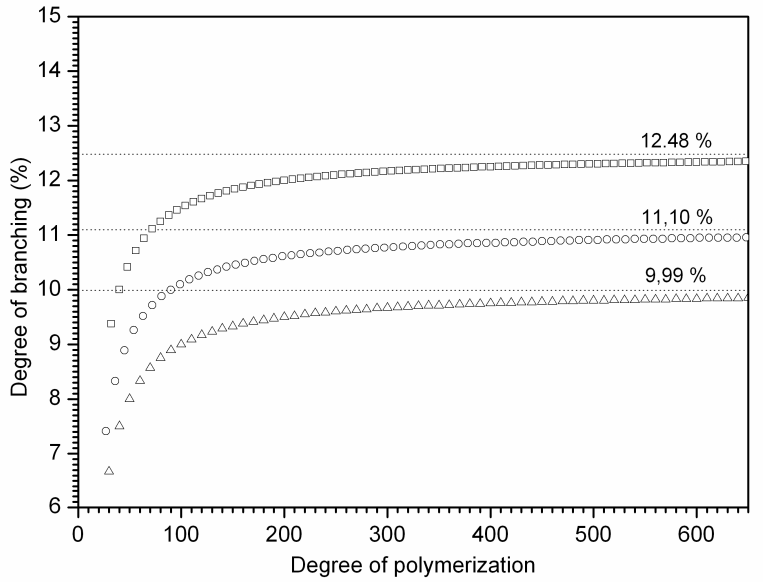

FIGURE 2.11: (□) theoretical average side chain lenght of 8 glucose residues; (○)theoretical average side chain length of 9 glucose residues; (△) theoretical average side chain length of 10 glucose residues.

Branching enzymes transfer a range of glucans with different chain lengths rather than one specific chain length. However, the proposed evolution of the degree of

branching should apply to the combined biocatalysis if the branching enzyme affinity to the donor substrate stays constant during the course of the reaction.

EXPERIMENTAL DETERMINATION OF THE DEGREE OF BRANCHING

To obtain the course of branching as a function of time of the combined biocatalysis, the reaction was followed by methylation analysis and the combined BCA/anthron assay. The RSD assay results are considered as not accurate and are discarded since the samples were not G-1-P free. These results together with the evolution of the degree of polymerization in time is plotted in FIGURE 2.12.

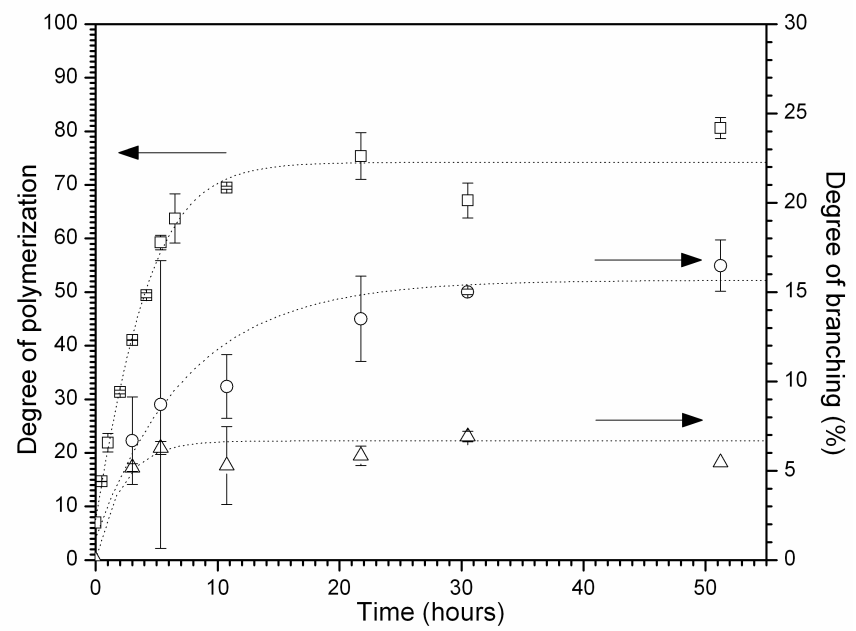

FIGURE 2.12: (□) Evolution of the degree of polymerization in time. Evolution of the degree of branching in time measured via (○) BCA/anthrone assay and (△) methylation procedure. All dashed lines are guide lines to the eye.

The degree of branching levels of to a value of 15.7 % and 6.7 % for, respectively, the BCA/anthron assay and the methylation analyis. The degree of branching does reach the expected plateau (as shown in FIGURE 2.11) but the difference between the two methods is rather substantial. Both the methylation analysis and the combined BCA/anthrone assay consists of a complex and laborious multi-step procedure which makes this method susceptible to inaccurate values due to accumulated experimental errors.

An alternative method is found in ^{1}H-NMR spectroscopy. By taking the ratio of the $\alpha(1\rightarrow6)$ and $\alpha(1\rightarrow4)$ signal, the degree of branching can be calculated in a fast and accurate manner.

DETERMINATION OF THE DEGREE OF BRANCHING BY ^{1}H-NMR

In the next section, the degree of branching is determined with ^{1}H-NMR spectroscopy. Again, the degree of branching and the degree of polymerization were followed during the course of a tandem polymerization. FIGURE 2.13 shows the combined results.

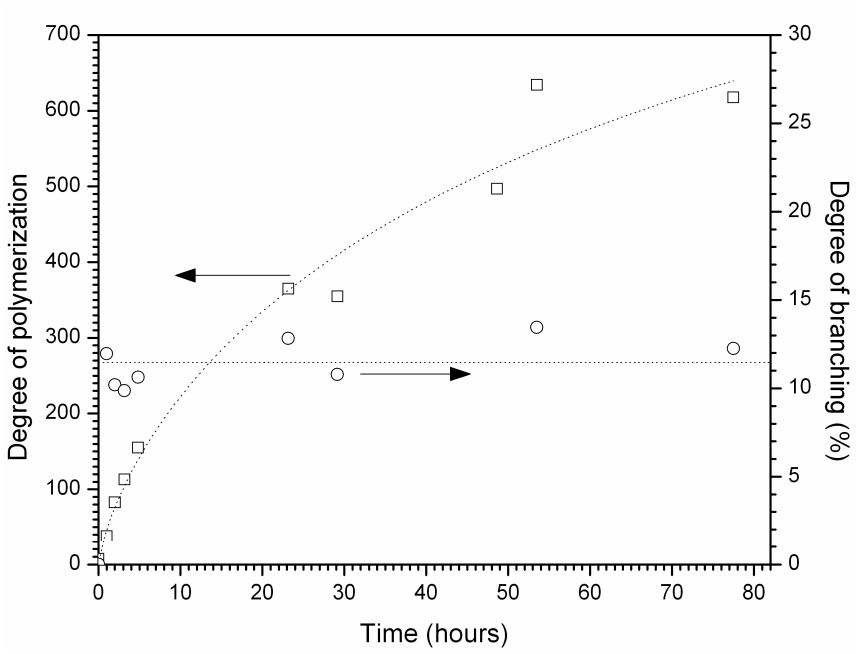

FIGURE 2.13: (□) Evolution of the degree of polymerization in time. (○) Evolution of the degree of branching in time measured via ^{1}H-NMR. Dashed lines are guide lines to the eye.

FIGURE 2.13 nicely illustrates that the degree of branching is independent of the degree of polymerization at higher molecular weights. This is in accordance with the theoretical calculated asymptote as shown in FIGURE 2.11.

The initial part of the reaction course does not show the expected increase in the degree of branching, instead values of around 11 % are measured during the complete course of the reaction. This is caused by the fact that measurements of the

degree of branching of samples with a DP<50 is difficult due to the necessary dialysis step in order to purify the sample.

The experimentally obtained data is fitted with the proposed theoretical evolution of the degree of branching in the case of an average side chain length of 9 glucose residues (see FIGURE 2.14).

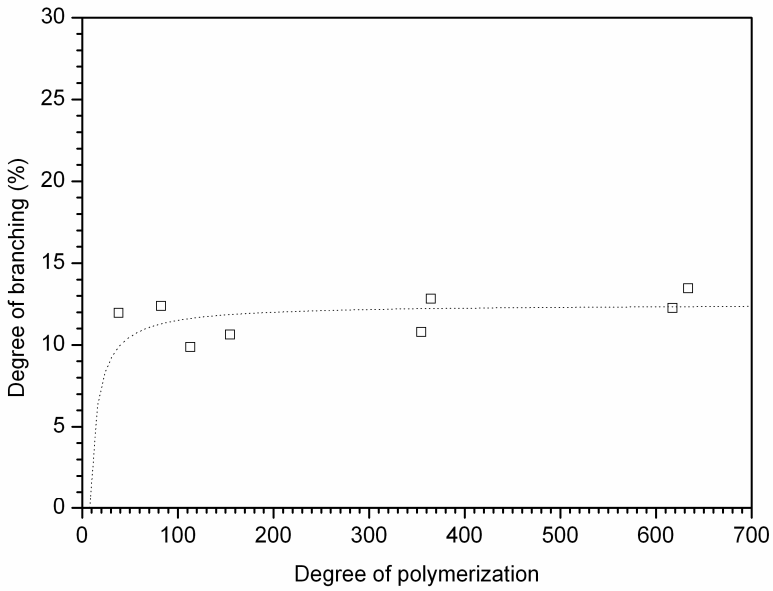

FIGURE 2.14: (□) Experimental data as determined with ^{1}H-NMR. (dashed line) Theoretical average degree of branching on the basis of a side chain length of 9 glucose residues.

On the basis of these results it is concluded that the hyperbranched products have on average side chain lengths of 9 glucose residues. However, branching enzymes transfer a range of side chains to the $\alpha(1\rightarrow6)$ positions rather than one specific length. Therefore the side chain length pattern is further elucidated with MALDI-ToF experiments.

DETERMINATION OF THE SIDE CHAIN LENGTH DISTRIBUTION BY MALDI-TOF

Matrix assisted laser desorption/ionization – time of flight (MALDI-ToF) mass spectrometry allows the mass analysis of biopolymers via a soft ionization technique. The technique requires a suitable matrix in which the analyte is mixed. Upon irradiation the matrix/analyte mixture with short laser pulses, ionized analyte molecules are co-desorbed with the matrix and are accelerated and analyzed by a ToF-MS detector.

It is rather difficult to ionize large neutral polysaccharides such as amylose and the branched structures as synthesized in this chapter. Therefore it is not possible to directly determine the mass with MALDI-ToF. However, linear α-glucans with a DP below 30 can be detected.

Therefore synthesized hyperbranched polysaccharides are debranched with the enzyme isoamylase. With this approach it becomes possible to determine the side chain length distribution with MALDI-ToF as isoamylase selectively catalyses the hydrolysis of α(1→6) linkages. The resulting mixture of linear oligosaccharides is measured with MALDI-ToF spectroscopy (see FIGURE 2.15).

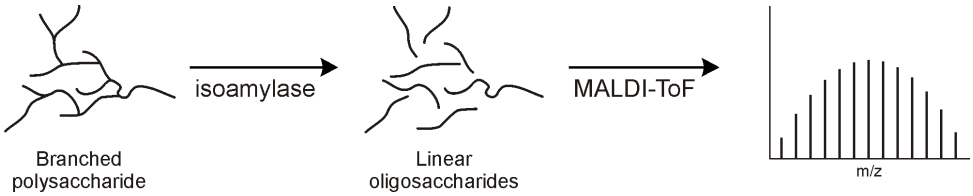

FIGURE 2.15: The followed procedure in order to obtain the side chain distribution with MALDI-ToF spectrometry.

^{1}H-NMR spectroscopy is used to ensure complete hydrolysis of all α(1→6) linkages. As can be seen in FIGURE 2.16, the α(1→6) signal at 5.0 ppm is indistinguishable from the debranched product, proving that the selective hydrolysis of the α(1→6) linkages has gone to completeness.

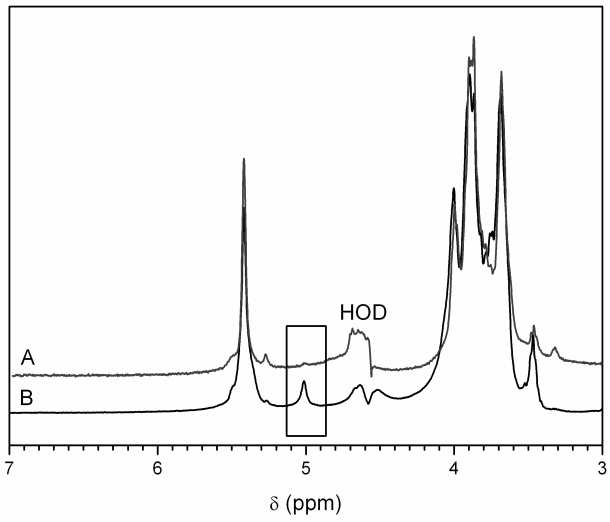

FIGURE 2.16: A) α-glucan after debranching with isoamylase, B) branched α-glucan.

FIGURE 2.17 shows the MALDI-ToF spectrum of a debranched polyaccharide. The mixture of resulting oligosaccharides after debranching gives a rather narrow distribution of side chains with a DP between 4 and 15 glucose residues, with a preference for oligosaccharides with a length of 6-8 glucose residues.

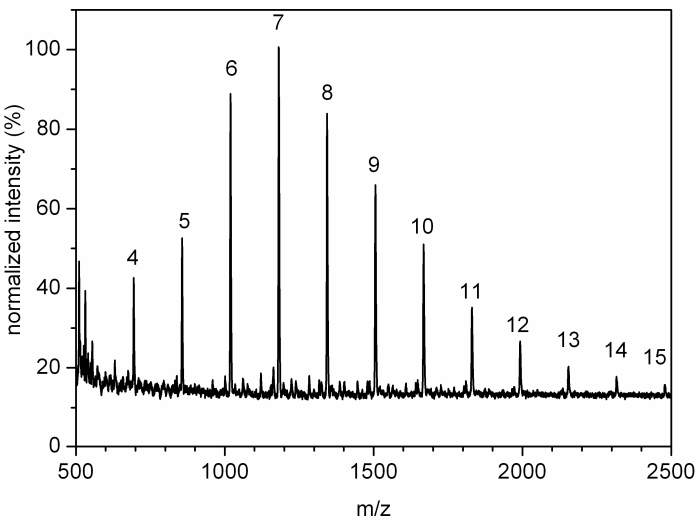

FIGURE 2.17: Chain lenght distribution profile of a debranched polysaccharide with an original DP of 600. The relative difference between signals is 162 m/z and corresponds to the mass of 1 glucose residue.

Palomo et al.[23] incubated amylose V with GBE_{DG} and determined the side chain pattern with high performance anion exchange chromatography with a pulsed amperometric detector (HPAEC-PAD). The resulting distribution consisted of side chains with a DP between 4 and 17 glucose residues, with a preference for oligosaccharides with a length of 6-7 glucose residues.

The results as obtained here by MALDI-ToF fit well with the average side chain length as obtained by ^{1}H-NMR and with the results published by Palomo et al.

2.4 CONCLUSION

The one pot synthesis of a hyperbranched α-glucan via an enzyme catalyzed tandem polymerization is demonstrated. The production of hyperbranched structures includes glucose-1-phosphate (G-1-P) as donor substrate, maltoheptaose as primer and the enzymes phosphorylase and the branching enzyme of *Deinococcus geothermalis* (GBE_{DG}). Potato phosphorylase is able to catalyze the linear α(1→4) chain growth of maltoheptaose at the non-reducing site using glucose-1-phosphate as donor substrate while GBE_{DG} catalyses the *in situ* branch formation by a transglycosylation reaction in which an α(1→4) linkage of the donor substrate is cleaved, followed by an attachment of the released oligosaccharide to an acceptor substrate via an α(1→6) linkage.

The course of the reaction can be followed by UV spectroscopic measurement of the released organic phosphate by complexing it with molybdate. Via this technique, the degree of polymerization and conversion of the reaction can be determined during the course of reaction. In general 70 % of the G-1-P is converted. The size of the hyperbranched polysaccharide can be predetermined by controlling the feed ratio of G-1-P which acts as the donor substrate.

A fast and accurate determination of the degree of branching as well as the determination of the average side chain length is achieved with ^{1}H-NMR spectroscopy. The maximum attainable degree of branching is independent of the degree of polymerization and is 11 %.

The side chain distribution is determined with MALDI-ToF. The side chain distribution consists of rather short chains with a narrow side chain distribution. The distribution proves that GBE_{DG} preferentially transfers oligosaccharides with a length of 6 to 9 glucose residues. This length is also optimal for the phosphorylase catalyzed chain growth. Moreover, it is known that short side chains retard the retro-degradation process and enhance the water solubility[24]. These are important features for the use of hyperbranched polysaccharides in the biomedical field and the food industry.

The hyperbranched polysaccharides have a degree of branching and side chain distribution comparable to amylose V samples that are incubated with GBE_{DG}. However, the procedure described in this chapter allows complete control over the degree of polymerization.

2.5 REFERENCES

1. W.N. Haworth, S. Peat, E.J. Bourne, *Nature*, **1944**, *154,* 236
2. A. Biwer, G. Antranikian, E. Heinzle, *Appl. Microbiol. Biotechnol.*, **2002**, *59,* 609-617
3. C.F. Cori, G.T. Cori, *Proc. Soc. Exp. Biol. Med.*, **1936**, *34,* 702
4. C. Weibull, *Arkiv för Kemi, Mineralogi och Geologi*, **1945**, *21B,* 1-4
5. W.J. Whelan, J.M. Bailey, *Biochem. J.*, **1954**, *58,* 560-569
6. T. Suganuma, J.I. Kitazono, K. Yoshinaga, S. Fujimoto, T. Nagahama, *Carbohydr. Res.*, **1991**, *217,* 213-220
7. B. Pfannemüller, W. Burchard, *Die Makromolekulare Chemie*, **1969**, *121,* 1-17
8. B. Pfannemüller, *Naturwissenschaften*, **1975**, *62,* 231-233
9. J. Staerk, H. Schlenk, *Biochim. Biophys. Acta*, **1967**, *146,* 120
10. M. Pajatsch, A. Bock, W. Boos, *Carbohydr. Res.*, **1998**, *307,* 375-379
11. H. Hokse, *Carbohydr. Res.*, **1974**, *37,* 390-392
12. K. Balasing, W. Ferdinan, *Biochem. J.*, **1970**, *118,* 15
13. C.H. Fiske, Y. Subbarow, *J. Biol. Chem.*, **1925**, *66,* 375
14. O.H. Lowry, J.A. Lopez, *J. Biol. Chem.*, **1946**, *162,* 421-428
15. S. Hizukuri, S. Osaki, *Carbohydr. Res.*, **1978**, *63,* 261-264
16. D.D. Mcintyre, C. Ho, H.J. Vogel, *Starch*, **1990**, *42,* 260-267
17. H. Sugiyama, T. Nitta, M. Horii, K. Motohashi, J. Sakai, T. Usui, K. Hisamichi, J. Ishiyama, *Carbohydr. Res.*, **2000**, *325,* 177-182
18. G.S. Nilsson, K.E. Bergquist, U. Nilsson, L. Gorton, *Starch*, **1996**, *48,* 352-357
19. S. Kralj, G.H. van Geel-Schutten, M.M.G. Dondorff, S. Kirsanovs, M.J.E.C. van der Maarel, L. Dijkhuizen, *Microbiology-Sgm*, **2004**, *150,* 3681-3690
20. P.H. Hidy, H.G. Day, *J. Biol. Chem.*, **1945**, *160,* 273-282
21. H.P. Guan, P. Li, J. Imparl-Radosevich, J. Preiss, P. Keeling, *Arch. Biochem. Biophys.*, **1997**, *342,* 92-98
22. P. Roger, M.A.V. Axelos, P. Colonna, *Macromolecules*, **2000**, *33,* 2446-2455
23. M. Palomo Reixach, S. Kralj, M.J.E.C. van der Maarel, L. Dijkhuizen, *Appl. Environ. Microbiol.*, **2009**, *75*
24. C.K. Lee, Q.T. Le, Y.H. Kim, J.H. Shim, S.J. Lee, J.H. Park, K.P. Lee, S.H. Song, J.H. Auh, S.J. Lee, K.H. Park, *J. Agric. Food Chem.*, **2008**, *56,* 126-131

CHAPTER 3

Hyperbranched polysaccharide brushes

SUMMARY

A method is presented to produce hyperbranched polyglucan brushes on silica substrates. The brushes are grafted from specially prepared substrates via an enzyme catalyzed process. First the Si wafer is aminosilanized, second the enzyme recognition site maltoheptaose is anchored via a reductive amination. The third step consists of an enzyme catalyzed tandem polymerization. For the growth of linear α-polyglucan brushes phosphorylase is utilized while GBE_{DG} catalyzes the *in situ* branch formation in order to obtain hyperbranched polyglucan brushes. Polysaccharide functionalized surfaces are expected to function as an antibacterial layer similar to the glycocalyx of endothelial blood vessel cells. The hyperbranched brushes are expected to cover a larger area per polymer chain due to the divergent growth of the polyglucan.

3.1 INTRODUCTION

3.1.1 Biofouling

Biofouling is, in general terms, the undesired accumulation of microorganisms, plants, algae and animals. Biofouling causes problems in many dissimilar fields. Algal growth on ship's hulls increases the drag of the ship which is economically unfavourable[1]. Biofilm formation on biomedical implants may cause inflammation reactions[2,3,4] and bacterial growth on food technology equipment and water transport/storage systems may contaminate food and water[5,6].

Surfaces bearing hydrophilic polymer brushes are known to delay protein adsorption and hence retard biofouling[7,8]. PEG (poly ethylene glycol) brushes have been a topic of interest in the preparation of protein resistant surfaces [9,10,11,8,7]. PEG has an exceptionally high resistance to non-specific protein binding and is biocompatible. However, PEG has some limitations. It is for instance susceptible to thermal and oxidative degradation[12,13,14], the long term stability of PEG is limited[15], it can only be functionalized at its chain ends and it is not biodegradable.

Endothelial blood vessel cells are covered with a saccharide layer which forms a barrier around cells to prevent the undesirable non-specific adhesion of other cells and molecules. This exterior is known as the glycocalyx.

Biomimicking the glycocalyx provides a good alternative for PEGylated surfaces/systems and is a potential solution to clinical problems associated with implantable devices [16,15,17,18,19,20,21].

The use of polysaccharides in protein resistant surfaces has advantages such as the ability to incorporate active groups via a linkage with the hydroxy moiety of the sugar residues and the biocompatible and biodegradable character. Moreover, the use of *hyperbranched* polysaccharides can overcome the difficulty of engineering a high surface density polymer brush as a hyperbranched brush covers a larger surface area than a linear chain.

3.1.2 Polymer brush coatings

Polymer brush coatings refer to polymer systems in which one end of the polymer chain is attached to a surface or interface. In the 1950's Van der Waarden[22,23], Mackor[24,25] and Clayfield[26,27] discovered the potential of polymer brushes on colloidal particles to prevent flocculation.

When the independent chains of a polymer brush are densely packed they are forced to stretch perpendicular to the surface in order to avoid overlapping. The stretching of the chains lowers the monomer-monomer interactions and hence the interaction energy per chain (F_{int}) decreases. However, the free elastic energy of the chain increases with the stretching of the chain. The interplay between F_{int} and F_{el} determines the equilibrium thickness of the polymer brush. The theoretical work of Alexander[28] on the thermodynamics of densely packed polymer brushes is the basis of the scaling approach as presented in TABLE 3.1.

TABLE 3.1: Relationship between the dimensions of a polymer chain and the amount of statistical segments (N)[29].

	Tethered polymer chain	Free polymer chain
Good solvent	$L/a \approx N(a/d)^{2/3}$	$R_g \propto N^{3/5}$
Theta solvent	$L/a \approx N(a/d)$	$R_g \propto N^{1/2}$
Bulk state	$L \propto N^{2/3}$	$R_g \propto N^{1/2}$

Where a *is the statistical segment diameter,* N *is the amount of segments,* L *is the brush thickness and* d *is the polymer to polymer distance. The symbol ≈ means* approximately equal to *and the symbol ∝ means* proportional to*.*

Most remarkable characteristic of polymer brushes as compared to free polymer chains is the linear relation of L with N, i.e. the thickness of the brush increases linearly with the degree of polymerization. This in contrary to a free polymer chain in a good solvent, were the radius of gyration (R_g) scales with $N^{3/5}$. The range in which the polymer to polymer distance (d) is smaller than R_g is known as the brush regime. A less densely packed system (i.e. $d>R_g$) results in the mushroom regime. In this regime, the polymer chains do not interact with each other, the brush thickness is not related to the grafting density and the independent polymer coils have a dimension that corresponds closely to the dimensions of a free undisturbed random coil.

Polymer brush coatings can be prepared by two different approaches. The polymer chains can be covalently attached to the substrate (chemosorption) or can be adsorbed to the surface (physiosorption). In the case of chemosorbtion, the brushes can be prepared via a *grafting from* and a *grafting to* method. *Grafting to,* refers to the method in which polymers with a functional group react with a reactive site on the surface. *Grafting from* refers to the method in which an immobilized initiator molecule on the substrate starts a polymerization, as a result polymer chains grow directly from the surface. The *grafting from* technique results generally in thicker and more densely packed brushes as compared to the *grafting on* technique. However, in

terms of analysis (molecular weight, polydispersity) the *grafting to* technique is advantageous, because the preformed polymers can be easily analyzed.

This chapter covers the functionalization of silicon wafers with hyperbranched polyglucan brushes. These brushes are grafted according to the *grafting from* principle. After aminosilanization and covalent attachment of the maltoheptoase primer to the substrate, a phosphorylase driven polymerization is used to grow linear polyglucan brushes. With the addition of the branching enzyme, GBE_{DG}, hyperbranched polyglucan brushes were grown from the substrate (see FIGURE 3.1).

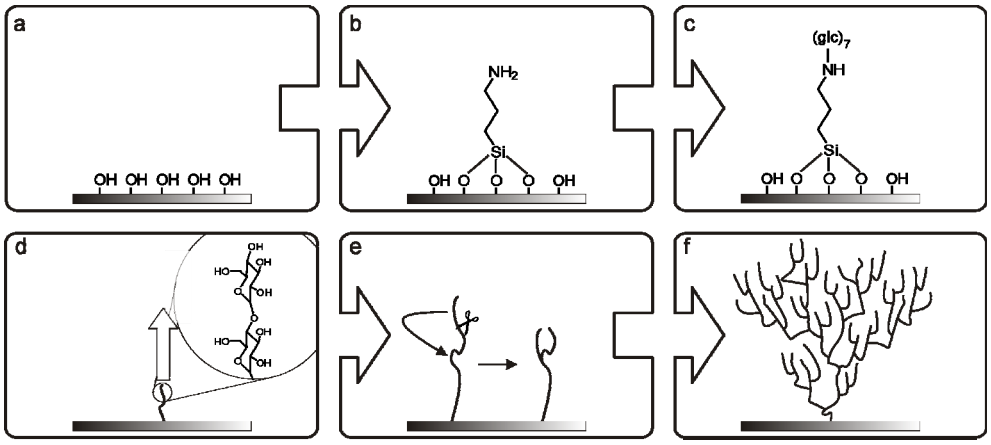

FIGURE 3.1: Schematic representation of the preparation of surface bound hyperbranched brushes. ***a)*** *Si wafer covered with hydroxy groups, oxidized with piranha.* ***b)*** *Aminosilanization of the substrate in order to introduce amine groups.* ***c)*** *Maltoheptaose, $(glc)_7$, is anchored to the amine groups via a reductive amination.* ***d)*** *The anchored maltoheptaose acts as acceptor substrate in the phosphorylase driven surface initiated polymerization of polyglucans.* ***e)*** *The branching enzyme catalyzes the hydrolytic chain scission of an $\alpha(1\rightarrow4)$ linkage and transfers the non reducing terminal fragment to a C6 hydroxyl position thereby introducing an $\alpha(1\rightarrow6)$ branch point.* ***f)*** *After multiple cycles in which phosphorylase elongates the chains and the branching enzyme reshuffles the non reducing terminal fragments a surface bound hyperbranched polysaccharide is formed.*

3.2 EXPERIMENTAL

3.2.1 Materials and chemicals

Double sided polished silicon wafers were purchased from TOPSIL (Frederikssund, Denmark). Toluene (Labscan) was freshly distilled from sodium and DMSO (Labscan) was distilled from CaH_2. Sodium cyanoborohydride, 3-aminopropyltriethoxysilane (APTES) and anthraldehyde (all purchased from Aldrich) were used as received. Water was purified with a Milli-Q system from Millpore.

3.2.2 Analysis and equipment

TRANSMISSION FOURIER TRANSFORM INFRARED (TRANSMISSION FT-IR)

Transmission FT-IR measurements were performed at a resolution of 3 cm^{-1}, under vacuum on a Bruker V/S FT-IR spectrometer equipped with a MIR DTGS detector. A sample shutter accessory was used for interleaved sample and background scanning. A clean double sided polished silicon wafer was used as reference.

ATOMIC FORCE MICROSCOPY

Atomic force microscopy (AFM) was carried out on a Digital Intruments EnviroScope AFM equipped with a Nanoscope IIIa controller in tapping mode using Veeco RTESPW silicon cantilevers. Surface flattening, analysis and visualization was performed with the WSxM 4.0 software package[30].

X-RAY PHOTOELECTRON SPECTROSCOPY

XPS spectra were recorded on a surface science intrument SSX-100 photoelectron spectrometer with a monochromatic AlKα X-ray source ($h\nu = 1486.6$ eV). Measurements were carried out at a photoelectron take off angle of 35° with respect to the sample surface. The resolution of the survey scans was set to 4 and the acquisition of C_{1s} signal was done at constant pass energy of 50 eV. All spectra are the averaged results of 4 measurements. Data analysis was performed with the software package Winspec 2.09. The elemental compositions were calculated with the relative sensitivity factors as shown in TABLE 3.2

TABLE 3.2: Relative sensitivity factors of selected elements.

Element	Sensitivity factor
O_{1s}	2.49
N_{1s}	1.68
C_{1s}	1
Si_{2s}	1.03
Si_{2p}	0.90

SPECTROSCOPIC ELLIPSOMETRY

Spectroscopic ellipsometry was performed on a VASE VB-400 ellipsometer in the range of 400 to 1000 nm. The angle of incidence was varied between 74° and 76° with an interval of 1°. The software package WVASE32 was used to make a model consisting of different layers with characteristic values for the refractive indices. A cauchy dispersion layer was used to determine the thickness of the APTES, maltoheptaose and polysaccharide layer. A refractive index of 1.336 was used for maltoheptaose and the α-glucan brush[31] and a refractive index of 1.465 for APTES[32].

3.2.3 Methods, synthesis and procedures

SURFACE PREPARATION AND MODIFICATION

The wafers were cut in pieces of 10 mm x 20 mm and ultrasonically rinsed with ethanol, dichloromethane and finally submerged in a hot piranha solution. After 1 hour, the substrates were extensively rinsed with Milli Q water and sonicated with methanol and toluene, respectively. The cleaned surfaces were immediately silanized as described below.

AMINOSILANIZATION

The aminosilanization process was carried out in a 2 % (V/V) APTES solution in freshly distilled toluene at room temperature in a shaking incubator. After 1.5 hour the substrates were rinsed with toluene and placed in a soxleth apparatus for 24 hours to remove the excess of APTES[33]. Finally the substrates were baked at 120 °C for 30 minutes.

SYNTHESIS OF MALTOHEPTAOSE

See experimental section CHAPTER 2.

ANCHORING THE PRIMER RECOGNITION SITE

The amino functionalized wafers were submerged in a DMSO solution containing 1 % (V/V) acetic acid, 10 mg·mL^{-1} maltoheptaose, 2.5 mg·mL^{-1} $NaCNBH_3$ and 4 Å molsieves. The reductive amination was carried out at a temperature of 60 °C for 3 days in a shaking incubator. Substrates were after reaction rinsed and sonicated with Milli Q water and ethanol.

SPECTROPHOTOMETRIC DETERMINATION OF THE AMINE DENSITY

Imine formation. 50 mg (242.4 μmol) anthraldehyde was dissolved in 50 ml distilled DMSO containing 12.5 μL acetic acid. The amine bearing surfaces were immersed in 2 ml of the above described solution and 4 Å molsieves were added. The samples, incubated at 60 °C for 20 hours, were afterwards rinsed with DMSO, Milli Q water and dry methanol and dried *in vacuo*.

Hydrolysis. Hydrolysis of the formed imines was realized by immersing the substrates in 1 mL Milli Q water containing 0.8 % (V/V) acetic acid. This solution was heated to 30 °C for 30 minutes. The absorbance of the solution was measured at a wavelength of 262 nm.

Calibration. A calibration curve of anthraldehyde in water containing 0.8 % (V/V) acetic acid was made in the range of 27-1300 nM. Absorptions were measured at a wavelength of 262 nm.

ISOLATION AND PURIFICATION OF POTATO PHOSPHORYLASE

See experimental section CHAPTER 2.

CLONING, EXPRESSION AND PURIFICATION OF THE GLYCOGEN BRANCHING ENZYME

See experimental section CHAPTER 2.

ENZYME CATALYZED SYNTHESIS OF POLYGLUCAN BRUSHES

A maltoheptaose functionalized wafer was submerged in a buffered solution containing G-1-P (250 nM), phosphorylase (5 U.mL^{-1}) and GBE_{DG} (250 U.mL^{-1}). Citrate buffer (pH 6.2, 50 mM) was used when phosphorylase was utilized and a MOPS buffer (pH 8.0, 50mM) was used in the case of a tandem polymerization. The submerged wafer was, depending on the enzymes used, incubated for 3 days at 37 °C (tandem polymerization) or 38°C (phosphorylase) in a shaking incubator. Afterwards

the substrates where thoroughly rinsed with Milli Q water, dried with a stream of air and stored *in vacuo*.

3.3 RESULTS AND DISCUSSION

Before the enzyme catalyzed tandem polymerization can be performed on solid Si substrates, the Si surface needs first to be modified. This modification includes: aminosilanization and tethering the primer to the aminosilanization agent (see FIGURE 3.2) and is discussed in the next paragraphs.

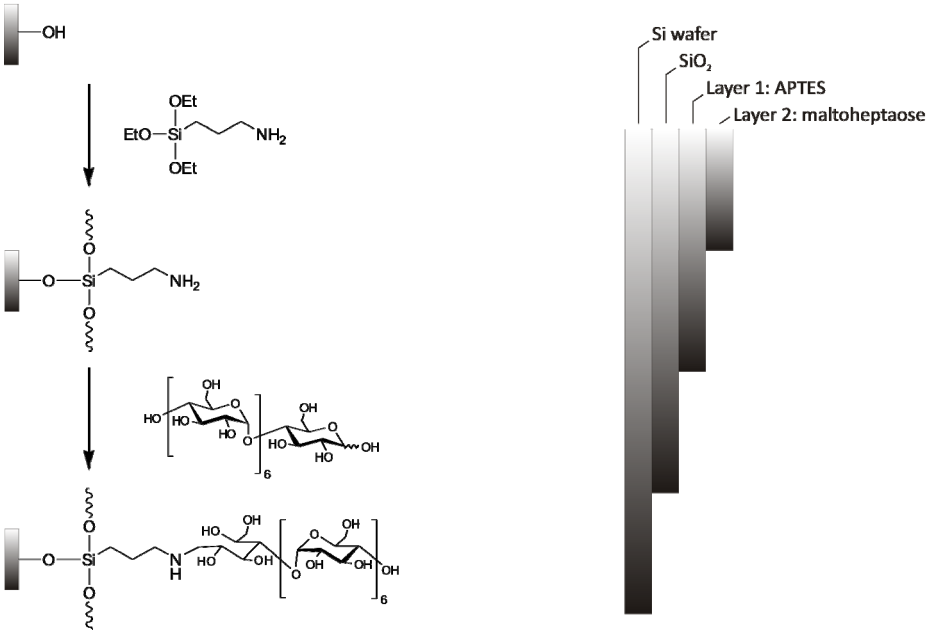

FIGURE 3.2: Schematic model of the different layers deposited on top of the Si wafer. The SiO_2 layer is the native oxide layer of the wafer. Layer 1, APTES: APTES is covalently bond to the native SiO_2 surface of the Si wafer and provides amine functionality to the surface. Layer 2, maltoheptaose: Maltoheptaose acts as acceptor substrate for the phosphorylase driven reaction.

3.3.1 Layer 1: Aminosilanization

The trifunctional APTES is used as an amine functionalized silanization agent. It is known that each APTES molecule makes on average 1 to 2 covalent attachments to the surface hydroxy groups. Leaving the remaining free ethoxy groups available for bonding with neighbouring APTES molecules[34]. The aminosilanized wafer is analyzed by XPS and ellipsometry.

X-RAY PHOTONELECTRON SPECTROSCOPY

XPS is a quantitative spectroscopic technique that measures the elemental composition of the top 10 nm of a surface. The XPS has an X-ray source that irradiates a surface in an ultra high vacuum. The (sample surface) electrons escape upon impact of the X-ray beam and the kinetic energy as well as the amount of electrons are analyzed, subsequently the binding energy is calculated. Due to differences in binding energy, elements can be distinguished. Moreover, the chemical environment of elements can be distinguished.

After the aminosilanization process, electrons from the N(1s) orbital and C(1s) core levels from the APTES can be detected by XPS. The Si(1s) and Si(2p) signals originate from the Si wafer (see FIGURE 3.4). This proves that the APTES molecules are covalently attached to the surface. Since there are still Si signals detected the APTES layer is <10 nm.

The C(1s) signal is deconvoluted in FIGURE 3.5 into 3 signals which are attributed to carbon atoms in different chemical environments as displayed in TABLE 3.3.

TABLE 3.3: Deconvolution of the C(1s) signal of an aminosilanized Si wafer.

element	binding energy (eV)	relative composition (%)
C-C	285.4	77.5
C-N	286.8	16.5
C-O	288.6	6.0

The 6.0 % attribution of the C-O signal indicates that there are still unreacted ethoxy groups present. It can be concluded that the baking of the wafers (120 °C for 30 minutes) was not sufficient to condensate all of the ethoxy groups. However, a value of 6 % is acceptable and not expected to have consequences for further procedures.

A soxleth extraction is used to remove all of the unreacted 'free' APTES molecules. Unreacted APTES can be quantified via XPS by comparing the C(1s) signal to the N(1s) signal. The C(1s)/N(1s) ratio of the respective signals is 3 for fully condensated APTES and 9 for 'free' APTES (see FIGURE 3.3). Therefore, the ratio of the surface area below the C(1s) and N(1s) signals of the respective core level regions is calculated and determined to be 3.63 (the sensitivity factors used are given in TABLE 3.2).

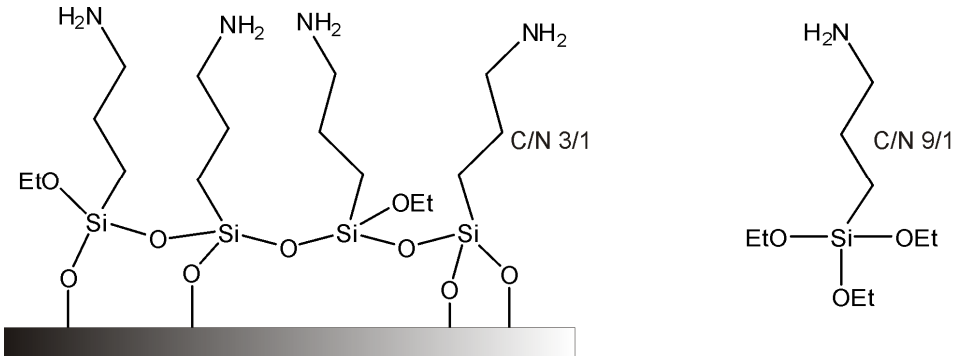

FIGURE 3.3: C/N ratio of condensated APTES molecules (left) and C/N ratio of 'free' APTES (right).

From the XPS measurements it can be concluded that unreacted APTES is effectively removed via a soxleth extraction. However 6 % of the ethoxy groups are not condensated.

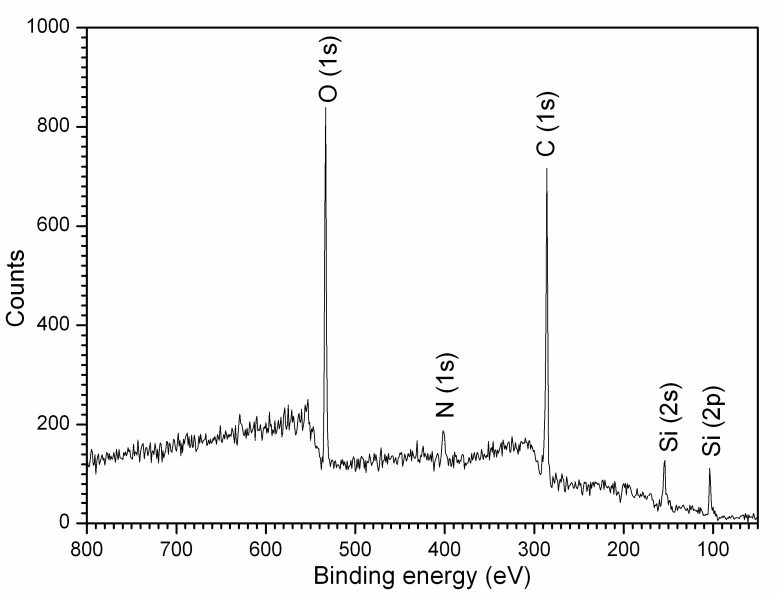

FIGURE 3.4: XPS survey spectrum of aminosilanized Si wafer.

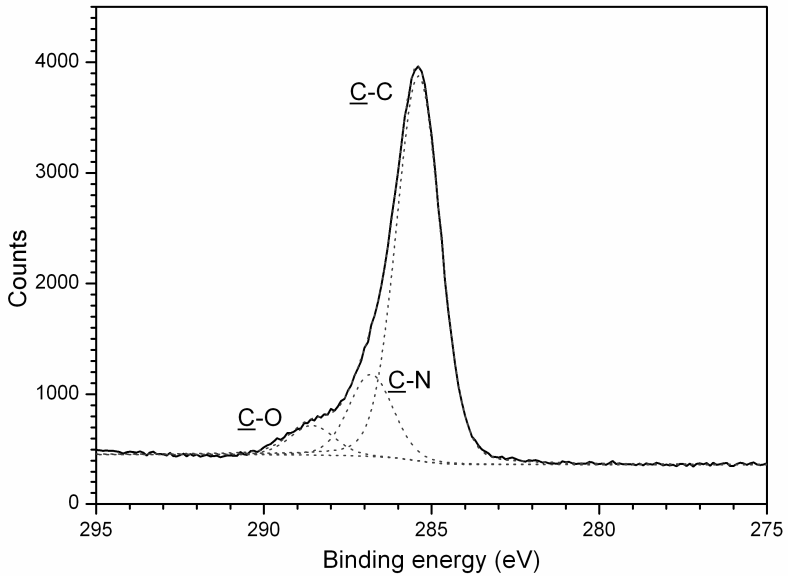

FIGURE 3.5: C(1s) core level region of the silicon wafer after aminosilanization.

SPECTROSCOPIC ELLIPSOMETRY

The layer thickness of the SiO_2, APTES and maltoheptaose layer is determined with spectroscopic ellipsometry. Ellipsometry is a measurement technique that uses polarized light to characterize thin films. In principle, ellipsometry measures the polarization state of a reflected light beam modified by an optical system (the sample substrate). The measured values are expressed as psi (Ψ) and delta (Δ) and are known as the ellipsometric parameters. The thickness and optical constants can be determined when the ellipsometric parameters are fitted in a suitable model. Here we use a cauchy dispersion model to calculate the thickness of the different layers. An overview of the ellipsometric data can be found in TABLE 3.4.

TABLE 3.4: Thickness of the the SiO_2-, APTES- and maltoheptaose layers.

Sample	SiO_2 thickness (nm)	APTES thickness (nm)	G7 thickness (nm)
1	3.606 ± 0.0224	4.661 ± 0.0206	3.388 ± 0.12
2	3.875 ± 0.0234	4.114 ± 0.0211	2.817 ± 0.0451
3	3.266 ± 0.0209	4.529 ± 0.0195	3.412 ± 0.0452
4	3.614 ± 0.0202	4.792 ± 0.0239	3.138 ± 0.0583
5	3.733 ± 0.0242	4.740 ± 0.0180	4.743 ± 0.0842
Average	**3.62 ± 0.23**	**4.57 ± 0.27**	**3.50 ± 0.74**

First a cleaned Si wafer was measured at 5 different positions to determine the average thickness of the SiO_2 layer. The average thickness was determined on 3.6 nm ± 0.2. This value is used in the ellipsometric model for the subsequent determination of the APTES- and maltoheptaose- layer thickness. The APTES layer thickness varied between 4.1 nm and 4.9 nm. An APTES monolayer is ~0.7 nm[32] meaning that multilayers of approximately 6 to 7 APTES molecules are formed. This kind of multilayer formation is quiet common for the type of aminosilanization agent used.

3.3.2 Layer 2: Primer functionalization of Si surfaces

In order to grow α-D-glucose residues on the amino functionalized substrate, first a short oligosaccharide has to be anchored to the APTES functionalized substrate. In this research maltoheptaose is anchored to the surface via a reductive amination with $NaCNBH_3$ as a reducing agent (see CHAPTER 1). After reaction, the substrates were sonicated with Milli Q water and ethanol in order to remove 'free' maltoheptaose. A small decrease in layer thickness is observed by ellipsometery suggesting that 'free' maltoheptaose is initially adsorbed to the Si wafer. Subsequent soxleth extraction with ethanol did not result in a further decrease in layer thickness.

So, the cleaning step as provided by ultrasonification is sufficient to remove unbounded maltoheptaose.

The layer thickness of maltoheptaose is as well measured by ellipsometry and is determined to be 3.5 ± 0.7 nm (see TABLE 3.4). This is in good agreement with the length of 1 maltoheptaose molecule. The (virtual) bond length of one glucose residue is 4.2 Å[35]. Taking 4.2 Å as unity, maltoheptaose would have a maximum length of 0.42*7 = 2.9 nm. Since maltoheptaose can take up to 10 % of (atmospheric) water, thicker layers can be observed.

The formation of the maltoheptaose layer is confirmed with transmission FT-IR spectrometry (see FIGURE 3.6).

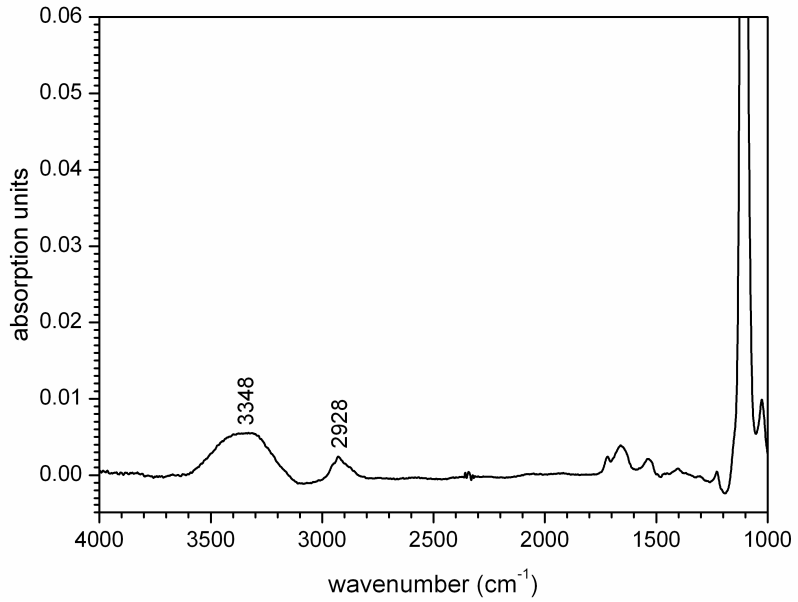

FIGURE 3.6: FT- IR transmission spectrum of a maltoheptaose functionalized Si wafer.

The maltoheptaose functionalized substrate was examined with transmission FT-IR and a clean double sided polished Si wafer was used as reference and is subtracted from the spectrum. Due to the small amount of material present on the wafer only a weak signal is visible. However, the typical CH and CH_2 vibration is visible at 2923 cm^{-1} and the sugar hydroxy moiety absorption can be observed between 3100 cm^{-1} and 3500 cm^{-1}.

The transmission FT-IR and ellipsometry measurements prove that the maltoheptaose layer is anchored to the amine functionalized Si wafer.

MALTOHEPTAOSE BRUSH CHARACTERISTICS

The amount of hydroxy groups per square nm was determined for a large number of amorphous silicas by Zhuravlev[36]. Zhuravlev found values around 4.9 $OH \cdot nm^{-2}$ for all determined surfaces.

The amount of aminosilanization agent per square nm is, after silanization, significantly lower. Moon et al.[37] and Zhao et al.[38] found values of 2.5 and 2.1 $amines \cdot nm^{-2}$, respectively.

The surface density of amine groups is an important value as it will determine the maximum brush density on the wafer. In this section the results as obtained via the method of Zhao[38] are discussed. The amine density on the wafers is determined:

- After silanisation *and*
- After anchoring maltoheptaose.

The method of Zhao consists of exposing the amine functionalized substrates to an anthraldehyde solution. This will convert all free available amines to the corresponding imines. Subsequently, the imine bearing substrates are hydrolyzed in a known volume of water and the UV absorption of this solution is measured at 260 nm.

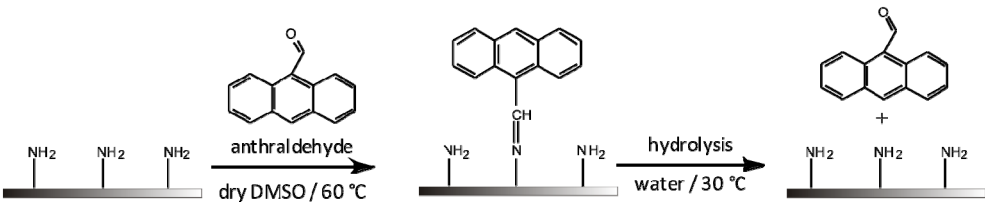

FIGURE 3.7: Reaction steps for the determination of the amine density.

Already small concentrations of anthraldehyde can be detected by UV spectroscopy due to the high absorption coefficient of the aromatic system.

Via this method the amine density was determined to be 2.8 $NH_2 \cdot nm^{-2}$ and is in good agreement with literature.

No absorption from the hydrolyzed anthraldehyde is measured after anchoring the maltoheptaose. This means that the amine functionalized substrate is completely converted to a maltoheptaose functionalized substrate or –and more likely– the maltoheptaose molecules cover the free amines and block thereby the reaction with anthraldehyde.

As the method of Zhao did not yield the expected primer density profile but only an amine density another approach is used: The primer density is calculated on the basis of EQUATION 3.1[39].

$$\sigma = L\rho N_a / M_n \qquad 3.1$$

Where *L* is the layer thickness as obtained with spectroscopic ellipsometry (3.5 nm, see TABLE 3.4), ρ is the density of maltoheptaose (1.0386 $g \cdot mL^{-1}$)[40], N_a is the constant of Avagadro and M_n is the molecular weight of maltoheptaose (1153 $g \cdot mol^{-1}$), yielding a grafting density of 1.89 nm^{-2}. This means that 67 % ([1.89/2.8]*100 %) of the amine groups are converted to maltoheptaose.

Loos et al.[41] reported that every third amine group react on average with maltoheptaose on amine functionalized silica beads. The difference can be explained by the reaction circumstances and analysis method.

It can be concluded that approximately 67 % of the amine groups react with maltoheptaose and a final primer density of almost 2 nm^{-2} is reached.

SURFACE TOPOLOGY

The surface topologies of the functionalized wafers are examined with AFM in tapping mode and give information about surface roughness and homogeneity. FIGURE 3.8represents 5 μm x 5 μm 3D views of a Si wafer, APTES functionalized wafer and a maltoheptaose functionalized wafer. The root mean square (RMS) roughness of the Si surface increases from 0.28 nm to 4.2 nm after the aminosilanization step. A further increase in the surface roughness to 5.4 nm is seen after the attachment of the maltoheptaose primers. The examined maltoheptaose substrates show a homogeneous surface over an area of 5 μm x 5 μm proving that the surface is completely covered with maltoheptaose.

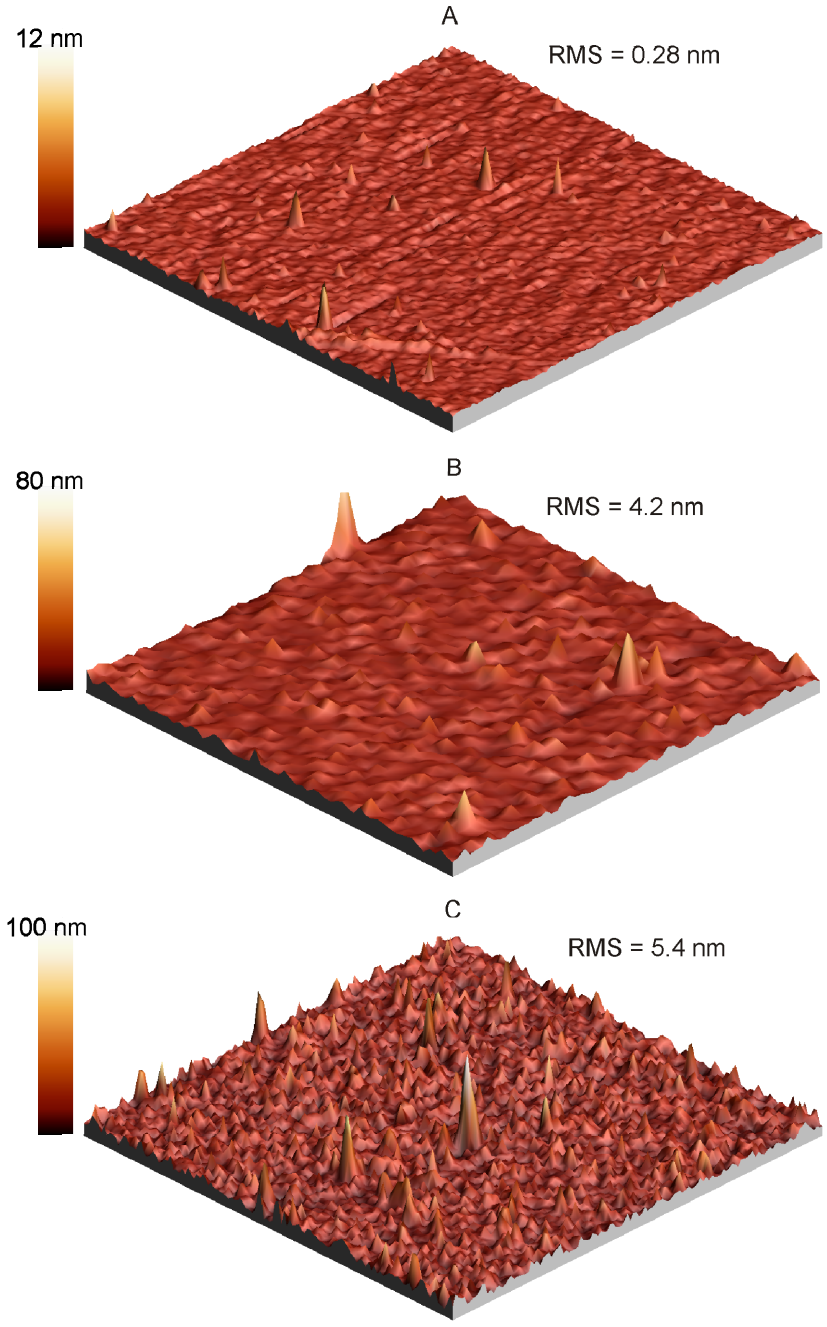

FIGURE 3.8: 3D AFM images of (A) Si wafer, (B) APTES functionalized wafer and (C) maltoheptaose functionalized wafer. Image size: 5 μm x 5 μm. (RMS roughness determined from a 10 μm x 10 μm area).

3.3.3 Enzyme catalyzed brush formation on Si surfaces

Taking the maltoheptaose functionalized wafers as starting material for the enzyme catalyzed surface initiated polymerization, polysaccharide brush coatings are grafted from solid supports. Linear as well as hyperbranched brushes are synthesized depending on the enzyme system used.

An important feature of a polymer brush coating used for anti-bacterial purposes is, next to the grafting density, the thickness. However, the degree of polymerization can not be followed with the modified[42] method of Fiske and Subbarow[43] as used in CHAPTER 2 because the amount of released P_i is below the detection limit. The average degree of polymerization is therefore estimated from the layer thickness as determined with ellipsometeric measurements.

Amylose forms by nature a helical structure consisting of a double-stranded left-handed helix. However, the linear brushes as grafted form the surface forms single stranded helices similar to Amylose V. Amylose V has a pitch of 8.05 Å with six glucose residues per turn[44]. By determining the layer thickness the amount of pitches and glucose residues can be calculated. For the sake of simplicity, the tilt angles of the chains are neglected (90°; perpendicular to the surface). In reality the tilt angle is equal to or smaller then 90°, resulting in a higher degree of polymerization.

The polymer brush thickness of linear, synthetic, amylose brushes as well as hyperbranched brushes are displayed in TABLE 3.5. The amount of pitches and the corresponding degree of polymerization are calculated for the linear brushes. An estimation of the amount of incorporated glucose residues for the hyperbranched brush coatings is unfortunately not possible with this method.

TABLE 3.5: Polyglucan brush thickness and the corresponding degree of polymerization.

Type of brush	Incubation time (days)	Thickness (nm)	# of pitches	Degree of pol.
Linear	3	16.719 ± 0.1440	20.8	125
Linear	3	20.171 ± 0.0405	25.1	150
Linear	3	15.214 ± 0.0314	18.9	113
Linear	3	19.435 ± 0.0557	24.1	144
Linear	3	19.654 ± 0.0700	24.4	146
Hyperbranched	3	16.903 ± 0.0432	--	--
Hyperbranched	3	12.223 ± 0.0242	--	--

The feed ratio G-1-P is in the order of 1000 (i.e. there are 1000 molecules G-1-P available per primer molecule). The results in CHAPTER 2 reveal that about 70 % of

the G-1-P is consumed by phosphorylase in the case of 'free' maltoheptaose. From this point of view synthetic amylose brushes with a DP of 700 could be expected. However, the degree of polymerization of the brushes as grafted on the Si wafers is between 100 and 146 glucose residues. Prolonged incubation of the wafers did not result in an increased layer thickness suggesting that the obtained layer thickness is limited to approximately 20 nm. Similar results are obtained by Breitinger[45] who obtained a degree of polymerization of between 100 and 250 depending on the length of the spacer used in between the surface and the primer recognition site. The highest degree of polymerizations (DP 250) is reached with longer spacers. So, the thickness of the brush layers as described in this chapter may be improved by using a long flexible spacer in between the surface and the maltoheptaose primer.

In CHAPTER 2 it was proven that a mixture of phosphorylase and GBE_{DG} catalyzes the formation of hyperbranched polyglucans with a degree of branching of 11 %. The determination of the degree of branching and the degree of polymerization of *grafted* hyperbranched polyglucan brushes is with the system as applied here not possible. However, it is not likely that the catalytic activity of GBE_{DG} or the activity of phosphorylase is altered in the grafting process. It is expected that the enzymes catalyze the growth of the brush until steric hindrance limits the catalytic activity of the enzymes.

In the future we hope to obtain more detailed data of the polyglucan brushes via XPS measurements. Another approach would be the use of a cleavable spacer in between the support and the maltoheptaose primer. With this it becomes possible to analyze the cleaved polymer chains with the same methods as described in CHAPTER 2.

SURFACE ANALYSIS OF THE HYPERBRANCHED BRUSHES

The surface topology of the hyperbranched brushes and the linear, amylose, brushes are investigated with AFM. Multiple areas are scanned and the roughness is determined. While the APTES- and maltoheptaose coatings were homogeneous and more or the less smooth, with the introduction of linear and hyperbranched brushes the surface becomes more rough. RMS roughness values differ from 7.2 (for hyperbranched brush coating) to 12.8 nm (for 'amylose' brush coating).

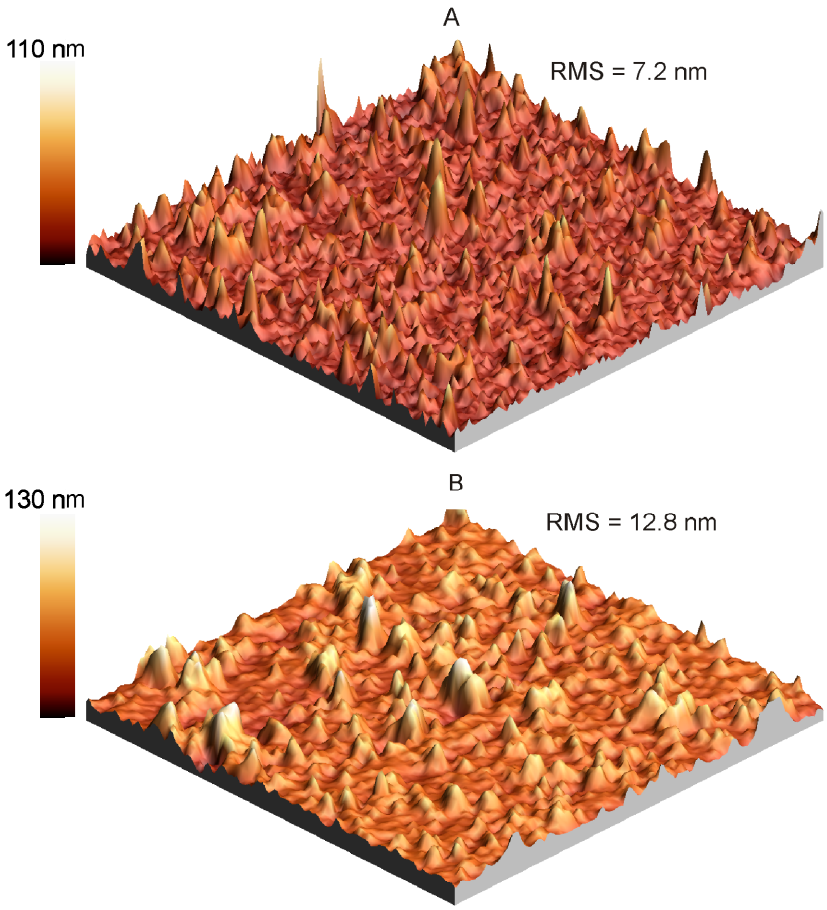

FIGURE 3.9: A) 3D AFM image of a hyperbranched brush coating grafted from a Si wafer. B) 3D AFM image of a linear polysaccharide brush coating grafted from a Si wafer. Image size: 5 μm x 5 μm. (RMS roughness determined from a 10 μm x 10 μm area).

3.4 CONCLUSION

It is shown that linear and hyperbranched polyglucan brushes can be grafted from maltoheptaose functionalized Si wafers via an enzyme catalyzed procedure. The resulting brush coatings have thicknesses of between 12 and 20 nm.

The procedure to make a polysaccharide brush coating starts with aminosilanization of the surface. Aminosilanization with APTES results in a multilayer deposit with a thickness of 4.6 nm and an amine density of 2.8 nm^{-2}. In the subsequent step, 67 % of the amines react with maltoheptaose. Maltheptaose acts herein as a primer recognition site for phosphorylase and linear polyglucan brushes can be grafted from the surface in the presence of G-1-P. Hyperbranched polyglucan brush coatings can be produced with the introduction of GBE_{DG}. The thickness of the brush coating is limited to approximately 20 nm. Steric hindrance of the densely packed chains is responsible for this limitation. By introducing more flexible spacers, an improvement in layer thickness is expected.

3.5 REFERENCE LIST

1. D.L. Schmidt, R.F. Brady, K. Lam, D.C. Schmidt, M.K. Chaudhury, *Langmuir*, **2004**, *20,* 2830-2836
2. R.D. Frank, H. Dresbach, H. Thelen, H.G. Sieberth, *Journal of Biomedical Materials Research*, **2000**, *52,* 374-381
3. P. Thomsen, C. Gretzer, *Current Opinion in Solid State & Materials Science*, **2001**, *5,* 163-176
4. L.J. Douglas, *Trends in Microbiology*, **2003**, *11,* 30-36
5. L.F. Melo, T.R. Bott, *Experimental Thermal and Fluid Science*, **1997**, *14,* 375-381
6. H.C. Flemming, T. Griebe, G. Schaule, *Water Sci. Technol.*, **1996**, *34,* 517-524
7. M. Amiji, K. Park, *Biomaterials*, **1992**, *13,* 682-692
8. Y.C. Tseng, T. McPherson, C.S. Yuan, K. Park, *Biomaterials*, **1995**, *16,* 963-972
9. M. Amiji, K. Park, *Journal of Biomaterials Science-Polymer Edition*, **1993**, *4,* 217-234
10. D. Leckband, S. Sheth, A. Halperin, *Journal of Biomaterials Science-Polymer Edition*, **1999**, *10,* 1125-1147
11. T. McPherson, A. Kidane, I. Szleifer, K. Park, *Langmuir*, **1998**, *14,* 176-186
12. S. Han, C. Kim, D. Kwon, *Polym. Degrad. Stab.*, **1995**, *47,* 203-208
13. S. Han, C. Kim, D. Kwon, *Polymer*, **1997**, *38,* 317-323
14. L. Yang, F. Heatley, T.G. Blease, R.I.G. Thompson, *Eur. Polym. J.*, **1996**, *32,* 535-547
15. C. Perrino, S. Lee, S. Won Choi, A. Maruyama, N.D. Spencer, *Langmuir*, **2008**, *24,* 8850-8856
16. M. Metzke, J.Z. Bai, Z. Guan, *J. Am. Chem. Soc.*, **2003**, *125,* 7760-7761
17. S.P. Massia, J. Stark, D.S. Letbetter, *Biomaterials*, **2000**, *21,* 2253-2261
18. Q. Yang, Z.K. Xu, M.X. Hu, J.J. Li, J. Wu, *Langmuir*, **2005**, *21,* 10717-10723
19. M. Metzke, Z. Guan, *Biomacromolecules*, **2008**, *9,* 208-215
20. N.B. Holland, Y.X. Qiu, M. Ruegsegger, R.E. Marchant, *Nature*, **1998**, *392,* 799-801
21. E. Monchaux, P. Vermette, *Langmuir*, **2008**, *23,* 3290-3297
22. M. Vanderwaarden, *Journal of Colloid Science*, **1950**, *5,* 317-325
23. M. Vanderwaarden, *Journal of Colloid Science*, **1951**, *6,* 443-449
24. E.L. Mackor, *Journal of Colloid Science*, **1951**, *6,* 492-495
25. E.L. Mackor, J.H. Vanderwaals, *Journal of Colloid Science*, **1952**, *7,* 535-550
26. E.J. Clayfield, E.C. Lumb, *J. Colloid Interface Sci.*, **1966**, *22,* 269
27. E.J. Clayfield, E.C. Lumb, *J. Colloid Interface Sci.*, **1966**, *22,* 285
28. S. Alexander, *Journal de Physique*, **1977**, *38,* 977-981
29. B. Zhao, W.J. Brittain, *Progress in Polymer Science*, **2000**, *25,* 677-710

30. I. Horcas, R. Fernandez, J.M. Gomez-Rodriguez, J. Colchero, J. Gomez-Herrero, A.M. Baro, *Rev. Sci. Instrum.*, **2007**, *78*
31. W.J. Hoover, A.I. Nelson, R.T. Milner, L.S. Wei, *J. Food Sci.*, **1965**, *30,* 253
32. E.T. Vandenberg, L. Bertilsson, B. Liedberg, K. Uvdal, R. Erlandsson, H. Elwing, I. Lundstrom, *J. Colloid Interface Sci.*, **1991**, *147,* 103-118
33. A. Simon, T. Cohen-Bouhacina, M.C. Porte, J.P. Aime, C. Baquey, *J. Colloid Interface Sci.*, **2002**, *251,* 278-283
34. P.A. Heiney, K. Gruneberg, J.Y. Fang, C. Dulcey, R. Shashidhar, *Langmuir*, **2000**, *16,* 2651-2657
35. V.S.R. Rao, N. Yathindr, P.R. Sundarar, *Biopolymers*, **1969**, *8,* 325
36. L.T. Zhuravlev, *Langmuir*, **1987**, *3,* 316-318
37. J.H. Moon, J.W. Shin, S.Y. Kim, J.W. Park, *Langmuir*, **1996**, *12,* 4621-4624
38. J. Zhao, Y. Li, H. Guo, L. Gao, *Chinese Journal of Analytical Chemistry*, **2006**, *34,* 1235-1238
39. I. Luzinov, D. Julthongpiput, H. Malz, J. Pionteck, V.V. Tsukruk, *Macromolecules*, **2000**, *33,* 1043-1048
40. J.A. Johnson, R. Srisuthep, *Cereal Chem.*, **1975**, *52,* 70-78
41. K. Loos, V. von Braunmühl, R. Stadler, *Macromol. Rapid. Comm.*, **1997**, *18,* 927-938
42. O.H. Lowry, J.A. Lopez, *J. Biol. Chem.*, **1946**, *162,* 421-428
43. C.H. Fiske, Y. Subbarow, *J. Biol. Chem.*, **1925**, *66,* 375
44. S. Immel, F.W. Lichtenthaler, *Starch*, **2000**, *52,* 1-8
45. H.G. Breitinger, *Tetrahedron Lett.*, **2002**, *43,* 6127-6131

CHAPTER 4

Hyperbranched polysaccharide sugar balls

SUMMARY

Linear and hyperbranched polyglucan multi-arm architectures are synthesized by a phosphorylase driven reaction. First multivalent primers were synthesized by the functionalization of butanediamine (BDA) and tris(2-aminoethyl)amine (TREN) with maltoheptaose via a reductive amination. Purification with Amberlite IR-120 (H^+) beads yielded fully substituted primers that were used to start the enzyme catalyzed reaction. Depending on the monomer-primer ratio different lengths of polyglucan arms could be realized. The addition of the branching enzyme, GBE_{DG}, resulted in hyperbranched multi arm structures. The hydrodynamic radii of the structures are determined with DLS and an increase in radius with increasing arm length is observed.

4.1 INTRODUCTION

The unique properties of hyperbranched polymers and dendrimers make them valuable in various fields. The abundant amount of (functional) end groups at the periphery can for example be used for post-polymerization reactions or to interact with their surroundings.

The polysaccharides glycogen and amylopectin are nature's realization of hyperbranched polymers. They have abundant hydroxy groups at the periphery and possess unique properties regarding the biocompatibility, biodegradability and bioactivity. Also, their renewable character can attribute to a sustainable development and environment conservation.

4.1.1 Dendrimers versus hyperbranched polymers

Dendrimers are perfectly branched macromolecules. Ideally, dendrimers consist of 100 % dendritic units and are spherical in structure. There are roughly two approaches to synthesize dendrimers. The convergent approach consists of the synthesis of dendrons that are linked to a central molecule[1]. The divergent approach starts the synthesis from a central molecule and the structure is built up towards the periphery[2,3]. This synthesis is usually based on a tedious multi-step protocol in which protection and de-protection steps are involved for each additional generation. The number of generations is limited by the steric hindrance occurring at the periphery of the dendrimer since the dendrimer grows exponentially with the number of generations and the available volume increases cubically[4].

Hyperbranched polymers consist of dendritic and linear units and are from the viewpoint of a dendrimer not perfectly branched. However, the production of hyperbranched polymers can usually be performed in a 1-pot synthesis and key features of dendrimers, such as: dense surface packing of functional groups, host-guest interaction, spherical in shape and low viscosity, are also valid for hyperbranched polymers[5]. Therefore it is not impossible that hyperbranched (glyco)polymers can be used in the same area of interest as (glyco)dendrimers.

The large scale availability of natural hyperbranched polysaccharides is limited, amylopectin, being one of them. The need to increase the variety of hyperbranched polysaccharides is multiple and includes:

- *Model compounds*. Synthetic hyperbranched polysaccharides can be used to understand biological processes such as the multivalent or cluster effect on carbohydrate-protein interactions[6,7]. But they are also important to elucidate the structure of amylopectin and glycogen and the enzyme catalyzed synthesis of them. In addition, the hyperbranched polysaccharides can be used as models for synthetic hyperbranched polymers.
- *New hyperbranched biomaterials*. Hyperbranched polysaccharides can be used to replace olefin based hyperbranched systems, for instance in coatings. And, due to the unique properties, hyperbranched polysaccharides can fulfil (new) functions in for example the food industry and the biomedical field.

The classical approach to obtain (semi)synthetic hyperbranched polysaccharides is the ring-opening multibranching polymerization of cyclic latent AB_m-type monomers. Schuerch et al. [8] reported the synthesis of branched polysaccharides in the 1950's by the acid catalyzed ring-opening polymerization of anhydrohexopyranoses in the solid phase. Kakuchi[9,10] optimized this synthesis using a thermal induced cationic initiation to polymerize anhydrohexopyranoses in solution. Kadokawa[11] used a oxazoline sugar having two hydroxyl groups that act as a latent AB_2-type monomer to produce a hyperbranched aminopolysaccharide.

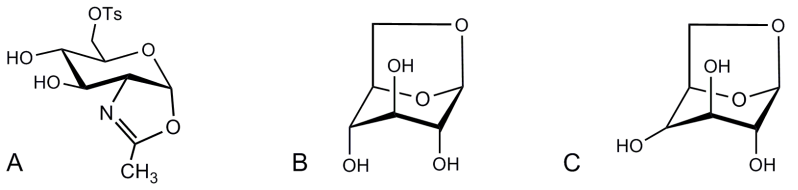

FIGURE 4.1: AB_m monomers used for the synthesis of hyperbranched polysaccharides. A) sugar oxazoline. B) 1,6-anhydro-β-D-mannopyranose. C) 1,6-anhydro-β-D-galactopyranose.

This approach results in randomly branched polymers with a degree of branching of 50 %[9,12]. α- and β-D-linkages were found and the polymerization is hence not stereoselective.

4.1.2 Glycoconjugated architectures

Glycoconjugates are in nature present as sugar containing lipids, proteins and peptides and are involved in cell-cell interaction, cell recognition, cell growth regulation, etc[13,14]. Synthetic glycoconjugates are synthesized in the form of polymers containing pendant sugar residues[15], glycoclusters[16], carbohydrate coated

dendrimers[17,18,19] or carbohydrate based dendrimers and mimic to some degree biological functions[20].

The hyperbranched structures as outlined in CHAPTER 2 can be covalently linked to a central molecule. In this way a hyperbranched glycoconjugate can be obtained with a central core molecule and hyperbranched polysaccharide arms.

Glycogen is also built up around a core molecule. The protein glycogenin acts as a primer for the *in vivo* biosynthesis of glycogen[21]. Glycogen appears in 2 different types. Spherical β-particles are 20 to 40 nm in diameter while α-particles are aggregrates of β-particles and can be found in the form of rosettes which can approach 200 nm in diameter[22].

This chapter covers the enzymatic synthesis of architectures consisting of multiple hyperbranched polyglucan chains connected to 1 central primer molecule. The synthesis and purification of di- and tri-valent primers is first described. Then the use of these primers as a starter for the enzyme catalyzed production of hyperbranched arms connected to a central core molecule is outlined (see FIGURE 4.2). The process can be compared with the divergent synthesis of dendrimers in which the structure is built up from the core molecule. Finally, the hydrodynamic radii of the obtained products are measured with DLS.

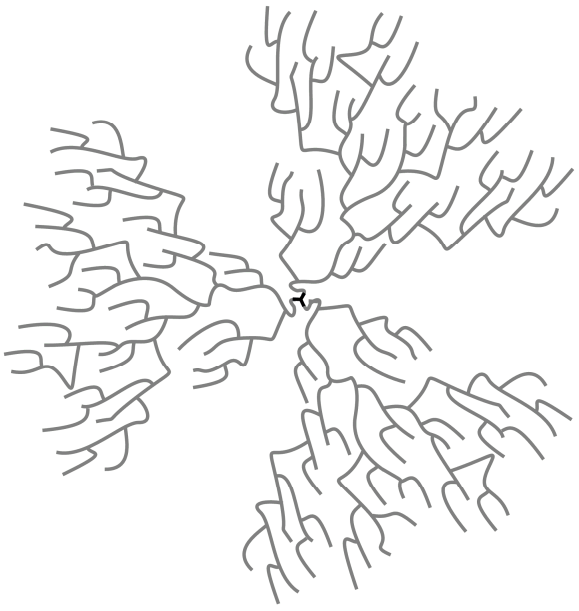

FIGURE 4.2: Impression of 3 hyperbranched arms connected to a central core molecule.

4.2 EXPERIMENTAL

4.2.1 Materials and chemicals

Butanediamine (BDA, Aldrich) was recrystalized before use and tris(2-aminoethyl)amine (TREN, Aldrich) was purified via a Kugelrohr distillation before use. The column material Amberlite IR-120 (H^+) ion exchange resin and were purchased at Aldrich. Dimethyl sulphoxide (DMSO, Labscan) was distilled from CaH_2 prior to use. Products were dialysed using dialysis tubing from Spectra/Por (MWCO 1000).

4.2.2 Analysis and equipment

DYNAMIC LIGHT SCATTERING (DLS)

DLS measurements were performed on an ALV CGS-3 goniometer equipped with an ALV LSE-5005 multiple τ digital correlator at angles of between 30° and 150° with a 10° interval at room temperature. Measurements were done in triplicate and averaged values are displayed. Fitting of the autocorrelation function was performed with the CONTIN algorithm.

Sample preparation

All samples were dissolved in water R.O. (1 $mg \cdot mL^{-1}$) and filtered (0.45 μm teflon filter).

^{1}H-NMR SPECTROSCOPY

^{1}H-NMR spectra were recorded on a Varian VXR spectrometer operating at 300 or 400 MHz at ambient temperatures. Dimethyl-2-silapentane-5-sulfonic acid (DSS) was used as an external reference.

^{1}H-NMR spectra used for the determination of the degree of branching were recorded on a Varian Inova 500 MHz spectrometer at 50 °C with pre-saturation of the HOD resonance. 2,2-dimethyl-2-silapentane-5-sulfonic acid (DSS) was used as an external reference. Complete relaxation of the protons was ensured by taking a 10 second pause between pulses.

INFRA-RED SPECTROSCOPY

Attenuated total reflection fourier transform infra-red (ATR FT-IR) spectra were recorded on a Bruker IFS88 spectrometer equipped with a MCT-A detector at a resolution of 4 cm^{-1} using an average of 50 scans for sample and reference.

ELEMENTAL ANALYSIS

Elemental analysis was performed on an EA3000 from EuroVector.

4.2.3 Methods, synthesis and procedures

ISOLATION AND PURIFICATION OF POTATO PHOSPHORYLASE

See experimental section CHAPTER 2.

CLONING, EXPRESSION AND PURIFICATION OF THE GLYCOGEN BRANCHING ENZYME

See experimental section CHAPTER 2.

ACTIVITY ASSAY PHOSPHORYLASE

See experimental section CHAPTER 2.

ACTIVITY ASSAY GLYCOGEN BRANCHING ENZYME

See experimental section CHAPTER 2.

SYNTHESIS OF MALTOHEPTAOSE

See experimental section CHAPTER 2.

SYNTHESIS OF DIFUNCTIONAL PRIMER

BDA (100 mg, 1 molar eq.), maltoheptaose (1.31 g, 1 molar eq.) and $NaCNBH_3$ (107 mg, 1.5 molar eq.) were dissolved in 6 mL DMSO containing 1 V/V % acetic acid and 3 Å molsieves. This mixture was placed in an incubator at 65 °C and was shaken for 6 days. After 3 days 1.5 molar eq. $NaCNBH_3$ and 0.9 molar eq. maltoheptaose were added. The reaction mixture was precipitated in ethanol, filtrated over a p4 glass filter, washed with acetone and ethanol and dried *in vacuo*, yielding a yellow powder (2.77 g). The product was dissolved in 50 mL water containing Amberlite IR-

120 (H^+) beads and was shaken overnight in an incubator at 40 °C. The solution was lyophilized yielding a yellow powder (1.69 g / 61 %).

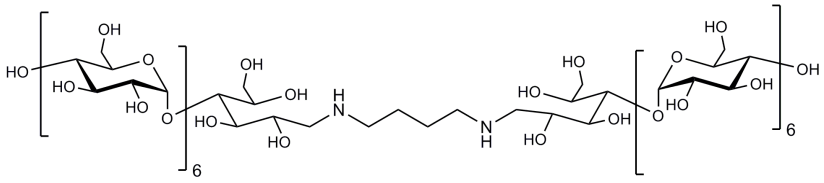

FIGURE 4.3: Fully functionalized BDA. BDA-$(G7)_2$.

^{1}H-NMR (D_2O, 300 MHz). 5.39 ppm: H1(m) and H1(n) of glucose residue, 5.11 ppm: C$\underline{H_2}$-NH, 4.12-3.51 ppm: glucose residue, 3.41 ppm: H4(m).
FT-IR. OH stretching glucose residues: 3683-2991 cm^{-1}, CH and CH_2 stretching: 2923 cm^{-1}, water deformation band: 1640 cm^{-1}, OH: 1358 cm^{-1}
Elemental analysis

	C (%)	H (%)	N (%)
Theoretical	44.74	6.66	1.19
Observed	39.67	5.98	1.23

SYNTHESIS OF TRIFUNCTIONAL PRIMER

TREN (100 μL, 1 molar eq.), maltoheptaose (1.16 g, 1.5 molar eq.) and $NaCNBH_3$ (126 mg, 3 molar eq.) were dissolved in 6 mL DMSO containing 1 V/V % acetic acid and 3 Å molsieves. This mixture was placed in an incubator at 65 °C and was shaken for 6 days. 1.5 molar eq. $NaCNBH_3$ and 1.4 molar eq. maltoheptaose were added after 3 days. The reaction mixture was precipitated in ethanol, filtrated over a p4 glass filter, washed with acetone and ethanol and dried *in vacuo*, yielding a yellow powder (2.26 g). The product was dissolved in 50 mL water containing amberlite IR-120 (H^+) beads and was shaken over night in an incubator at 40 °C. The solution was lyophilized yielding a yellow powder (1.01 g / 45 %).

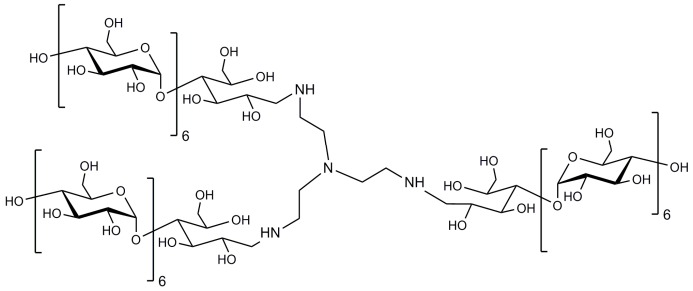

FIGURE 4.4: Fully functionalized TREN. TREN-(G7)$_3$.

^{1}H-NMR (D_2O, 300 MHz). 5.39 ppm: H1(m) and H1(n) of glucose residue, 5.11 ppm: C$\underline{H_2}$-NH, 4.12-3.51 ppm: glucose residue, 3.41 ppm: H4(m).
FT-IR. OH stretching glucose residues: 3683-2991 cm^{-1}, CH and CH_2 stretching: 2923 cm^{-1}, water deformation band: 1640 cm^{-1}, OH: 1358 cm^{-1}
elemental analysis

	C (%)	H (%)	N (%)
Theoretical	44.57	6.63	1.58
Observed	41.4	6.26	1.53

TYPICAL ENZYME CATALYZED POLYMERIZATION

Primer (0.5 mM), G-1-P (25-500 mM), phosphorylase (5 U·mL^{-1}) and GBE_{DG} (250 U·mL^{-1}) were mixed and filled to 5 mL MOPS buffer (pH 7.0, 50 mM). When only phosphorylase is utilized a citrate buffer (pH 6.2, 50mM) was used. Different ratios G-1-P to primer were used by varying the G-1-P concentration. The solution was depending on the enzymes used incubated at 37 °C (tandem polymerization) or 38°C (phosphorylase) in a shaking incubator. The released amount of phosphate was measured with a modified[23] method of Fiske and Subbarow[24]. Upon reaching equilibrium conditions the reaction was stopped by a heat treatment (5 minutes in boiling water). Denaturated enzymes were removed by means of centrifugation. Dialysis (MWCO1000) and lyophilization of the remaining solution yields the hyperbranched structures.

SPECTROSCOPIC PHOSPHATE DETERMINATION

See experimental section CHAPTER 2.

4.3 RESULTS AND DISCUSSION

Phosphorylase is able to catalyze the linear chain formation of, α(1→4) linked, maltodextrins with a minimum primer length of 3 glucose residues. Linear amylose chains can be synthesized in this way. In order to make more complex structures, bi- and tri-valent primers are synthesized. The primer sites needed for the enzymatic catalyzed elongation are therefore respectively coupled to butanediamine (BDA, see FIGURE 4.3) and tris(2-aminoethyl)amine (TREN, see FIGURE 4.4).

Coupling takes place via a reductive amination with $NaCNBH_3$ as reducing agent. The reducing group of the maltoheptaose reacts herein with the primary amines of the amine functionalized core molecules and the formed imine intermediate is subsequently reduced to a secondary amine.

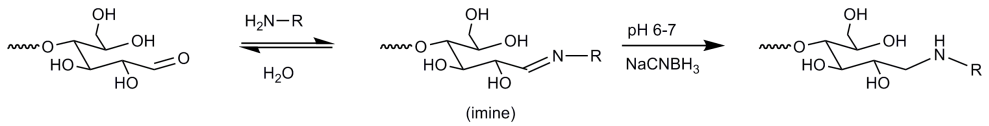

FIGURE 4.5: General formulation of the coupling of an amine to a reducing sugar group.

A large excess of maltoheptaose would increase the reaction speed and would guarantee a high yield of fully functionalized product. However, the excess of maltoheptaose is difficult to remove after the reaction and therefore this is not a good option.

Instead a small excess of amine groups to maltoheptaose is used together with long reaction times. This method results in a mixture of completely primer functionalized core molecules and partly functionalized core molecules, having one or more unreacted amine groups. This mixture is easier to separate if compared with the previously suggested method. All possible reaction products are shown in FIGURE 4.6.

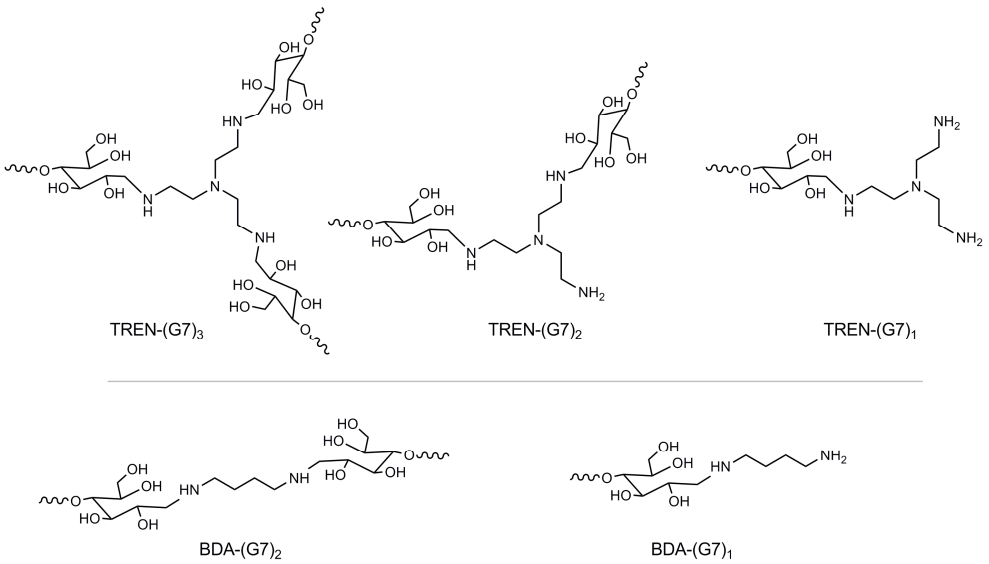

FIGURE 4.6: Different reaction products after the reductive amination of maltoheptaose and amine functionalized core molecules in order to obtain di- and trivalent primers.

4.3.1 Purification of the multivalent primers

Purification of the above described mixture is possible with Amberlite IR-120 (H^+) resin. This strong cation-exchange resin is able to adsorb amine functionalized molecules[25,26]. The unreacted and partly reacted starting material can therefore be separated from the product. The adsorbed side products are eluted with a 10 % ammonia solution. The 2 fractions are analysed with ^{1}H-NMR spectroscopy, IR spectroscopy and elemental analysis for the nitrogen content.

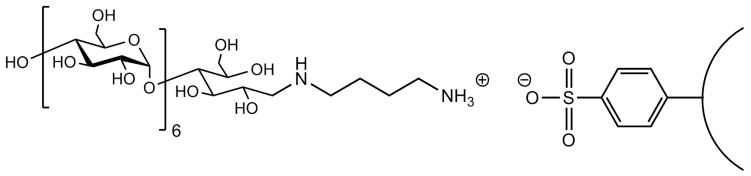

FIGURE 4.7: Adsorbtion of BDA-(G7)$_1$ to the functional, sulfonic acid, group of the amberlite beads. Elution with 10 % ammonia retrieves these products.

NITROGEN CONTENT ANALYSIS

The nitrogen content of the fully substituted products and the partly substituted products differ approximately a factor 2. Therefore determination of the nitrogen

content by elemental analysis is a good method to distinguish the fully substituted products from the partly substituted products. The results are listed in TABLE 4.1.

TABLE 4.1: Elemental analysis results after purification with Amberlite IR-120 (H+).

Compound	Washed with	Nitrogen content (%) Theoretical	Nitrogen content (%) Observed
BDA-$(G7)_2$	Water	1.19	1.23
BDA-(G7)	10 % Ammonia	2.29	3.67
TREN-$(G7)_3$	Water	1.58	1.53
TREN-$(G7)_2$, TREN-$(G7)_1$	10 % Ammonia	2.31 4.37	3.05

The nitrogen content of BDA-$(G7)_1$ is 1.9 times higher than BDA-$(G7)_2$. The nitrogen content of TREN-$(G7)_1$ and TREN-$(G7)_2$ is, respectively, 2.8 and 1.5 times higher when compared to the nitrogen content of TREN-$(G7)_3$. This significant difference in nitrogen content of the different functionalized products is a clear indication that the main compound in the water eluted fraction is the fully substituted product, BDA-$(G7)_2$ or TREN-$(G7)_3$, respectively.

^{1}H-NMR SPECTROSCOPY

A competitive side reaction during the reductive amination is the reduction of the sugar aldehyde group to an alcohol.

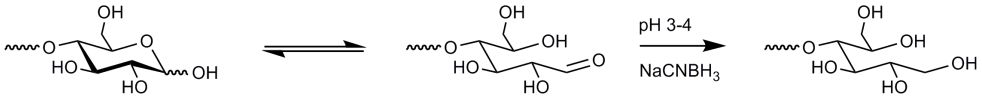

FIGURE 4.8: The unwanted reduction of the sugar aldehyde group.

Formation of a secondary amine and thus coupling is inhibited when the aldehyde group is reduced to an alcohol. A blank reaction was performed under the same reaction conditions as outlined in the experimental section with the difference that an amine bearing group is absent and a 10-fold excess of $NaCNBH_3$ is used. This will promote the side reaction as depicted in FIGURE 4.8. ^{1}H-NMR spectroscopy showed an intact reducing group after reaction proving that this side reaction does not occur under the circumstances chosen.

FIGURE 4.9 shows the ^{1}H-NMR spectra of BDA-$(G7)_2$ and BDA-$(G7)_1$ after the purification process with Amberlite IR-120 (H^+) beads. *Spectrum A* is the product obtained after elution with water and *spectrum B* is the product obtained after elution with 10 % ammonia. The complete disappearance of the H2β (3.26 ppm)

signal of the reducing sugar proves that maltoheptaose is reduced and coupled to BDA at both sides (spectrum A). The aliphatic protons of the core molecule are not visible in the complete functionalized BDA-$(G7)_2$ as aggregate formation shields the protons in the core molecule making them invisible.

Spectrum B does show the aliphatic core molecules of BDA. A broad signal between 1.49 and 1.84 ppm is attributed to the 2 inner methylenes while the broad signal between 2.68 and 2.92 ppm and 2.92 and 3.29 ppm are attributed to the methylenes next to the primary amine and secondary amine, respectively. The signal at 5.11 ppm, visible in spectrum A and B, originates from the methylene next to the secondary amine.

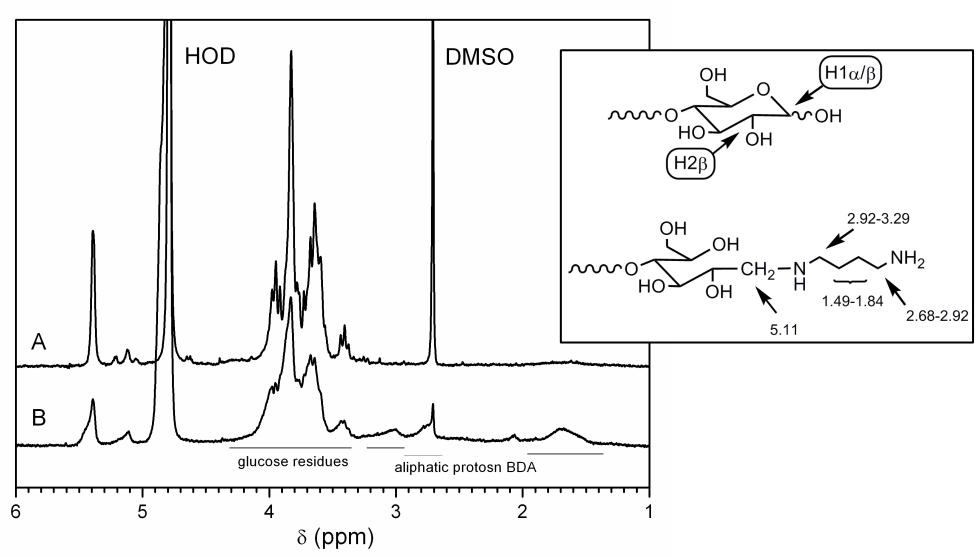

FIGURE 4.9: ^{1}H-NMR spectra of BDA functionalized products after purification with Amberlite IR-120 (H^+) beads. A) BDA-$(G7)_2$. Obtained after elution with water. B) BDA-$(G7)_1$. Obtained after elution with 10 % ammonia.

FIGURE 4.10 shows the ^{1}H-NMR spectra of the TREN functionalized products after purification with Amberlite IR-120 (H^+). Spectrum C is the product obtained after elution with water and spectrum D is the product obtained after elution with 10 % ammonia. The aliphatic core methylene groups are just like in spectrum A not visible in spectrum C but are visible in spectrum D as a very broard signal ranging from 2.33-3.14 ppm. The signals at 5.23 and 4.65 ppm indicate the presence of unreacted maltoheptaose (spectrum D).

On the basis of of the ^{1}H-NMR results it can be concluded that the side reaction as depicted in FIGURE 4.8 does not occur and that the reducing group of the sugar reacts with the primary amines as can be concluded from the disappearance of the H2β signal of maltoheptaose. However, traces of unreacted maltoheptaose are still present.

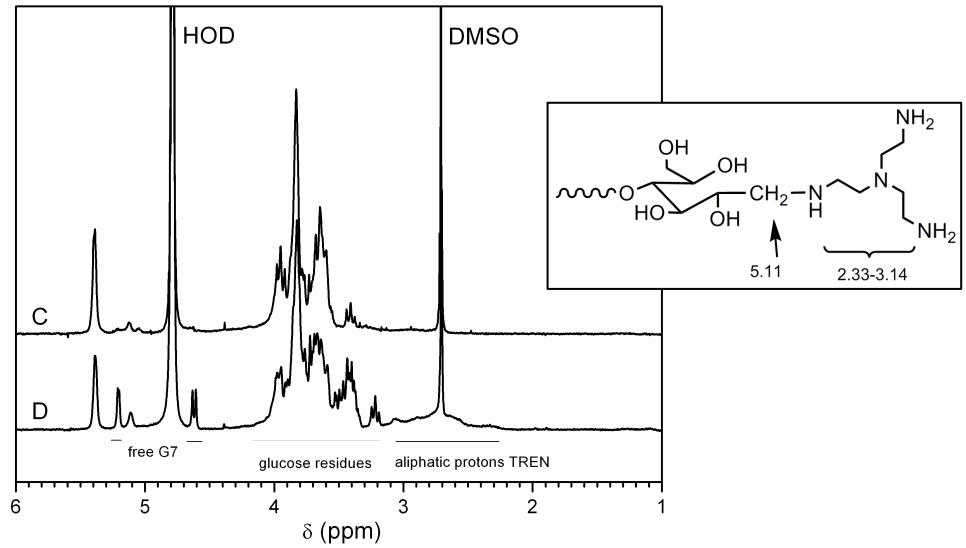

FIGURE 4.10: ^{1}H-NMR spectra of TREN functionalized products after purification with Amberlite IR-120 (H^{+}) beads. C) TREN-$(G7)_3$. Obtained after elution with water. D) TREN-$(G7)_1$ and TREN-$(G7)_2$. Obtained after elution with 10 % ammonia.

ATR FTIR SPECTROSCOPY

The unreacted amine groups present in partly substituted material are well visible with ATR FTIR spectroscopy (see FIGURE 4.11 and FIGURE 4.12) and can be used to distinct partly substituted material from fully substituted material. The N-H bend vibration of primary amines is visible at 1593 cm^{-1}. This band is only visible in the ammonia eluted products, proving that the purification with the Amberlite IR-120 (H^{+}) beads is quantitative. The signal at 1640 cm^{-1} that partly overlaps the N-H bend vibration originates from absorbed water[27] and is visible in all spectra (water deformation band). Prolonged drying of the products is necessary to remove the water. The N-H stretch vibrations are overshadowed by the sugar hydroxy groups (3670-2988 cm^{-1}) and can not be used to indentify the products.

Only BDA-$(G7)_2$ and TREN-$(G7)_3$ are present in the water eluted samples. Primary amines are only found in the ammonia eluted samples. The separation of the fully functionalized core molecules and partially substituted products is therefore according to the results of ATR FTIR spectroscopy complete.

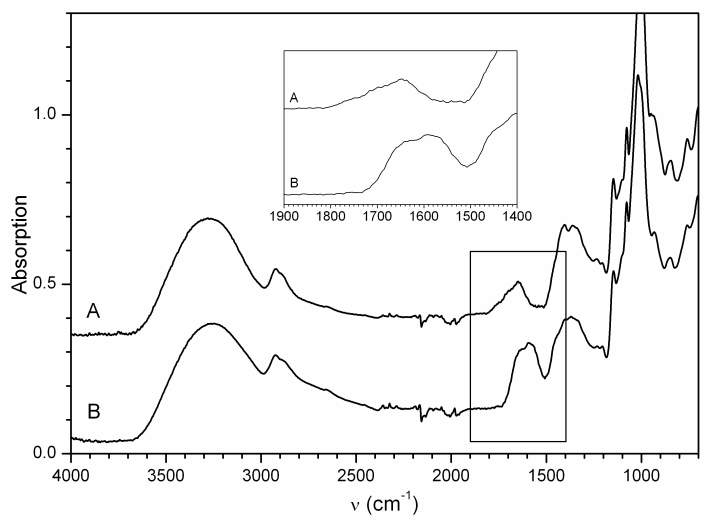

FIGURE 4.11: ATR FTIR spectrum of A) BDA-(G7)$_2$, B) BDA-(G7)$_1$.

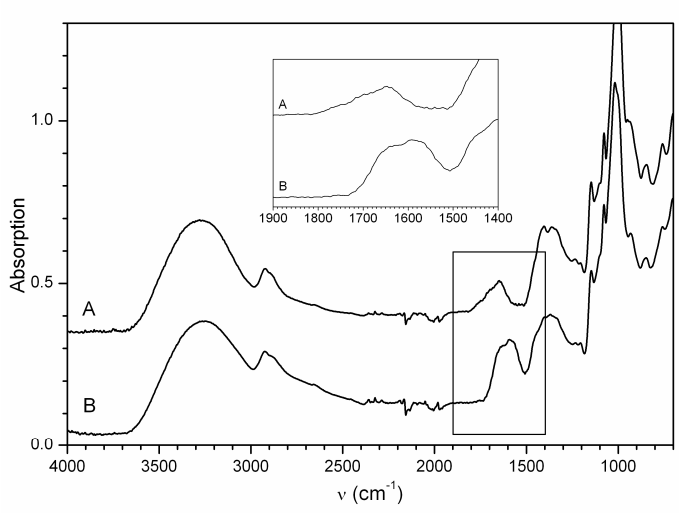

FIGURE 4.12: ATR FTIR spectrum of C) TREN-(G7)$_3$, D) TREN-(G7)$_1$ and TREN-(G7)$_2$.

4.3.2 Tandem reaction starting from multifunctional primers

KINETICS OF PHOSPHORYLASE CATALYZED POLYMERIZATION

BDA-$(G7)_2$ and TREN-$(G7)_3$ are successfully used as a multifunctional primer for the production of synthetic amylose. The initial reaction course is followed and compared with a maltoheptaose primed reaction (see FIGURE 4.13). The primer concentration is kept low in order to perform the reaction in a regime where the primer concentration is rate determining. On the other hand the G-1-P concentration is kept high (500 fold excess) to ensure that only the initial, linear, part of the reaction is monitored. The reaction course as presented in FIGURE 4.13 has after 90 minutes a conversion below 20 %. This is considered as the linear part of the reaction.

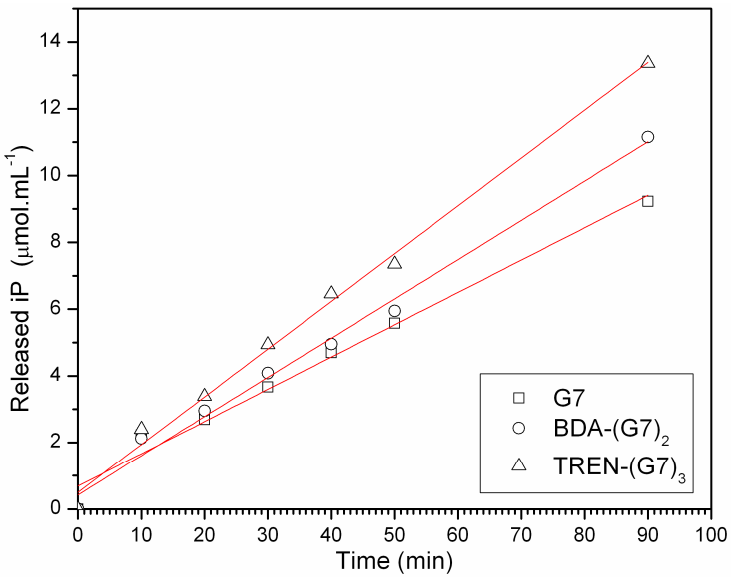

FIGURE 4.13: Initial reaction course of a phosphorylase driven polymerization started from G7, BDA-$(G7)_2$ and TREN-$(G7)_3$. Reaction performed in 0.5 ml citrate buffer (pH 6.2, 50 mM) at 38°C with a primer concentration of 0.05 mM, 25 mM G-1-P and 2.2 U·mL^{-1} phosphorylase.

The slope of the line is taken as the reaction rate. Since BDA-$(G7)_2$ and TREN-$(G7)_3$ carry, respectively, 2 and 3 maltoheptaose moieties per mole multivalent primer, the reaction rate exceeds the maltoheptaose primed reaction (see TABLE 4.2.)

TABLE 4.2: The rate of reaction of phosphorylase catalyzed polymerizations started from different (multivalent) primers.

Primer	Primer concentration (mM)	Reaction rate * ($\mu M \cdot sec^{-1}$)	Theoretical reaction rate ($\mu M \cdot sec^{-1}$)
G7	0.05	1.61	--
BDA-$(G7)_2$	0.05	1.96	3.22
TREN-$(G7)_3$	0.05	2.39	4.83

** The reaction rate is expressed as the amount of released P_i ($\mu M \cdot sec^{-1}$).*

The experimental obtained reaction rates are lower than the expected reaction rates, which is caused by:

- Phosphorylase is not able to elongate the maltoheptaose moieties of the multivalent primers at the same time. Sterical hindrance, especially in the initial part of the polymerization, may be the cause.
- The maltoheptaose moieties of the multivalent primers are too densely packed. Sterical hindrance is again responsible for the suppression of the reaction rate. Pfannemüller et al. experienced this behaviour in the case of densely packed multivalent primers[28,29]. Moreover, similar results were obtained in CHAPTER 3 where grafted polyglucan brushes were limited to 20 nm in thickness.

TANDEM POLYMERIZATION STARTED FROM MULTIVALENT PRIMERS

Phosphorylase and GBE_{DG} are employed in order to construct hyperbranched multi-arm architectures. Different arm lengths were realized by varying the feed ratio of G-1-P. Furthermore, the maximum conversion of the the BDA-$(G7)_2$ and TREN-$(G7)_3$ primed polymerization were determined in equilibrium conditions. FIGURE 4.14 shows the obtained arm lengths for a given feed ratio of G-1-P. The observed linear trend is a proof for the living character of the polymerization while the slope of the function represents the conversion of the reaction. Each data point represents an enzyme catalyzed tandem reaction with a specific feed ratio of G-1-P.

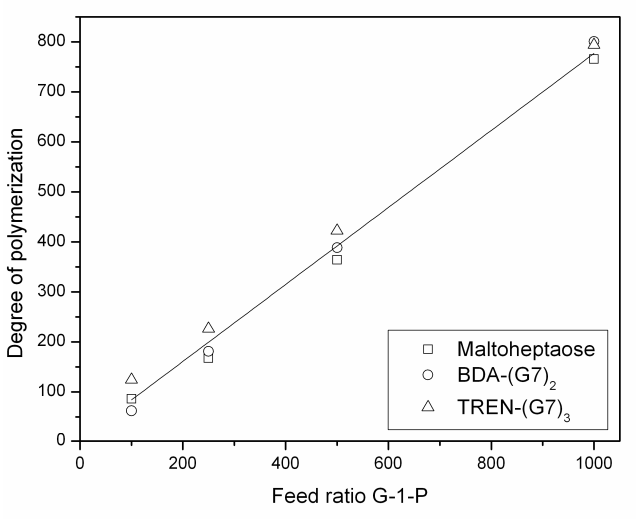

FIGURE 4.14: Average degree of polymerization for a given feed ratio of G-1-P . The slope of the linear trend line represents the conversion of G-1-P (only one trend line is displayed). Reactions performed in 5 ml MOPS buffer (pH 7.0, 50 mM) at 37°C with a primer concentration of 0.1 mM, 10-100 mM G-1-P, 4 U·mL^{-1} phosphorylase and 280 U·mL^{-1} GBE$_{DG}$.

The conversion of the multivalent primed reactions and the degree of polymerization are presented in TABLE 4.3.

The conversion of the different primed reactions varies from 74 % for maltoheptaose primed reactions to 80 % for TREN-(G7)$_3$ primed reactions. It is believed that this difference is within the experimental error. In general, reactions catalyzed with phosphorylase result in conversions of between 60 % and 80 %.

The degree of polymerization increases linear with the feed ratio of G-1-P. This is in line with the results as presented in chapter 2. By choosing the right feed ratio G-1-P, the length of the hyperbranched polyglucan chain can be predetermined. With the current method only average arm lengths can be determined rather than individual values.

TABLE 4.3: Conversion and final degree of polymerization of the enzyme tandem reaction starting from multifunctional primers.

Primer	Feed ratio G-1-P	Conversion (%)[A]	# Incorporated glc. residues (/arm) [B]	
G7	100	74	86	
	250		168	
	500		364	
	1000		765	
BDA-$(G7)_2$	100	78	62	(31)
	250		181	(91)
	500		388	(194)
	1000		800	(400)
TREN-$(G7)_3$	100	80	124	(41)
	250		226	(75)
	500		422	(141)
	1000		794	(265)

[A] *The conversion as displayed in the table is the slope of the linear solid line in FIGURE 4.14*
[B] *The amount of incorporated glucose residues is determined via the modified[23] inorganic phosphate assay as described by Fiske and Subarrow[24].*

DEGREE OF BRANCHING

The degree of branching of the polysaccharide part of the multi arm architectures is determined with ^{1}H-NMR. The ratio of the $\alpha(1\rightarrow6)$ signal relative to the $\alpha(1\rightarrow4)$ signal is taken as the degree of branching (see CHAPTER 2 for more information). FIGURE 4.15 shows the degree of branching for a given feed ratio of G-1-P. The trend line gives the theoretical degree of branching if on average every 9th glucose residue acts as a branching point and approaches a degree of branching of 11 %, as was determined in CHAPTER 2.

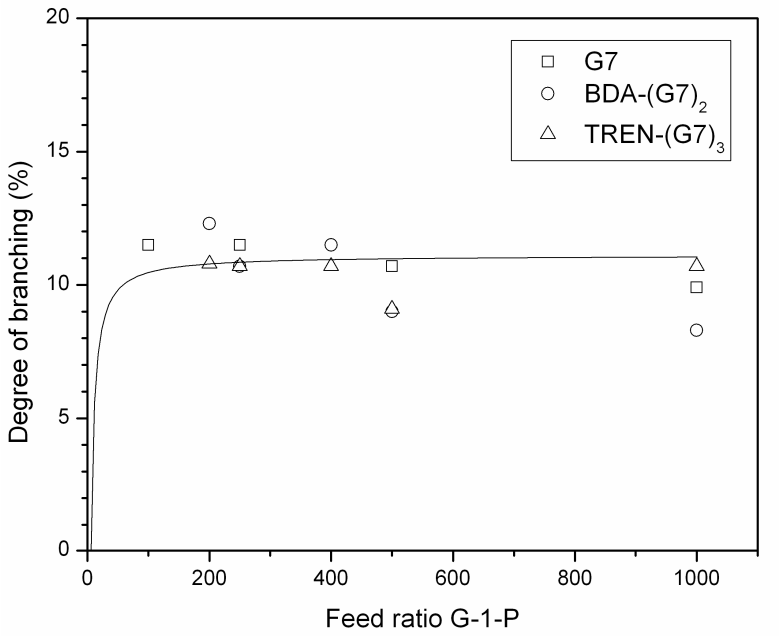

FIGURE 4.15: The final degree of branching of G7, BDA-(G7)$_2$ and TREN-(G7)$_3$ primed products, as determined by ^{1}H-NMR. The solid line gives the theoretical degree of branching with a side chain length of 9 glucose residues.

The hyperbranched amylose arms have, independent of the primer used, an average degree of branching of 10.5 %. This corresponds with an average side chain of 9.5 glucose residues. Palomo et al.[30] reported that GBE_{DG} transfers oligosaccharides with a preference for chains with a length of 6-7 glucose residues. However, they found a side chain distribution between 4 and 17. This same characteristic branching pattern is confirmed by MALDI-ToF measurements for *in situ* branched products (see CHAPTER 2).

In conclusion, phosphorylase, as well as GBE_{DG}, catalyze the synthesis of synthetic hyperbranched amylose chains started from multivalent primers. GBE_{DG} performs this task unhindered while suppression in the rate of the reaction is seen for the phosphorylase catalyzed elongation of the multivalent primers.

4.3.3 Particle size determination

The hyperbranched structures as described in the previous paragraphs are subjected to dynamic light scattering measurements in order to determine the particle size. DLS measurements show diameters in the order of 14-28 nm depending on the feed ratio G-1-P.

The DLS autocorrelation functions of the hyperbranched polysaccharides were recorded with DLS in triplo, the CONTIN algorithm is used to calculate the decay rates (Γ) of the distribution functions at different scattering vectors (q) (see FIGURE 4.16). The translational diffusion coefficient (D_t) is obtained from the decay time (τ), according to the relationship as displayed in EQUATION 4.1.

$$\frac{1}{\tau} = \Gamma = q^2 D_t \qquad 4.1$$

The mean translational diffusion coefficient is determined from the slope of the function $\Gamma(q^2)$ as depicted in FIGURE 4.17.

A linear variation of Γ versus q^2 passing through the origin is characteristic of a translational diffusive process typical for spherical particles[31].

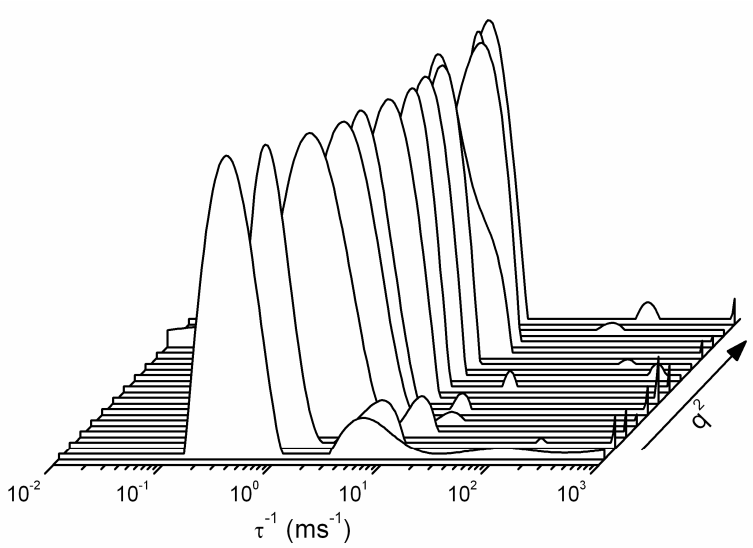

FIGURE 4.16: Example of the distribution functions as obtained by the CONTIN algorithm at different scattering vectors.

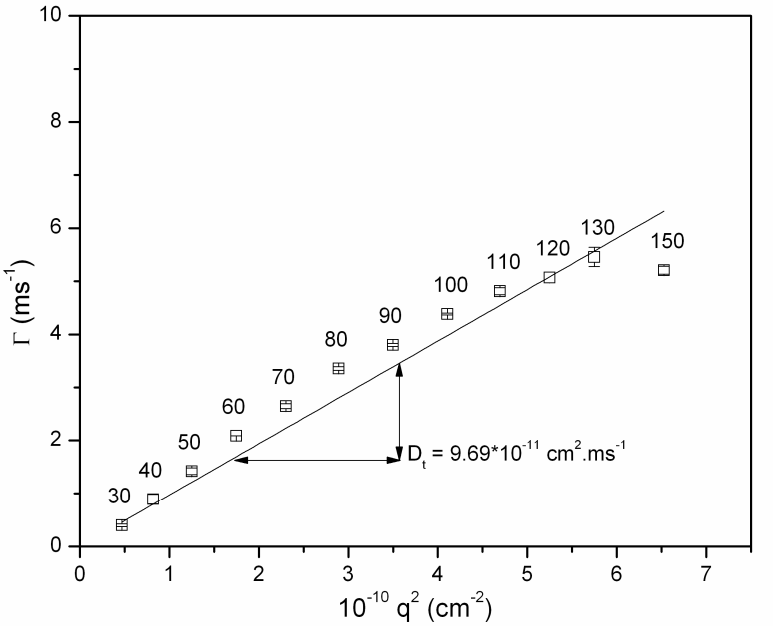

FIGURE 4.17: Linear fit of Γ versus q^2. The decay rates are obtained from the maximum values of the main signals of FIGURE 4.16.

The diffusion coefficient is related to the hydronamic radius (R_H) via the Stokes-Einstein equation. Since the Stokes-Einstein relation is only valid for hard spherical particles the term apparent hydrodynamic radius is introduced ($R_{H(app)}$).

$$R_{H(app)} = \frac{k_B T}{6\pi\eta D_t} \qquad 4.2$$

Where k_B, T and η are the Boltzmann constant, temperature (K) and the solvent viscosity.

FIGURE 4.18 shows the relationship of the hydrodynamic radii and the feed ratio G-1-P. The hydrodynamic radii of the structures increase with increasing feed ratio G-1-P. A difference in size is observed if the different core molecules are compared. G7 > TREN-$(G7)_3$ > BDA-$(G7)_2$. Since the degree of polymerization and the degree of branching is comparable for the different structures this effect has to originate from the central core molecules.

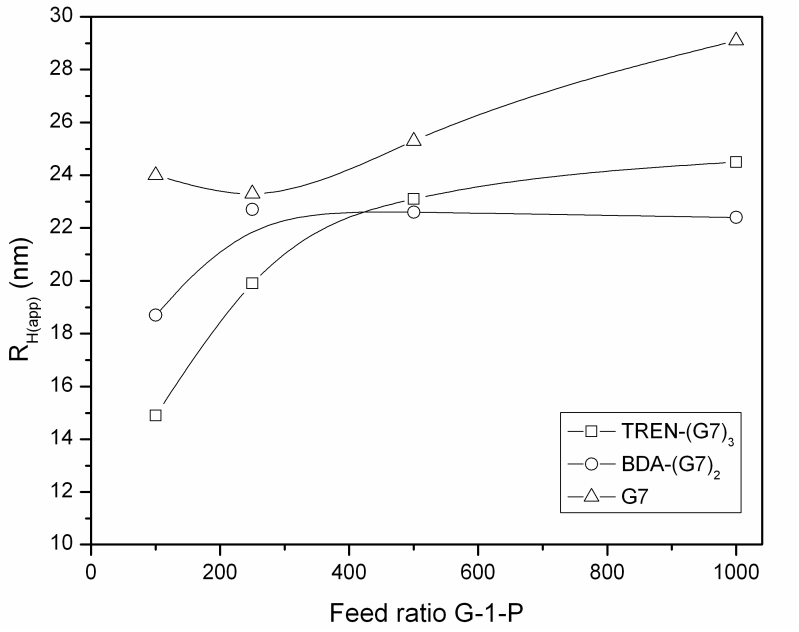

FIGURE 4.18: The hydrodynamic radii as obtained by DLS measurements of different primed enzyme catalyzed tandem polymerizations with different feed ratios G-1-P.

It is known that hyperbranched polymers form more compact structures as compared with their linear analogues due to the branched character. The size of hyperbranched structures is therefore not only dependent on the degree of

polymerization but also on the degree of branching[32]. FIGURE 4.18 shows an initial increase of the radius for polymerizations primed with G7, BDA-$(G7)_2$ and TREN-$(G7)_3$.

At higher feed ratios of G-1-P, the increase in radius levels off for the BDA-$(G7)_2$ and TREN-$(G)_3$ initiated polymerizations. This phenomenon is also seen for dendrimers at higher generations[4]. The volume required for the exponential growth of dendrimers at higher generations is not available since the volume increases only cubically. The hyperbranched structures with BDA-$(G7)_2$ and TREN-$(G7)_3$ as core molecules can be compared with the initiator cores used in the divergent synthesis of dendrimers and the same limitation in growth is seen. The G7 primed products do not show this plateau because the available space for chain growth is hardly limiting.

4.4 CONCLUSIONS

Di- and trivalent primers were successfully synthesized and employed in an enzyme catalyzed tandem polymerization. Hyperbranched multi-arm architectures were obtained after a phosphorylase driven polymerization in the presence of GBE_{DG}.

The synthesis of the primers was realized by coupling maltoheptaose moieties to amine functionalized core molecules via a reductive amination. An efficient purification method was found in the form of the column material Amberlite IR-120 (H^+). Partly functionalized core molecules adsorb to the Amberlite IR-120 (H^+) beads while fully functionalized core molecules do not show interaction with Amberlite beads. Nitrogen content analysis and FT-IR spectroscopy of the multivalent primers demonstrate that the fully functionalized primers are quantitatively separated from the partly functionalized products. However, trace amounts of maltoheptaose are visible with ^{1}H-NMR spectroscopy.

The multifunctional primers were successfully used to start the phosphorylase driven polymerization and linear $\alpha(1\rightarrow4)$ linked artificial amylose chains are connected to the central core molecule. The addition of the branching enzyme GBE_{DG} during polymerization resulted in the *in situ* branching of the multi arm structures. A degree of branching of 10.5 % was determined with ^{1}H-NMR measurements.

The hydrodynamic radii of the hyperbranched multi-arm structures were measured with DLS analysis. Hydrodynamic radii ranging from 14 nm to 29 nm were measured. The size of the maltoheptaose primed hyperbranched amylose increased from 24 nm to 29 nm, while for the BDA-$(G7)_2$ and TREN-$(G)_3$ a maximum radius at a high G-1-P feed ratio was observed. Steric hindrance at the periphery is the limiting factor.

4.5 REFERENCES

1. C.J. Hawker, J.M.J. Frechet, *J. Am. Chem. Soc.*, **1990**, *112,* 7638-7647
2. G.R. Newkome, X.F. Lin, *Macromolecules*, **1991**, *24,* 1443-1444
3. D.A. Tomalia, A.M. Naylor, W.A. Goddard, *Angew. Chem. -Int. Edit.*, **1990**, *29,* 138-175
4. D. Boris, M. Rubinstein, *Macromolecules*, **1996**, *29,* 7251-7260
5. J.M.J. Frechet, C.J. Hawker, I. Gitsov, J.W. Leon, *Journal of Macromolecular Science-Pure and Applied Chemistry*, **1996**, *A33,* 1399-1425
6. Y. Miura, *Journal of Polymer Science Part A-Polymer Chemistry*, **2007**, *45,* 5031-5036
7. S.G. Spain, M.I. Gibson, N.R. Cameron, *Journal of Polymer Science Part A-Polymer Chemistry*, **2007**, *45,* 2059-2072
8. J. da Silva Carvalho, W. Prins, C. Schuerch, *J. Am. Chem. Soc.*, **2002**, *81,* 4054-4058
9. T. Satoh, T. Imai, H. Ishihara, T. Maeda, Y. Kitajyo, A. Narumi, H. Kaga, N. Kaneko, T. Kakuchi, *Macromolecules*, **2003**, *36,* 6364-6370
10. T. Satoh, T. Imai, H. Ishihara, T. Maeda, Y. Kitajyo, Y. Sakai, H. Kaga, N. Kaneko, F. Ishii, T. Kakuchi, *Macromolecules*, **2005**, *38,* 4202-4210
11. J. Kadokawa, H. Tagaya, *Polymers and Advanced Technologies*, **2000**, *11,* 122-126
12. T. Satoh, T. Kakuchi, *Macromolecular Bioscience*, **2007**, *7,* 999-1009
13. R.A. Dwek, *Chemical Reviews*, **1996**, *96,* 683-720
14. H. Lis, N. Sharon, *Chemical Reviews*, **1998**, *98,* 637-674
15. A.B. Tuzikov, A.S. Gambaryan, L.R. Juneja, N.V. Bovin, *J. Carbohydr. Chem.*, **2000**, *19,* 1191-1200
16. R.T. Lee, Y.C. Lee, *Bioconjugate Chem.*, **1997**, *8,* 762-765
17. K. Aoi, K. Itoh, M. Okada, *Macromolecules*, **1995**, *28,* 5391-5393
18. A. Narumi, S. Yamane, Y. Miura, H. Kaga, T. Satoh, T. Kakuchi, *Journal of Polymer Science Part A-Polymer Chemistry*, **2005**, *43,* 4373-4381
19. H. Kaga, S. Yamane, A. Narumi, T. Satoh, T. Kakuchi, *Macromolecular Symposia*, **2004**, *217,* 29-38
20. W.B. Turnbull, S.A. Kalovidouris, J.F. Stoddart, *Chemistry-A European Journal*, **2002**, *8,* 2988-3000
21. C. Smythe, P. Cohen, *Eur. J. Biochem.*, **1991**, *200,* 625-631
22. R. Geddes, *Biosci. Rep.*, **1986**, *6,* 415-428
23. O.H. Lowry, J.A. Lopez, *J. Biol. Chem.*, **1946**, *162,* 421-428
24. C.H. Fiske, Y. Subbarow, *J. Biol. Chem.*, **1925**, *66,* 375
25. I. Perdivara, E. Sisu, I. Sisu, N. Dinca, K.B. Tomer, M. Przybylski, A.D. Zamfir, *Rapid Commun. Mass Spectrom.*, **2008**, *22,* 773-782
26. E. Sisu, W.T.E. Bosker, W. Norde, T.M. Slaghek, J.W. Timmermans, J. Peter-Katalinic, M.A. Cohen-Stuart, A.D. Zamfir, *Rapid Commun. Mass Spectrom.*, **2006**, *20,* 209-218
27. M. Kacurakova, R.H. Wilson, *Carbohydr. Polym.*, **2001**, *44,* 291-303
28. G. Ziegast, B. Pfannemüller, *Carbohydr. Res.*, **1987**, *160,* 185-204
29. W.N. Emmerling, B. Pfannemüller, *Starch*, **1981**, *33,* 202-208
30. M. Palomo Reixach, S. Kralj, M.J.E.C. van der Maarel, L. Dijkhuizen, *Appl. Environ. Microbiol.*, **2009**, *75*
31. J.F. Le Meins, C. Houg, R. Borsali, D. Taton, Y. Gnanou, *Macromolecular Symposia*, **2009**, *281,* 113-118
32. X. Ba, H. Wang, M. Zhao, M. Li, *Macromolecules*, **2002**, *35,* 4193-4197

CHAPTER 5

Hyperbranched polyglucan diblock copolymers

SUMMARY

Biohybrid diblock copolymers of poly(ethylene)glycol carrying hyperbranched polysaccharide chains are reported. Hyperbranched polysaccharides are grown from maltoheptaose functionalized PEG chain-ends by the enzyme catalyzed synthesis with potato phosphorylase and GBE_{DG}. Maltoheptaose acts as a primer recognition site for phosphorylase, making it possible to grow the hyperbranched structures from the PEG polymers. By varying the molar ratio of donor substrate (glucose-1-phosphate) to acceptor substrate (the PEG macroprimer), differently sized diblock copolymers are realized as proven with DLS.

5.1 INTRODUCTION

The ability of block copolymers to self-assemble into nanostructured morphologies in solution has been widely studied [1,2,3,4]. Block copolymers consisting of 2 parts, both synthetic and natural in origin, are known as polymer bioconjugates or polymer biohybrids and combine the properties of conventional block copolymers with the biodegradable and biocompatible character of natural polymers. When the natural part is sugar based, the biohybrid is known as a glycoconjugate. Research on glycoconjugates can lead to new applications in, for example, the biomedical field.

Several studies on the synthesis of block copolymers with a polysaccharide moiety are reported. Block copolymers consisting of a part dextran [5,6,7,8,9], hyaluronan [10,11] and amylose [12,13,14,15,16,17], are reported. The use of a glyco moiety as a part of a diblock copolymer can result in an amphiphilic system with interesting aggregation behaviour. Polystyrene-block-amylose (or dextran) amphiphiles aggregate in micelles, polymersomes or vesicles[18,12,19,20,8]. The saccharide part can be crosslinked with divinyl sulfone in order to fix the nanostructures[6]. Furthermore, a dextran-polyethylene glycol (PEG) diblock copolymer results in a double hydrophilic block copolymer (DHCB)[21]. A DHCB consist of two different water soluble blocks of different chemical nature. However, extern stimuli, such as a change in salinity or pH, can convert one block to a more hydrophobic one. An amylose-block-PEG diblock copolymer can form micelles in chloroform[22] and after converting the sugar hydroxy groups into carboxymethyl groups, a pH sensitive system is formed in water.

To date, only glyco block copolymers have been described as building up from two linear polymers. Here we describe the chemo enzymatic synthesis of a block copolymer consisting of a linear polyethylene glycol part and a hyperbranched polysaccharide part (see FIGURE 5.1). PEG is a unique polymer that dissolves in water and many organic solvents, such as chloroform and toluene. In addition, the biodegradable and biocompatible character of PEG fulfils requirements essential for use in the pharmaceutical and biomedical field.

In a block copolymer it is expected that the water soluble PEG chains prevent the retrogradation associated with polysaccharide based solutions[23]. In this chapter diblock copolymer of PEG are synthesized. However, it is also possible to start the enzyme catalyzed polymerization from water insoluble polymers such as polystyrene[14]. In theory, hyperbranched polyglucan copolymers can be made from virtually any polymer.

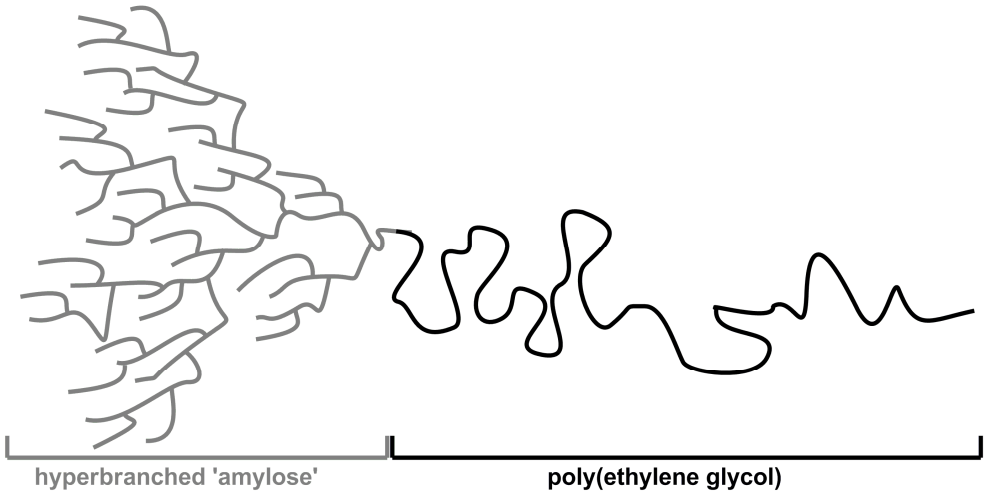

FIGURE 5.1: Schematic representation of a diblock copolymer build up from a hyperbranched α-glucan and poly(ethylene glycol).

5.2 EXPERIMENTAL

5.2.1 Materials and chemicals

Poly(ethylene glycol) methyl ether (PEG-OH; MW 2000 g·mol^{-1}, Aldrich) and PEG-NH_2 (MW 20000, Iris Biotech) were dried over P_2O_5 *in vacuo* before use. Phthalimide, triphenylphosphine (Ph_3P), diisopropylazodicarboxylate (DIAD), hydrazine monohydrate, sodiumcyanoborohydride and Amberlite IR-120 H^+ ion exchange resin were used as received (Aldrich).

5.2.2 Analysis and equipment

DYNAMIC LIGHT SCATTERING (DLS)

DLS measurements were performed on an ALV CGS-3 goniometer equipped with an ALV LSE-5005 multiple τ digital correlator at angles of between 30° and 150° with a 10° interval at room temperature. Measurements were performed in triplicate and averaged values are displayed. Fitting of the autocorrelation function was performed with the CONTIN algorithm.

Sample preparation

All samples were dissolved in water R.O. (1 mg·mL^{-1}) and filtered (0.45 μm teflon filter).

^{1}H-NMR SPECTROSCOPY

^{1}H-NMR spectra were recorded on a Varian VXR spectrometer operating at 300 or 400 MHz at ambient temperatures. Dimethyl-2-silapentane-5-sulfonic acid (DSS) was used as an external reference. ^{1}H-NMR spectra used for the determination of the degree of branching were recorded on a Varian Inova 500 MHz spectrometer at 50 °C with pre-saturation of the HOD resonance. 2,2-dimethyl-2-silapentane-5-sulfonic acid (DSS) was used as an external reference. Complete relaxation of the protons was ensured by taking a 10 second pause between pulses.

INFRA-RED SPECTROSCOPY

Attenuated total reflection fourier transform infra-red (ATR FT-IR) spectra were recorded on a Bruker IFS88 spectrometer equipped with a MCT-A detector at a resolution of 4 cm^{-1} using an average of 50 scans for sample and reference.

MALDI-TOF MASS SPECTROMETRY

MALDI-ToF mass spectrometry measurements were performed on a Voyager-DE PRO spectrometer in linear (positive ion) mode with 2,5-dihydroxybenzoic acid (DHB) as a matrix. The matrix solution was made by dissolving DHB (0.2 M) in a 1:1 v/v water/acetonitrile solution. Analyte solution was made by dissolving the product in water R.O. (4 mg·mL^{-1}). Matrix and analyte were mixed in 1:1 v/v ratio. 5 μL of this mixture was deposited on the target and dried *in vacuo* at 40 °C

5.2.3 Methods, synthesis and procedures

SYNTHESIS OF PEG-PHTHALIMIDE INTERMEDIATE (MITSUNOBU)

PEG-OH (5 g, 2.5 mmol, mw 2000 g·mol^{-1}), triphenylphosphine (0.62 g, 10 mmol), phthalimide (1.47 g, 10 mmol) and THF (50 ml) were mixed in a round-bottomed flask equipped with a magnetic stirrer at 0 °C under a N_2 atmosphere. To this mixture diisopropyl azodicarboxylate (1.9 ml, 10 mmol) was added drop wise. After the addition, the temperature was raised to 25°C and the reaction mixture was allowed to stir for 24 hours. Ethanol (200 ml) was added and the reaction mixture was stirred

for another 30 minutes. The solvent was evaporated by means of rotation evaporation and the resulting PEG-phthalimide was dissolved in water. The excess starting material was extracted with 3 portions of diethyl ether and discarded. Finally, the product was lyophilized, yielding a white powder (4.7 g, 94 %).

^{1}H-NMR (d-DMSO, 300 MHz): 7.8 ppm: benzylic protons endgroup, 3.7 ppm: C$\underline{H_2}$-phtalimide, 3.5 ppm: O-C$\underline{H_2}$ PEG backbone, 3.2 ppm: C$\underline{H_3}$ endgroup.
ATR FTIR: 2880 cm^{-1}: C-H stretching, 1712 cm^{-1}: C=O stretching, 1396 cm^{-1}: C-N stretching, 1100 cm^{-1}: C-O stretching (PEG backbone).

SYNTHESIS OF PEG-NH_2 (HYDRAZYNOLYSIS)

4.7 g PEG-phthalimide and hydrazine monohydrate (5 ml) were added to ethanol (40 ml) in a round-bottomed flask equipped with a magnetic stirrer. The mixture was refluxed for 24 hours and the solvent was removed via rotation evaporation. The remaining product was dissolved in CH_2Cl_2 (100 ml) and the precipitated by-products were removed by filtration. The filtrate was precipitated in diethyl ether and dried *in vacuo*, yielding an off-white powder (3.7 g, 78 %).

^{1}H-NMR (d-DMSO, 300 MHz): 3.7 ppm: C$\underline{H_2}$-NH_2, 3.5 ppm: O-C$\underline{H_2}$ PEG backbone, 3.2 ppm: C$\underline{H_3}$ end group, 2.6 C$\underline{H_2}$-NH_2.
ATR FTIR: 2880 cm^{-1}: C-H stretching , 2327 cm^{-1}: NH_3^+ salt, 1665 cm^{-1}: phthalhydrazide impurity, 1582 cm^{-1}: N-H bending (primary amine), 1100 cm^{-1}: C-O stretching (PEG backbone).

PURIFICATION OF PEG-NH_2

PEG-NH_2 was purified with Amberlite IR-120 H^+ beads. See experimental section CHAPTER 4.

ISOLATION AND PURIFICATION OF POTATO PHOSPHORYLASE

See experimental section CHAPTER 2.

CLONING, EXPRESSION AND PURIFICATION OF THE GLYCOGEN BRANCHING ENZYME

See experimental section CHAPTER 2.

ACTIVITY ASSAY PHOSPHORYLASE

See experimental section CHAPTER 2.

ACTIVITY ASSAY GLYCOGEN BRANCHING ENZYME

See experimental section CHAPTER 2.

SYNTHESIS OF MALTOHEPTAOSE

See experimental section CHAPTER 2.

TYPICAL ENZYME CATALYZED POLYMERIZATION

Primer (0.5 mM), G-1-P (25-500 mM), phosphorylase (5 $U \cdot mL^{-1}$) and GBE_{DG} (250 $U \cdot mL^{-1}$) were mixed and filled to 5 mL MOPS buffer (pH 7.0, 50 mM). Different ratio's G-1-P to primer were used by varying the G-1-P concentration. The solution was incubated at 37 °C in a shaking incubator. The released amount of phosphate was measured with a modified[24] method of Fiske and Subbarow[25]. Upon reaching equilibrium conditions, the reaction was stopped by a heat treatment (5 minutes in boiling water). Denaturated enzymes were removed by means of centrifugation. Dialysis (MWCO1000) and lyophilization of the remaining solution yields the hyperbranched structures.

5.3 RESULTS AND DISCUSSION

Polyethylene glycol macroprimers are synthesized by reacting amine functionalized PEG with maltoheptaose in the presence of sodium cyanoborohydride. This reaction, known as reductive amination, results in a PEG polymer chain linked to maltoheptaose by a secondary amine linkage. In some cases the PEG-NH_2 is first converted from PEG-OH via the Mitsunobu-hydrazinolysis reaction as is described in the next section.

5.3.1 Synthesis of amine terminated polyethylene glycol

The terminal hydroxy group of poly(ethylene glycol) methyl ether is a weak nucleophile and restricts PEG-OH from wide application. However, the conversion of the end terminal hydroxy group to an amino group makes the PEG suitable for coupling to maltoheptaose. Various methods are reported on the conversion of a hydroxy group to an amino group[26,27,28,29,30,31]. Ryoo et al.[32] report on a conversion based on the Mitsunobu reaction[33], in which the hydroxy group is converted into a phtalimide in the presence of diisopropyl azodicarboxylate (DIAD) and triphenylphosphine (Ph_3P) (see FIGURE 5.2 A). Subsequent hydrazinolyzes in refluxing ethanol with hydrazine hydrate yield PEG-NH_2 (see FIGURE 5.2 B).

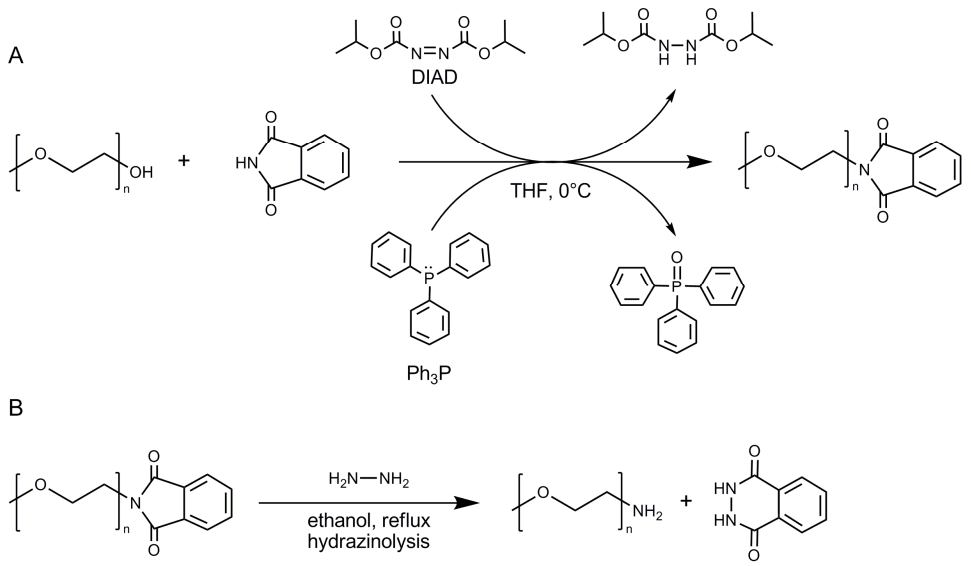

FIGURE 5.2: The Mitsunobu reaction with DIAD and Ph_3P is depicted in scheme A. Scheme B describes the subsequent hydrazinolysis of PEG-phtalimide to PEG-NH_2.

Reaction A and B as depicted in FIGURE 5.2 can be followed by ^{1}H-NMR[34] and appeared to be an efficient method to synthesize amino functionalized PEG.

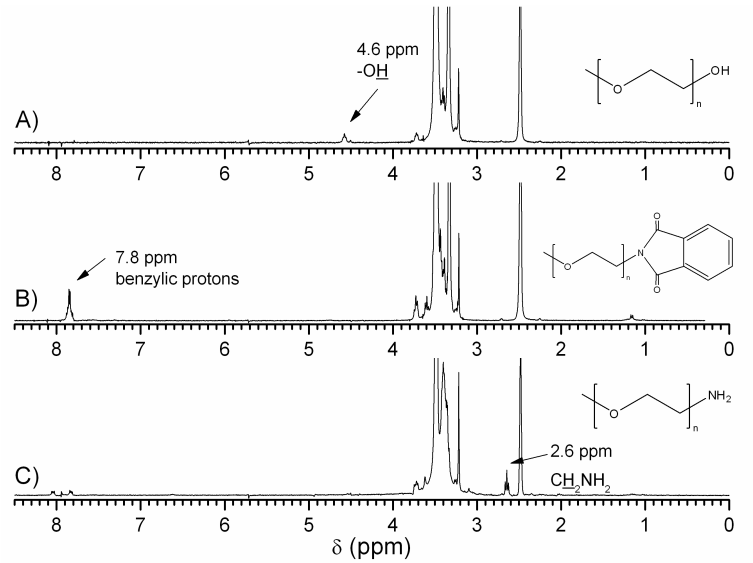

FIGURE 5.3: ^{1}H-NMR spectra (300MHz/d-DMSO) of: A) poly(ethylene glycol) methyl ether as received from Aldrich. B) PEG-phthalimide after the Mitsunobu reaction and C) PEG-NH_2 after hydrazinolysis of the PEG-phthalimide.

The quantitative conversion of PEG-OH into PEG-phthalimide is proven by the complete disappearance of the $\underline{C}H_2OH$ signal at 4.6 ppm and the appearance of the benzylic protons at 7.8 ppm of PEG-phthalimide. (^{1}H-NMR trace A and B in FIGURE 5.3). The subsequent hydrazinolysis results in a reduction of the signal at 7.8 ppm and the appearance of the (PEG)$C\underline{H}_2NH_2$ signal at 2.6 ppm (trace C). Remaining phthalhydrazide is responsible for the signals around 7.8-8.1 ppm and is difficult to remove. To purify the resulting amino functionalized PEG is dissolved in water together with Amberlite IR-120 H^+ beads. This ion exchange material absorbs only amino functionalized products. After flushing with a diluted ammonia solution, the amino functionalized product is released from the Amberlite IR-120 H^+ beads and collected by rotation evaporation and lyophilization.

5.3.2 Synthesis of poly(ethylene glycol) macroprimers

Maltoheptaose is effectively coupled to amine functionalized PEG polymers by a reductive amination (see FIGURE 5.4).

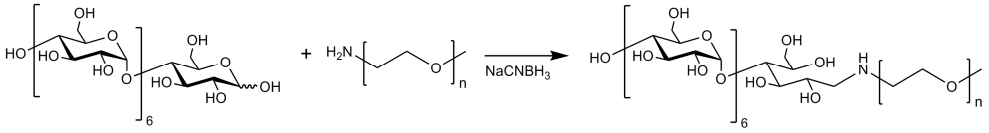

FIGURE 5.4: Reductive amination of the reducing group of maltoheptaose and amine functionalized PEG. The resulting macroprimer is able to start the enzyme catalyzed polymerization.

The reductive amination was performed in DMSO and DMF. No difference is observed in solubility, reactivity or yield regarding the solvent of choice. DMF may be preferred since it is from a practical point of view easier to remove.

An excess of PEG-NH_2 (compared to maltoheptaose) is used together with long reaction times. These precautions make sure that all the maltoheptaose reacts with the primary amine groups. Unreacted PEG-NH_2 is removed with Amberlite IR-120 H^+ beads, as described in the previous section.

The disappearance of the N-H bending vibration (1598 cm^{-1}) and the protonated NH_3^+ overtone (2329 cm^{-1}) in the IR spectrum is a clear indication that the primary amine reacted with the reducing end of maltoheptaose (see FIGURE 5.5 LEFT).

The disappearance of the anomeric protons of maltoheptaose can be followed with ^{1}H-NMR. The α– and β anomeric signal of maltoheptaose are normally visible at 5.2 and 4.6 ppm, respectively (see FIGURE 5.5 RIGHT). These signals disappear once

reacted with the PEG chain and proves again the coupling of maltoheptaose to the PEG chain.

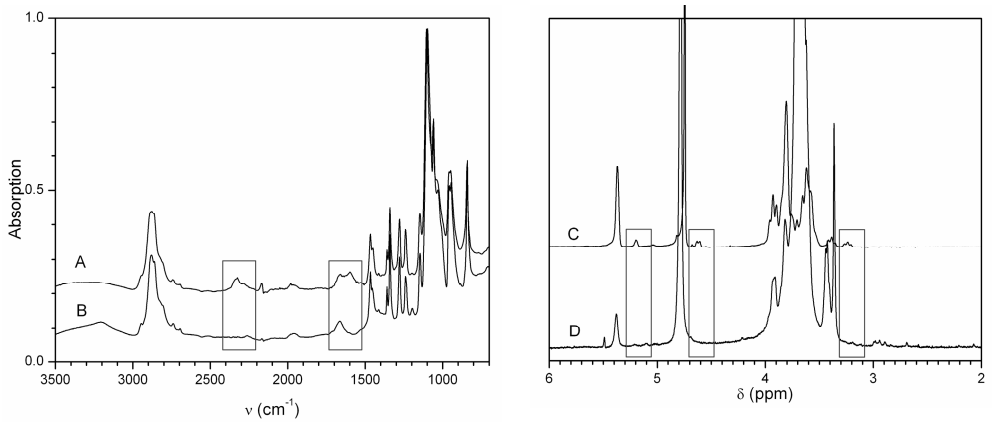

FIGURE 5.5: IR spectrum (left) of PEG-NH_2 (A) and PEG-G7 (B). The main differences between the spectra are boxed. After reaction the primary amine vibration (1598 cm^{-1}) and NH_3^+ overtone (2329 cm^{-1}) disappear.
^{1}H-NMR spectrum (right). The anomeric protons (5.2 and 4.6 ppm) of maltoheptaose (C) as well as the βH2 proton (3.3 ppm) are boxed. After reaction with PEG-NH_2 these signals disappear (D).

MALDI-TOF ANALYSIS

MALDI-ToF analysis of the macroprimer consisting of PEG_{mw2000} and $PEG_{mw20000}$ were also performed. Unfortunately, the right conditions for the $PEG_{mw20000}$ macroprimers were not found. The size of the polymer and the neutral character of the oligosaccharide are accountable for this fact.

The spectrum of the low molecular weight macroprimer (PEG_{mw2000}) is shown in FIGURE 5.6. Trace a) shows the PEG-OH polymer as received from Aldrich. The individual m/z difference between the peaks is 44 m/z and corresponds to the mass of one monomer unit of ethylene glycol. The optimum is around 2000 m/z. Trace b) shows the PEG macroprimer after purification with Amberlite IR-120 H^+.

Most remarkable is the huge amount of unreacted PEG-NH_2 in the spectrum. However, care has to be taken with the interpretation of the MALDI-ToF trace, as MALDI-ToF is not a quantitative method. Higher molecular weight polymer chains and/or neutral polymers are more difficult to detect with the MALDI-ToF setup due to the critical ionization step in the method. Without ionization, particles (polymer

chains) cannot reach the detector and will not be recorded. The ionization of large and neutral polymers can be more difficult and will show a lower count rate.

Although not visible with IR- and ^{1}H-NMR spectroscopy, PEG-NH_2 is present in the sample after purification. The PEG macro-primer is visible as a distribution around 3000 m/z. Individual differences between peaks are 44 m/z and correspond with an ethylene glycol monomer. The difference between the maxima of the bimodal distribution corresponds to the molecular weight of maltoheptaose (1153 g·mol^{-1}).

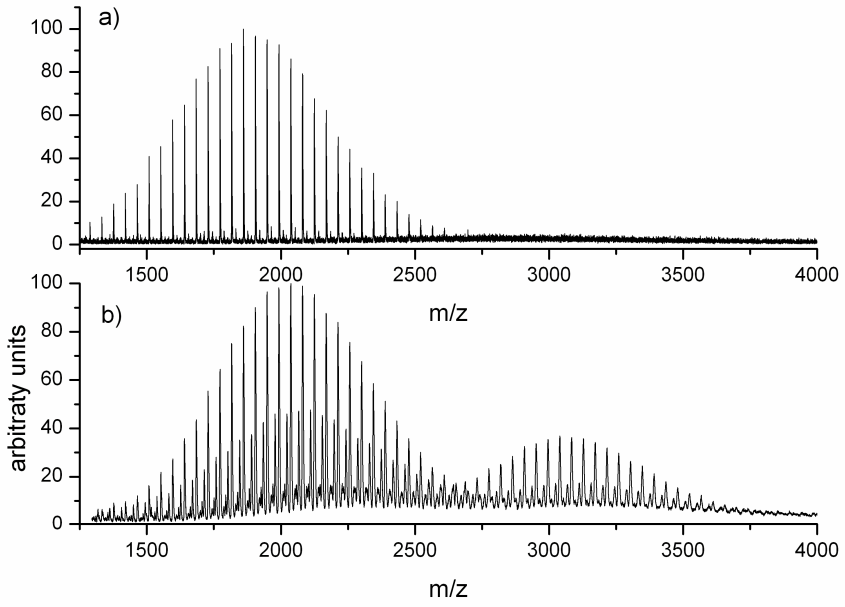

FIGURE 5.6: MALDI-ToF spectra of a) PEG-OH and b) PEG-G7. The bimodal distribution consists of the starting product (PEG-NH_2) and the actual macro-primer at a higher molecular weight.

5.3.3 Enzyme catalyzed synthesis started from macroprimers

The macro-primers as described in the previous section are used to start the enzymatic polymerization. Two different PEG macro-primers are synthesized:

- PEG_{MW2000}-G7 *and*
- $PEG_{MW20000}$-G7

The PEG macro-primers were used to start the polymerization of a series of PEG diblock copolymers carrying a hyperbranched α-polyglucan part and are compared to a hyperbranched polyglucan started from a 'normal' maltoheptaose primer. PEG

block copolymers are realized with different sized hyperbranched polysaccharides by changing the molar ratio of donor substrate (G-1-P) relative to the (macro-)primer (see TABLE 5.1).

TABLE 5.1: Overview of the results obtained after enzyme catalyzed synthesis with phosphorylase and GBE_{DG} starting from PEG macro-primers.

Primer	Feed ratio G-1-P	Incorporated glc. residues [A]	Conversion (%)[B]	Degree of braching (%)[C]	Hydrodynamic radius (nm)
G7	100	86	74	11.5	24.0
	250	168		11.5	23.3
	500	364		10.7	25.3
	1000	765		9.9	29.1
$PEG_{MW20000}$	100	129	67	9.1	26.4
	250	220		7.8	30.9
	500	n.d.		7.5	34.1
	1000	684		8.3	36.4
PEG_{MW2000}	100	92	62	10.7	29.2
	250	206		10.7	30.9
	500	436		8.3	30.8
	1000	643		8.4	36.9

[A] *The amount of incorporated glucose residues is determined via the inorganic phosphate assay as described in CHAPTER 2.*
[B] *The conversion is calculated as described in FIGURE 2.10.*
[C] *The degree of branching is calculated via ^{1}H-NMR (see CHAPTER 2).*

The reactions were terminated after reaching equilibrium conditions i.e. until the concentration released inorganic phosphate remained constant as determined with the inorganic phosphate assay (see CHAPTER 2). The conversion of the reactions started from the PEG macro-primers are lower as compared with the reaction started from maltoheptaose. However, in general conversions are observed between 60 % and 80 % independent of the primer used. This observation cannot be assigned to the macro-primers. This is in accordance to results as obtained in CHAPTER 2 and CHAPTER 4.

From TABLE 5.1 it becomes apparent that the degree of branching drops to values below 10 % at high feed ratio's G-1-P. Products based on the $PEG_{MW20000}$ primer do not even show branching characteristics above 10 %. Non-specific binding of the hydrophilic PEG chain with parts of the GBE_{DG} may result in a decreased activity of the enzyme resulting in a lowered degree of branching. Furthermore, reactions

where run for a minimum of 3 days it is possible that the phosphorylase catalyzed synthesis reached equilibrium conditions while the GBE_{DG} catalyzed reaction was not completed.

The (apparent) hydrodynamic radii as determined with DLS show an increasing trend with the amount of incorporated glucose residues.

The hydrodynamic radii of the PEG_{MW2000} en $PEG_{MW20000}$ based diblock copolymers are (in FIGURE 5.7) compared with a hyperbranched polysaccharide started from maltoheptaose.

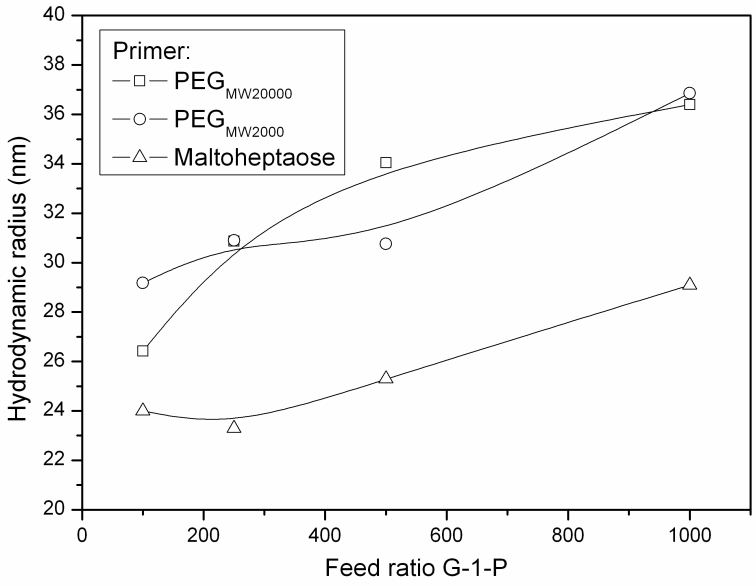

FIGURE 5.7: The hydrodynamic radii as obtained by DLS measurements of different primed enzyme catalyzed tandem polymerizations with different feed ratios G-1-P.

Water soluble hyperbranched polysaccharides tend to form aggregates in water due to intermolecular hydrogen bonding between the abundant hydroxy groups[35]. Therefore, the hydrodynamic radii as shown in FIGURE 5.7 represent the radii of aggregates rather than single polymer chains. The increase in feed ratio of G-1-P results in aggregates build up from larger hyperbranched polysaccharides. This aggregation behaviour is also observed in the BDA-$(G7)_2$ and TREN-$(G7)_3$ started polymerizations as shown in CHAPTER 4.

A clear shift in hydrodynamic radius is seen for the diblock copolymers as compared to the maltoheptaose started polysaccharides. However, the two different PEG

diblock copolymers can not be distinguished by hydrodynamic radius although the molecular weight of the PEG block varies from 2000 g·mol^{-1} to 20000 g·mol^{-1}.

This can be explained by the fact that the hydrodynamic volume of PEG_{MW2000} and $PEG_{MW20000}$ in water are an order smaller than the size of the aggregates. The hydrodynamic radius of PEG_{MW2000} and $PEG_{MW20000}$ are, respectively, ~1.3 nm and ~4.5 nm[36]. When the PEG chains are entangled (interpenetrating coils) inside the hyperbranched polyglucan aggregates it is difficult to observe a volume change with DLS.

To obtain more information about the aggregate formation light scattering measurements can be conducted with DMSO as solvent instead of water. DMSO is known to break the inter- and intramolecular hydrogen bonds of polysaccharides, leading to the dispersion of the aggregates and making it maybe possible to study individual polymer chains[37]. Furthermore, electron microscopy can give more information about the aggregation behaviour.

5.4 CONCLUSIONS

Two PEG macroprimers with different molecular weights were successfully synthesized. PEG-methylether with a molecular weight of 2000 g·mol^{-1} was first converted to a PEG-amine via the Mitsunobu-hydrazinolysis pathway. With this method, we obtained in a quantitative manner PEG-NH_2 as proven with ^{1}H-NMR.

PEG-NH_2 (MW 20000 g·mol^{-1}) and the synthesized PEG-NH_2 (MW 2000 g·mol^{-1}) were subsequently coupled to a maltoheptaose moiety via a reductive amination. ^{1}H-NMR and IR measurements show successful coupling between PEG-NH_2 and maltoheptaose. MALDI-ToF measurements reveal the presence of unreacted PEG-NH_2. The percentage of unreacted PEG-NH_2 remains unclear since MALDI-ToF is not a quantitative technique.

The resulting PEG-G7 macro-primers are used in an enzyme catalyzed synthesis. Potato phosphorylase and GBE_{DG} are utilized to obtain PEG diblock copolymers carrying a hyperbranched polysaccharide. The maltoheptaose moiety of the PEG macro-primer acts as a recognition site for phosphorylase making it possible to start polymerization solely from the PEG chain. By varying the feed ratio of G-1-P the amount of incorporated glucose residues can be controlled in the diblock. In this way, different sized diblock copolymers were synthesized. The hydrodynamic radii of the

diblock copolymers were measured with DLS. Because of the size of the hydrodynamic radii, it is likely that aggregates are formed.

5.5 REFERENCES

1. S.B. Darling, *Progress in Polymer Science*, **2007**, *32,* 1152-1204
2. J. Rodriguez-Hernandez, F. Checot, Y. Gnanou, S. Lecommandoux, *Progress in Polymer Science*, **2005**, *30,* 691-724
3. G. Riess, *Progress in Polymer Science*, **2003**, *28,* 1107-1170
4. A. Blanazs, S.P. Armes, A.J. Ryan, *Macromolecular Rapid Communications*, **2009**, *30,* 267-277
5. W.T.E. Bosker, K. Ágoston, M.A. Cohen Stuart, W. Norde, J.W. Timmermans, T.M. Slaghek, *Macromolecules*, **2003**, *36,* 1982-1987
6. C. Houga, J. Giermanska, S. Lecommandoux, R. Borsali, D. Taton, Y. Gnanou, J.F. Le Meins, *Biomacromolecules*, **2009**, *10,* 32-40
7. O.S. Hernandez, G.M. Soliman, F.M. Winnik, *Polymer*, **2007**, *48,* 921-930
8. C. Houga, J.F. Le Meins, R. Borsali, D. Taton, Y. Gnanou, *Chemical Communications*, **2007**, 3063-3065
9. C. Schatz, S. Louguet, J.F. Le Meins, S. Lecommandoux, *Angew. Chem. -Int. Edit.*, **2009**, *48,* 2572-2575
10. K.K. Upadhyay, J.F. Le Meins, A. Misra, P. Voisin, V. Bouchaud, E. Ibarboure, C. Schatz, S. Lecommandoux, *Biomacromolecules*, **2009**, *10,* 2802-2808
11. Y.L. Yang, K. Kataoka, F.M. Winnik, *Macromolecules*, **2005**, *38,* 2043-2046
12. K. Loos, A. Böker, H. Zettl, A.F. Zhang, G. Krausch, A.H.E. Müller, *Macromolecules*, **2005**, *38,* 873-879
13. K. Loos, A.H.E. Müller, *Biomacromolecules*, **2002**, *3,* 368-373
14. K. Loos, R. Stadler, *Macromolecules*, **1997**, *30,* 7641-7643
15. I. Otsuka, K. Fuchise, S. Halila, S. Fort, K. Aissou, I. Pignot-Paintrand, Y.G. Chen, A. Narumi, T. Kakuchi, R. Borsali, *Langmuir*, **2010**, *26,* 2325-2332
16. G. Ziegast, B. Pfannemüller, *Macromol. Rapid. Comm.*, **1984**, *5,* 373-379
17. A. Narumi, Y. Miura, I. Otsuka, S. Yamane, Y. Kitajyo, T. Satoh, A. Hirao, N. Kaneko, H. Kaga, T. Kakuchi, *Journal of Polymer Science Part A-Polymer Chemistry*, **2006**, *44,* 4864-4879
18. C. Houga, J. Giermanska, S. Lecommandoux, R. Borsali, D. Taton, Y. Gnanou, J.-F. Le Meins, *Biomacromolecules*, **2009**, *10,* 32-40
19. L.C. You, H. Schlaad, *J. Am. Chem. Soc.*, **2006**, *128,* 13336-13337
20. A. Narumi, I. Otsuka, T. Matsuda, Y. Miura, T. Satoh, N. Kaneko, H. Kaga, T. Kakuchi, *Journal of Polymer Science Part A-Polymer Chemistry*, **2006**, *44,* 3978-3985
21. O.S. Hernandez, G.M. Soliman, F.M. Winnik, *Polymer*, **2007**, *48,* 921-930
22. K. Akiyoshi, N. Maruichi, M. Kohara, S. Kitamura, *Biomacromolecules*, **2002**, *3,* 280-283
23. K. Akiyoshi, M. Kohara, K. Ito, S. Kitamura, J. Sunamoto, *Macromol. Rapid. Comm.*, **1999**, *20,* 112-115
24. O.H. Lowry, J.A. Lopez, *J. Biol. Chem.*, **1946**, *162,* 421-428
25. C.H. Fiske, Y. Subbarow, *J. Biol. Chem.*, **1925**, *66,* 375

26. S. Zalipsky, C. Gilon, A. Zilkha, *Eur. Polym. J.*, **1983**, *19,* 1177-1183
27. G. Ziegast, B. Pfannemüller, *Makromolekulare Chemie-Rapid Communications*, **1984**, *5,* 363-371
28. H. Gehrhardt, M. Mutter, *Polymer Bulletin*, **1987**, *18,* 487-493
29. V.N.R. Pillai, M. Mutter, E. Bayer, I. Gatfield, *J. Org. Chem.*, **1980**, *45,* 5364-5370
30. A.F. Buckmann, M. Morr, G. Johansson, *Makromolekulare Chemie-Macromolecular Chemistry and Physics*, **1981**, *182,* 1379-1384
31. E. Fabiano, B.T. Golding, M.M. Sadeghi, *Synthesis-Stuttgart*, **1987***,* 190-192
32. S.J. Ryoo, J. Kim, J.S. Kim, Y.S. Lee, *Journal of Combinatorial Chemistry*, **2002**, *4,* 187-190
33. O. Mitsunobu, *Synthesis-Stuttgart*, **1981***,* 1-28
34. K. Jankova, J. Kops, *J. Appl. Polym. Sci.*, **1994**, *54,* 1027-1032
35. Y.Z. Tao, L. Zhang, *Biopolymers*, **2006**, *83,* 414-423
36. S. Kuga, *Journal of Chromatography A*, **1981**, *206,* 449-461
37. P. Ostern, E. Holmes, *Nature*, **1939**, *144,* 34

Summary

Polysaccharides are versatile biopolymers that show their multiple characteristics in nature: cellulose, starch and chitin being examples. The molecular properties of such polysaccharides are excellent in terms of molecular weight and stereoregularity. These special properties are difficult to control with conventional polymer chemistry and hence most glycoscience is based on modifying natural polysaccharides rather than synthesizing them.

In nature, enzymes catalyze the *in vivo* polymerizations of the above mentioned polysaccharides. In this thesis it is shown that enzymes are also essential laboratory tools for the synthesis of biopolymers with control over macromolecular properties. Conventional polymer synthesis of polysaccharides is in many aspects inferior (or impossible) as compared to the enzyme catalyzed synthesis of polysaccharides investigated in this research. Here we present a method to enzymatically polymerize hyperbranched polysaccharides with control over stereoregularity, degree of branching and molecular weight. Moreover, the possibility to construct hybrid materials consisting of a hyperbranched polyglucan part connected to a synthetic substrate (e.g. polymer, surface, etc) is shown.

Using an enzymatic catalyzed tandem polymerization in which the unique properties of the enzymes potato phosphorylase and glycogen branching enzyme (GBE_{DG}; from *Deinococcus geothermalis*) are combined, a hyperbranched polyglucan was polymerized consisting of (1→4) linked α-D-glucose residues with branches at the glucose C6 hydroxy group. In this tandem polymerization, phosphorylase catalyzes the addition of (1→4) linked α-D-glucose residues from a short oligosaccharide, using glucose-1-phosphate (G-1-P) as donor substrate (monomer). Phosphorylase is the driving force behind the polymerization while GBE_{DG} introduces *in situ* branch points. More specifically, GBE_{DG} catalyzes the formation of α(1→6) branch points by the hydrolysis of an α(1→4) linked glycosidic linkage and subsequent inter- or intra-chain transfer of the non reducing terminal fragment to the C6 hydroxyl position of an α-glucan.

A property of phosphorylase, essential for the research as outlined in this thesis, is the donor substrate (primer) dependency. Polymerization is impossible without an oligomeric $\alpha(1\rightarrow4)$ linked D-glucose primer of at least 3 glucose residues.

Chapter 2 shows the fundamentals of the enzyme catalyzed tandem polymerization while chapters 3, 4 and 5 describe the various possible hybrid structures when this essential primer is first coupled to a synthetic substrate.

CHAPTER 2 describes the isolation and purification of the enzymes, as well as the optimum reaction conditions for a tandem polymerization. Both enzymes showed activity at 37 °C and a pH of 7. The primer used to start the polymerization from, was maltoheptaose, obtained via the acidic catalyzed hydrolysis of β-cyclodextrin. The enzyme catalyzed tandem polymerization showed characteristics of a living polymerization, including:

- the polymer chains grew linear with time;
- further addition of G-1-P resulted in regrowth of the polymer chain;
- a termination step was absent;
- polymers with a low polydispersity were obtained.

Furthermore, different methods were evaluated to characterize the degree of branching and the side chain distribution profile of the hyperbranched polyglucans. It was shown via ^{1}H-NMR that the degree of branching was 11 %. The side chain distribution was measured via MALDI-ToF spectrometry after the enzymatic hydrolysis of the $\alpha(1\rightarrow6)$ linkages. The resulting spectrum showed a rather narrow side chain distribution, ranging from 4 to 15 glucose residues with an optimum length of 7 glucose residues.

CHAPTER 3 shows the use of the previously described tandem polymerization for the construction of hyperbranched polysaccharide brushes. It is described how brushes were grown from functionalized Si wafers via the *grafting from* principle. First, a cleaned and oxidized Si wafer was functionalized with an aminosilanization agent. This resulted in a surface coverage of 2.8 amino groups nm^2. Subsequently, maltoheptaose was coupled to the introduced amino groups via a reductive amination. The conversion of the reaction with the amino groups and the reducing group of the maltoheptaose molecules was determined to be 67 %. These primer functionalized substrates were used to start the enzyme catalyzed tandem polymerization. The thickness of the resulting hyperbranched polysaccharide coating

was determined by ellipsometry and was in the range of 12-20 nm. Steric hindrance is expected to be the cause of the limited coating thickness.

CHAPTER 4 covers the enzyme catalyzed tandem polymerization started from di- and trivalent primers. Hence, maltoheptaose was coupled to core molecules carrying multiple amino groups. More specifically, di- and trifunctional primers were synthesized by reacting maltoheptaose with, respectively, butanediamine (BDA-$(G7)_2$) and tris(2-aminoethyl)amine (TREN-$(G7)_3$). This resulted in a mixture of completely and partly functionalized core molecules. It was found that only partly functionalized core molecules adhere to the column material Amberlite IR-120 (H^+) and hence purification of the mixture was possible with Amberlite beads. Approximately 50 % of the product was completely functionalized. Subsequently, the enzyme catalyzed tandem polymerization - started from the purified multivalent primers - was evaluated. An increase in reaction rate was observed as compared with a maltoheptaose primed reaction. However the increase was not as high as expected. The phosphorylase catalyzed reaction may be retarded due to the densely packed multivalent primers which result in a suppression in the reaction rate. By varying the amount of G-1-P, different sized hyperbranched multi arm architectures were polymerized, which was confirmed by DLS.

CHAPTER 5 details the functionalization of poly(ethylene)glycol (PEG) with maltoheptaose as confirmed by MALDI-ToF. This so-called macro-primer was used to start the enzyme catalyzed tandem polymerization, resulting in diblock copolymers consisting of a hyperbranched polysaccharide part and a linear PEG part. By varying the amount of G-1-P, different sized diblock copolymers were polymerized, which was confirmed by DLS measurements.

Samenvatting

Polysachariden of koolhydraten zijn veelzijdige biopolymeren. Dit komt tot uitdrukking in de vele functies die biopolymeren vervullen in de natuur. De polysachariden cellulose en pectine geven houtvezels hun structuur, zetmeel verzorgt de energieopslag in planten en chitin vind men in het exoskelet van krabben en insecten. De moleculaire eigenschappen van bovengenoemde polysachariden zijn uitstekend wat betreft het molecuulgewicht en stereoregulariteit. Het is moeilijk om de bovengenoemde structuren via conventionele (polymeer)chemie in het laboratorium te evenaren. Daarom is het meeste onderzoek die zich bezig houdt met polysachariden er op gefocust natuurlijke polysachariden te modificeren.

In de natuur maken enzymen de synthese van polysachariden mogelijk. De conventionele manier om polysachariden te synthetiseren (in een laboratorium) is in veel aspecten inferieur aan de enzym gekatalyseerde polymerisaties zoals beschreven in dit proefschrift. We beschrijven hier een enzym gekatalyseerd systeem waarmee hypervertakte polysachariden gesynthetiseerd kunnen worden met controle over molecuulgewicht, stereoregulariteit en vertakkingsgraad. Bovendien kunnen de hypervertakte polysachariden gekoppeld worden aan synthetische substraten (polymeer, oppervlak, etc.) zodat hybride structuren ontstaan.

De unieke eigenschappen van de enzymen aardappel fosforylase en glycogeen vertakkingsenzym worden in dit onderzoek gecombineerd voor de synthese van een hypervertakt polyglucaan bestaande uit α-D-glucose eenheden die met elkaar verbonden zijn via $\alpha(1\rightarrow4)$ glycosidische verbindingen. Vertakking vindt plaats op de C6 positie van de α-D-glucose eenheden.

Het enzym fosforylase katalyseert de additie van α-D-glucose eenheden via een $\alpha(1\rightarrow4)$ verbinding aan een kort oligoglucaan (acceptor substraat). Hierdoor ontstaat er een groeiende lineaire glucaanketen. Glucose-1-fosfaat wordt hierbij gebruikt als donor substraat (monomeer). Fosforylase is de drijvende kracht achter de enzymatische tandempolymerisatie terwijl het glycogeen vertakkingsenzym de *in situ* formatie van vertakkingspunten katalyseert via de introductie van $\alpha(1\rightarrow6)$ verbindingen. De exacte katalyse van het glycogeen vertakkingsenzym omvat de

hydrolyse van een $\alpha(1\rightarrow4)$ glycoside verbinding waarna het vrij gekomen terminale oligosacharide verplaatst wordt naar een C6 positie van een groeiende glucaanketen.

Een belangrijke eigenschap van fosforylase en essentieel voor het werk als beschreven in dit proefschrift is dat de aanwezigheid van een acceptor substraat een vereiste is voor de katalyse van lineaire glucaanketens.

Hoofdstuk 2 beschrijft de basisprincipes van de enzym gekatalyseerde tandempolymerisatie en de hoofdstukken 3, 4 en 5 laten voorbeelden zien van hybride structuren die ontstaan als het acceptor substraat eerst gekoppeld wordt aan bv. een synthetisch polymeer of oppervlakte.

HOOFDSTUK 2 beschrijft de isolatie en zuivering van de benodigde enzymen, de synthese van de uitgangsstoffen en de optimale reactie condities. Er wordt aangetoond dat beide enzymen voldoende activiteit vertonen bij 37 °C en een pH van 7 waardoor een tandempolymerisatie bij deze omstandigheden mogelijk is. Het donor substraat dat gebruikt is in dit onderzoek is maltoheptaose. Maltoheptaose is zuiver verkregen in een opbrengst van 10 % via de zuur gekatalyseerde hydrolyse van β-cyclodextrine.

De enzym gekatalyseerde tandempolymerisatie van hypervertakte polyglucanen gedraagt zich als een levende polymerisatie. De volgende kenmerken heeft de enzymatische polymerisatie gemeen met een levende polymerisatie:

- De polymeerketens groeien lineair met de tijd.
- Wanneer extra G-1-P toegevoegd wordt groeien de ketens verder.
- Een terminatiestap ontbreekt in het polymerisatiemechanisme.
- Polymeren met een lage polydispersiteit worden verkregen.

Daarnaast zijn er verschillende technieken gebruikt om de hypervertakte polysachariden te karakteriseren. De vertakkingsgraad is bepaald met ^{1}H-NMR spectroscopie en is 11 %. Na de specifieke hydrolyse van alle $\alpha(1\rightarrow6)$ is de ketendistributie van de producten bepaald met MALDI-ToF spectrometrie. De ketendistributie vertoont een minimum en maximum ketenlengte van respectievelijk 4 en 15 α-D-glucose eenheden met een maximum bij 7 α-D-glucose eenheden.

In HOOFDSTUK 3 worden de resultaten gepresenteerd van de hierboven beschreven tandempolymersatie gestart vanaf een speciaal geprepareerd silica (Si) oppervlak. De Si substraten zijn hiervoor eerst schoon gemaakt en geoxideerd waarna ze via een aminosilanisatieproces gefunctionaliseerd werden. Dit resulteerde in een amino

groep dichtheid van 2,8 per nm^2. Vervolgens is maltoheptaose aan de aminogroepen gekoppeld middels een reducerende aminering. Het is berekend dat de efficiëntie van deze koppeling 67 % is. De maltoheptaose gefuntionaliseerde Si substraten zijn gebruikt voor de enzym gekatalyseerde tandempolymerisatie met als resultaat een Si oppervlak bedekt met een laag covalent verbonden hypervertakte polyglucanen. De dikte van de hypervertakte coating is bepaald met ellipsometrie en varieerde tussen de 12 en 20 nm. Sterische hindering is waarschijnlijk de beperkende factor in het polymerisatieproces waardoor de dikte van de coating gelimiteerd is.

HOOFDSTUK 4 toont de resultaten die behaald zijn door de enzym gekatalyseerde tandempolymerisatie te starten vanaf multifunctionele acceptor substraten. Deze substraten werden gesynthetiseerd door amino dragende moleculen te functionaliseren met maltoheptaose. De exacte reactie omvat de reducerende aminering van maltoheptaose met butaandiamine (BDA) of tris(2-aminoethyl)amine (TREN). Aldus wordt er respectievelijk een difuntioneel (BDA-$(G7)_2$) en trifunctioneel (TREN-$(G7)_3$) acceptor substraat verkregen. De reactie als hierboven beschreven verloopt voor ongeveer 50 % en dat betekent dat er naast compleet gefunctionaliseerde amino-dragers ook onvolledige reactieproducten aanwezig zijn. Deze onvolledige reactieproducten werden selectief verwijderd met het kolom materiaal Amberlite IR-120 (H^+). Vervolgens werden de gezuiverde multifunctionele acceptor substraten gebruikt in de enzym gekatalyseerde tandempolymerisatie. De verwachtte toename in reactiesnelheid werd waargenomen maar was niet zo groot als theoretisch mogelijk. Vermoedelijk wordt de fosforylase gekatalyseerde reactie vertraagd door moeilijk bereikbare ketenuiteinden wat resulteert in een afname van de reactiesnelheid. Door de verhouding G-1-P/ACCEPTOR SUBSTRAAT tijdens de reactie te variëren konden hypervertakte structuren gepolymeriseerd worden met verschillende molecuulgewichten. Dit is bevestigd middels dynamische lichtverstrooiing.

HOOFDSTUK 5 demonstreert de resultaten die behaald zijn door de enzym gekatalyseerde polymerisatie te starten vanaf een acceptor substraat gekoppeld aan een polyethyleenglycol (PEG) polymeer. MALDI-ToF massa spectrometrie metingen bevestigen de koppeling tussen maltoheptaose en de PEG keten. Wanneer de enzym gekatalyseerde tandempolymerisatie gestart wordt in aanwezigheid van dit zogenaamde macrosubstraat ontstaan er diblok copolymeren bestaande uit een lineair PEG gedeelte en een hypervertakt polysacharide gedeelte. Door de verhouding G-1-P/MACROSUBSTRAAT tijdens de reactie te variëren konden hypervertakte

diblok copolymeren gepolymeriseerd worden met verschillende molecuulgewichten. Dit is bevestigd middels dynamische lichtverstrooiing.

Dankwoord

Het heeft langer geduurd dan gepland maar met het schrijven van dit dankwoord komt het einde van mijn promotietraject in zicht. Ik heb mogen ervaren dat wetenschap nooit klaar is. Meer dan eens ben ik het afgelopen jaar terug het lab op gegaan om het 'allerlaatste experiment' uit te voeren. Het 'allerlaatste experiment' nodigde echter steevast uit tot de formulering van nog een experiment. Het onderzoek loslaten en afronden bleken niet mijn sterkste punten. Nu dat afronden toch gelukt is, wil ik graag van de gelegenheid gebruik maken om alle mensen te bedanken die hebben bijgedragen aan de totstandkoming van dit proefschrift.

Katja, bedankt voor de leerzame tijd de afgelopen jaren. Ik begon als één van de eerste AIO's in je onderzoeksgroep. Je was toen nog assistent professor en je onderzoeksgroep aan het opstarten. Inmiddels is het Prof. dr. Loos en ben je mijn promotor geworden. Ik waardeer de enorme vrijheid die je mij gegeven hebt met het invullen van het onderzoek. Deze vrijheid heeft er ook wel eens toe geleid dat ik niet meer wist welke kant uit te gaan. Een bezoekje aan je kantoortje deed echter altijd wonderen. De deur stond, letterlijk en figuurlijk, altijd open. Bedankt!

Arend-Jan, je hebt mijn onderzoek vanaf de zijlijn gadegeslagen. Desalniettemin zijn op het juiste moment via jou belangrijke contacten gelegd met de onderzoeksgroep van Prof. Dijkhuizen. Bedankt voor het altijd nuchtere commentaar en de aangedragen oplossingen tijdens de werkbesprekingen.

I would like to thank the reading committee, Prof. Dijkhuizen, Prof. Gandini and Prof. Mischnick, who evaluated the manuscript both quickly and thoroughly. Many improvements have been made because of their thoughtful remarks.

Zoals eerder aangegeven is er een samenwerking ontstaan met de vakgroep van Prof. Dijkhuizen. De enorme kennis van de Microbial Physiology groep over enzymen is van onschatbare waarde geweest voor dit onderzoek. Naast Prof. Dijkhuizen wil ik ook graag Prof. Van der Maarel en Marta Palomo Reixach uit deze vakgroep bedanken voor de hulp aangaande de karakterisatie van polysachariden en het ter beschikking stellen van verschillende soorten glycogen branching enzymes. Marta, I enjoyed our cooperation during the last years. Lately the contact was only by email; nevertheless,

I enjoyed our (digital) conversations and coffee breaks when I visited the biology laboratories in Haren.

Een aantal leden van de vaste staf van polymeerchemie, Jur Wildeman, Joop Vorenkamp en Gert Alberda van Ekenstein, wil ik bedanken voor de tips & tricks die zij hebben aangedragen vanuit hun jarenlange ervaring bij de vakgroep. Ook de secretaresses van de vakgroep wil ik hier even in het zonnetje zetten. Karin, Hinke en Yvonne zonder jullie was ik allang verdwaald in de administratieve rompslomp die de universiteit rijk is. Karin, het was erg fijn om af en toe naar je kantoortje te kunnen "vluchten" voor een praatje.

Leendert, ik kon mij geen betere collega wensen om een kantoortje mee te delen. Wij zijn ongeveer tegelijkertijd begonnen als AIO en ongeveer tegelijkertijd (en later dan gepland) klaar. Hebben we het soms tè gezellig gehad op het lab en in de tussenkamer? Ik zal het gaan missen!

Een aantal (afstudeer)studenten en stagiairs hebben ook hun steentje bijgedragen aan dit proefschrift en wil ik bij deze bedanken voor hun inzet: Matthijs, Christa, Iris , Lia, Pradanti, Teunis, Martin en Lizette (Loen). This thesis is also filled with your results, graphs and tables and without your contributions this thesis would have been a lot thinner. I am very grateful to you all. Lia, Martin and Iris: good luck with your own PhD research. Lizette, ik noem je hier bij de "afstudeerders en stagiairs", dat is natuurlijk niet helemaal van toepassing op jou als ervaren organisch chemicus. Fantastisch dat jij me gedurende 6 weken wilde helpen met de laatste (experimentele) loodjes. Hierdoor kwam het hele project in een stroomversnelling.

Gedurende mijn werkzaamheden binnen de vakgroep heb ik heel wat leuke momenten gedeeld met een verscheidenheid aan mensen. Een aantal wil ik hier bij naam noemen: Jelger, Joost, Gerrit (jr.), Wendy, Frans, Nemanja. Jullie hebben de vakgroep alweer een tijdje verlaten maar ik ben jullie niet vergeten, bedankt voor alle leuke momenten. Gerrit (sr.), Ton, Andreas (sr.), Wouter, Ralph, Jacob, Diego, Alberto, Anke, Deepak, Minseok, Rachma, Erythrina, Salomeh, Lizette (Oudhuis), Albert, Anton, Vincent, Lieuwe-Jan, Jan-Willem, Steven, Laura, Jelena, Ivana, Milica, Danijela, Nienke (Brouwer) and all the people I forgot to mention: Thanks for the *gezellige* coffee breaks, V.v.P. drinks, BBQ's and other pleasant moments.

Groningen is leuk maar er gaat niets boven een bezoekje aan Schoonhoven. Pap en mam, een bezoekje aan Schoonhoven voelde altijd aan als een “weekendje weg”. Geen enkel sterren-hotel kan op tegen thuiskomen bij jullie! Bedankt voor het geduld, vertrouwen en de aanmoedigingen.

Lieve Nienke, ik heb je geduld aardig op de proef gesteld doordat ik mijn AIO-periode een aantal keer met een paar maanden wist te verlengen. Het was voor mij niet altijd even makkelijk om uit te leggen waarom dat nodig was. Nu is het dan toch ècht klaar!

Jeroen